# Appendix E:
# Speaker Abstracts

# 100 Years of Progress in Boundary-Layer Meteorology: A look to the past, questions for the future

Margaret A. LeMone
NCAR

(with contributions from Wayne Angevine, Fei Chen, Jimy Dudhia, Kristina Katsaros, Larry Mahrt, Jielun Sun, and Michael Tjernstrom)[1]

and input from
Chris Fairall, Jim Fleming, Ned Patton, Shuyi Chen, and Peter Sullivan[2]

We define the atmospheric boundary-layer (ABL) as that layer of air directly influenced by exchange of heat and energy with the surface. Our story of the ABL begins with surface fluxes, which are dependent on surface roughness and the exchange of energy between the surface and atmosphere. The ABL is typically divided into a surface layer, through which shear production of turbulence kinetic energy is as important as buoyancy production, a well-mixed inner layer, and a transition layer that is alternately occupied by turbulent and free-atmosphere air. This division is most straightforward for a cloudless, steady-state, unstable ABL.

Our history begins with the classical-physics roots from the 18th and 19th Centuries and their early applications to the atmospheric boundary layer, and the contributions from the early turbulence/boundary layer community, who developed the concept of the boundary layer and applied it to flow through wind tunnels, past aircraft wings, and sometimes in the atmosphere itself, with some reference to early discoveries from those more interested in agricultural applications.

From there, we examine the boundary layer from the surface on up, through a look at our understanding of the surface energy budget, exchange coefficients and flux-profile relationships in the surface layer over land and ocean, and the study of the entire cloud-free ABL under unstable and stable conditions. Each narrative follows early measurements and conceptual, laboratory, and numerical modeling efforts. And each provides an idea of what we consider "typical." As part of each narrative, we highlight major difficulties in measurements and models, some which have been resolved, and some which point to research directions in the future.

Even in the absence of clouds, the steady-state ABL is actually rather unusual during the day, occupying only a small part of the diurnal cycle over land during the early afternoon. Likewise, even the dry stable boundary layer is rarely steady-state, being influenced by inertial

[1] Wayne Angevine, CIRES/NOAA, Boulder; Fei Chen, Jimy Dudhia, and Jielun Sun, NCAR/Boulder, Larry Mahrt, Northwest Research Associates, Corvallis, Oregon; Michael Tjernstrom, Department of Meteorology, Stockholm University, Sweden.

[2] Chris Fairall, CIRES/NOAA, Boulder; Jim Fleming, Dept. of Science, Technology, and Society, Colby College, Waterville, ME, Ned Patton and Peter Sullivan, NCAR, and Shuyi Chen, Dept. of Atmospheric Sciences, University Washington, Seattle.

oscillations, baroclinic flows, and even the slightest terrain variation. In addition to its continuous evolution, ABL behavior is complicated by interactions with a heterogeneous surface and with clouds overhead. We present the Arctic boundary layer as a special case, since its properties are in a little-studied part of the ABL parameter space. Again, all topics point to research challenges and opportunities for the future.

We also provide a brief summary of the development of ABL parameterization schemes, many of which depend on a land-surface model for surface fluxes. Especially for the land-surface models, the challenges are not only to represent the "physics" correctly, but also to have the best possible input data on soil and vegetation properties and to represent heterogeneous grid boxes in a numerical model. Ocean-surface models (especially the COARE flux algorithm) have provided an excellent platform to test new ideas against new field data. The PBL models have evolved today to include not only "local" fluxes but also "non-local" fluxes by eddies that extend through the ABL. Unfortunately, even the most advanced models have not succeeded in transporting heat upward rapidly enough to avoid the formation of partially-resolved PBL eddies. Despite their artificiality, the eddies create cloud fields that often resemble satellite images; and the associated convective circulations have been implicated not only in the formation and propagation of precipitating convective systems, but the formation of tornadoes.
Several nagging problems emerged from this historical study. A partial list includes:

1. Why doesn't the surface energy budget balance?
2. How do we approach the apparent failures of Monin-Obukhov similarity theory?
3. How do we deal with surface-atmosphere interaction?
    a. Over the ocean, in the presence of waves, spray, and rain?
    b. Over land, in the presence of horizontally varying terrain?
    c. Over land, in the presence of canopies, canopies and terrain? Cities?
4. What are the values of key "constants" in surface-layer and PBL schemes, such as the ratios of the exchange coefficients of heat and moisture to exchange coefficients for momentum, as a function of stability? The surface roughness lengths for momentum, temperature, and scalars?
5. How do we best describe the evolving boundary layer?
6. How do we best describe the stable boundary layer? (Shouldn't critical parameters include terrain as well as atmospheric and other surface properties?)
7. How do cloud-topped PBLs evolve (for stratus, stratocumulus, cumulus, transitional, in the presence of precipitation, even mesoscale convective systems)?

Addressing these questions should include some lessons from history:

1. We must be aware that the part of boundary-layer parameter space each one of us explores is only part of that space.
    a. Even for clear skies, tropical marine boundary layers and Arctic boundary layers can behave quite differently from fair-weather boundary-layers over land, with vastly different entrainment constants for sensible heat and water vapor, and different depths.
    b. Horizontal advection makes possible entrainment of moist air at PBL top not only in the Arctic, but during the morning in the central U. S. when a southerly low-level jet is bringing moist air up from the Gulf of Mexico.

   c. Direct heating/cooling of the air by radiation during the day, given attention in the early 1970s, was forgotten by some researchers for a time.
2. Related to (1), though large eddy simulations (LES) are powerful tools, the cases simulated often focus on near steady state. Similarly, collection of aircraft flux profiles over land often focused on early afternoon, when the PBL is closest to steady state. Both practices can mislead us into expecting to observe steady-state type profiles in the evolving PBL.
3. Nevertheless, use of all our tools – theory, field observations, LES, laboratory studies. and comparison of PBL parameterizations in numerical weather predictions to observations or idealized LES cases – is important to make progress.
4. Improvement of all these approaches can correct mistakes and lead to new discoveries.
5. Nevertheless, we will often re-discover earlier findings.

# Atmospheric BL Over Land: Observations and Models

Alan K Betts
Atmospheric Research

## 1. INTRODUCTION

**I will only address the first few workshop goals, primarily over land and snow:**

- Overarching Science Question: What observations are needed (over land, ocean, and ice) to make meaningful progress in our understanding and modeling of the global atmospheric boundary layer?
- Examine our understanding of atmospheric boundary layer processes and interactions with land, ocean, and ice surfaces and science drivers, from observation, modeling, and data assimilation perspectives;
- Discuss key observing and modeling gaps and the science that could be accomplished by filling those gap

**My perspective** is to ask how well is the observed surface and BL climatology represented in global models (ECMWF model). Models should represent the real world, and observations tell us how the real world works. Data collection is of limited value, unless it can quantify critical coupled processes that are poorly understood. Given the complexity of real world weather, a forecast model framework is generally needed.

**Land conceptual issues.** BL is diurnally driven by SW and LW radiative processes, coupled to turbulent transport processes & the local cloud field. We can only model the fully coupled system with errors/biases. Disaggregating biases to separate components is tricky. There are unresolved modeling issues over heterogeneous terrain related to:

*Surface roughness, canopy and forests modeling, cloud radiative and BL flux coupling with heterogeneity; intermittent turbulence and ground coupling in stable BLs.*

**2. RECENT CANADIAN PRAIRIE STUDIES** based on a remarkable 55-yr hourly Prairie data set with opaque cloud fraction (fraction of the sky that obscures the sun, moon or stars) have identified several key features of northern latitude BL and surface climate:

Cloud forcing is the dominant BL driver

Cloud radiative forcing changes from negative to positive with snow cover.

Snow cover is a fast climate switch between cloud-coupled unstable and stable BLs with distinct non-overlapping climates.

Specifically temperature changes 10K with surface snow (Fig 1). This large signal means there is a linear relation between fraction of days with surface snow and mean cold season temperature (Fig 2). So over land, snow cover is a primary climate driver in winter.

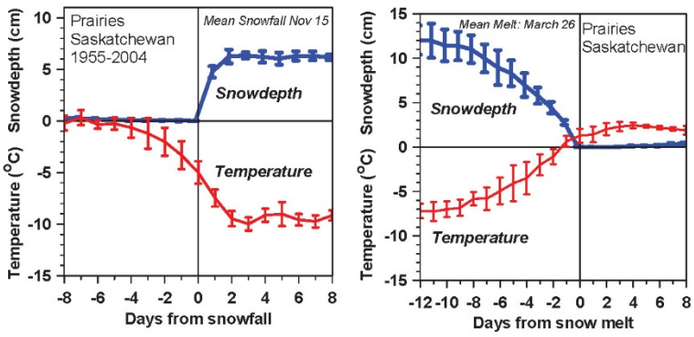


FIGURE 1. Change of 2-m temperature with first major snowfall (left) and (right) with snowpack melt in spring. (Adapted from Betts et al. 2014)

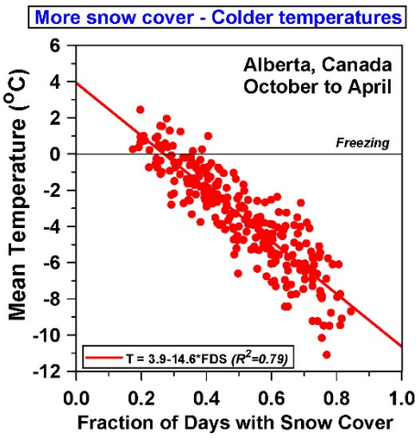


FIGURE 2. Relation between fraction of days with snow cover and mean cold season temperature. (Adapted from Betts et al. 2014)

The sign of the cloud forcing reverses sign with snow cover, so that the diurnal cycle of the BL stratified by opaque cloud cover switches between non-overlapping states (Fig 3). In the cold season with snow cover (which reflects 70% of the incoming SW on the Prairies), temperatures plunge under clear skies. In the warm season without snow cover, temperatures rise to the highest afternoon maximum under clear skies. Months like November (and April) show both of these non-overlapping climates.

The annual diurnal climatology of opaque cloud shows that there are two cloud regimes (Fig 4): the afternoon maximum characteristic of the daytime unstable BL, and a sunrise maximum at the end of the nocturnal cooling of the stable BL, which dominates the cold season.

**Our conclusion** is that the dominant drivers of the stable and unstable BLs over land are cloud cover (at all latitudes) and snow cover at high latitudes, because they control the surface radiative forcing that drives BL development. Unless these are a central focus of observational research on the fully coupled system, progress will be limited.

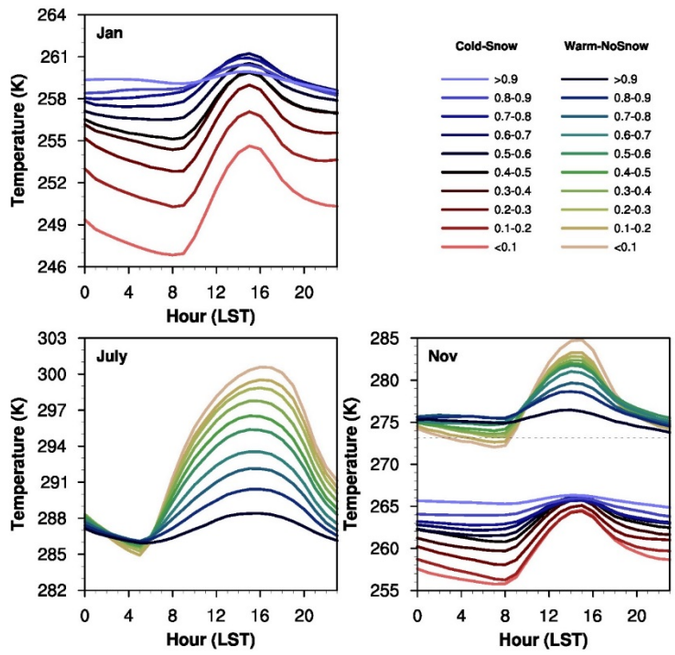


Figure 3. Diurnal cycle of 2-m temperature for January, July and November as a function of daily mean opaque cloud cover (Betts and Tawfik 2016).

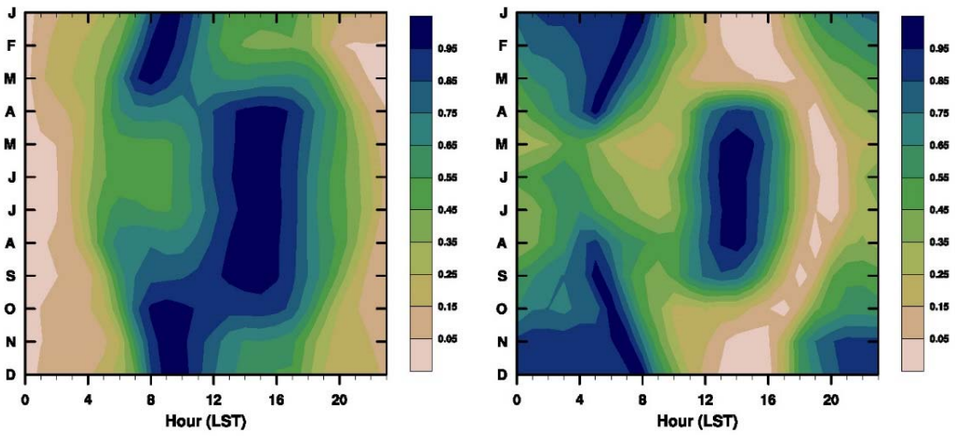


FIGURE 4. Normalized diurnal cycle of total opaque cloud cover fraction (left) and lowest-level opaque cloud fraction (right) over the annual cycle, where 1 is the diurnal maximum and 0 is the minimum (Betts and Tawfik 2016).

## 3. UNSTABLE BL CONSTRAINTS AND DIURNAL CYCLE IMBALANCE

Figure 5 shows two important characteristics of the observed fully coupled unstable BL over the Prairies in the warm season. The left panel shows that the key diurnal ranges of 2-m T and RH are tightly controlled by daily mean opaque cloud in the warm season. The right panel shows that climatologically the diurnal cycle is not in balance over the 24h period. There is a warming and drying at low cloud cover and a monotonic shift to cooling and moistening at high cloud cover, with significant precipitation, with a weak seasonal dependence as the surface warms in spring and cools in fall. We will show that ERA-Interim (ERAI) has biases that have a seasonal structure for $T_n$, $T_x$ and DTR.

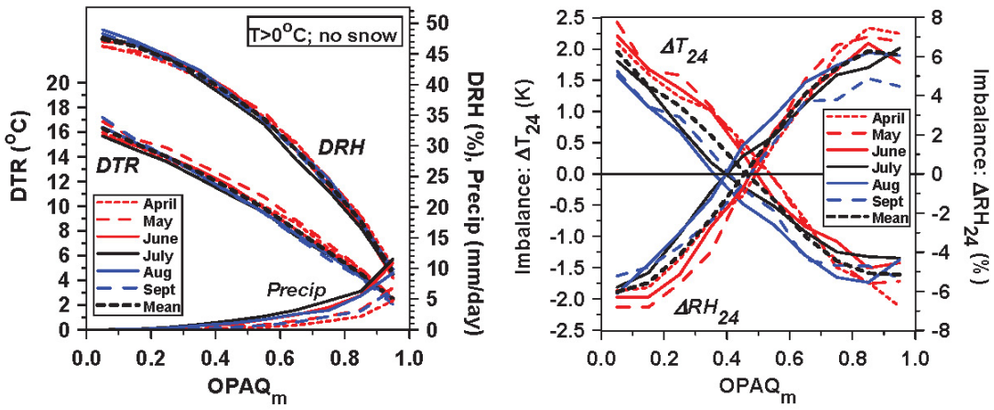


FIGURE 5. Tight coupling between opaque cloud and diurnal ranges: DTR and DRH (left), and (right) 24-h imbalance of the diurnal cycle.

## 4. BIASES IN ERA-INTERIM: DIFFERENCE FROM OBSERVATIONS (BETTS ET AL. JAMES 2017)

Figure 6 shows the large dependence of the ERAI biases (right panel) in $T_n$, $T_m$, $T_x$ (minimum, mean and maximum temperature) and DTR on observed opaque cloud cover in the warm season. The biases in $T_n$ and $T_x$ are of opposite sign, so the bias in DTR is large under clear skies, while the bias of $T_m$ is small.

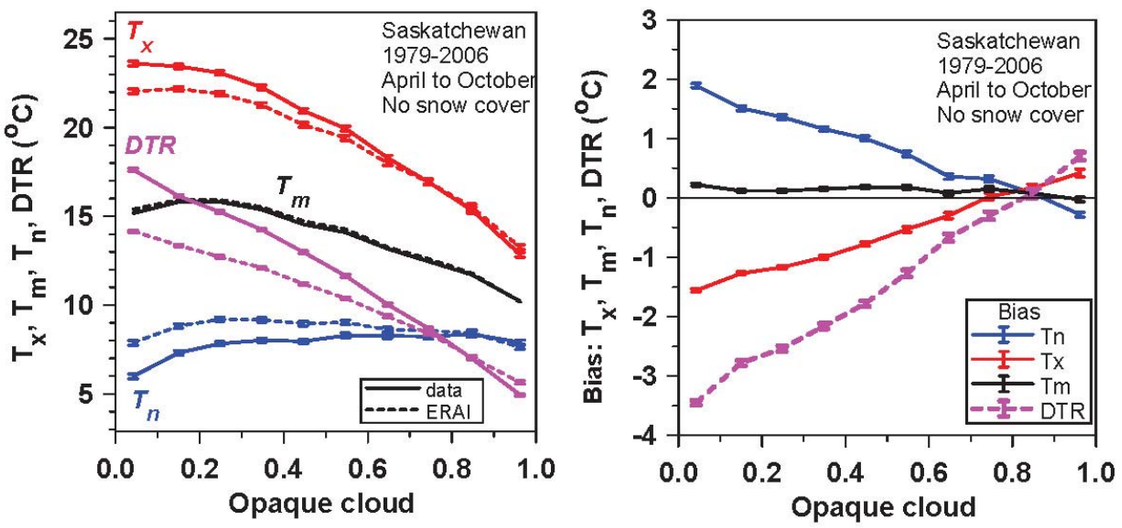

FIGURE 6. Opaque cloud dependence of Tn, Tm, Tx and DTR for observations and ERAI (left) and (right) corresponding ERAI biases in the warm season.

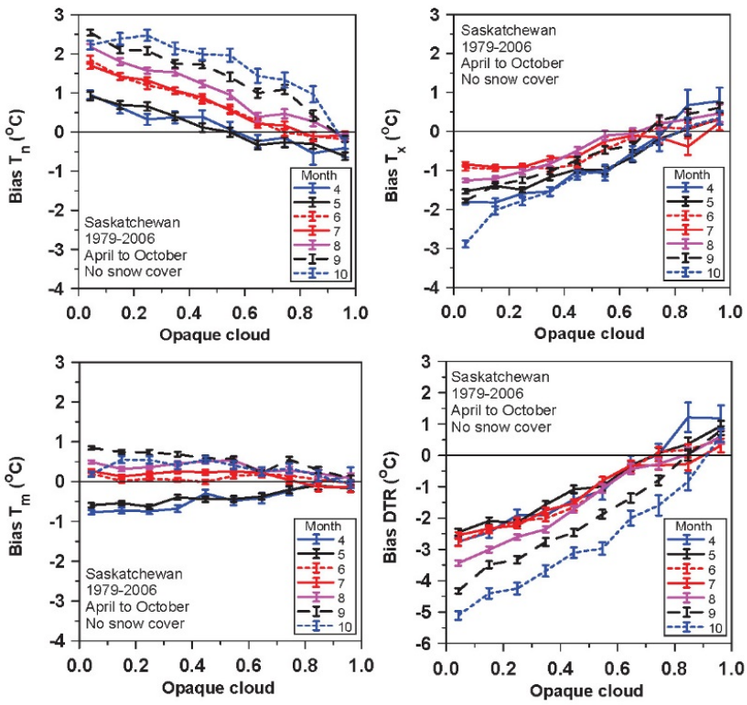


FIGURE 7. Opaque cloud dependence of monthly biases of Tn, Tx, Tm and DTR

Figure 7 shows the seasonal cycle (monthly) of the warm season biases of $T_n$, $T_m$, $T_x$ and DTR as a function of cloud. For the stable BL there is a nearly monotonic increase in the positive bias of $T_n$ a measure of the inversion strength of the stable BL at sunrise. For the unstable BL, $T_x$, a measure of the strength of the superadiabatic layer, has the smallest negative bias in mid-summer. Consequently the bias in $T_m$ shifts upward from spring to fall; and the bias in DTR becomes large negative in the fall.

Figure 8 is the corresponding seasonal cycle of the cold season biases with snow cover of $T_n$, $T_m$, $T_x$ and DTR as a function of cloud. The increase in the stable BL biases of $T_n$ increase into winter and then fall sharply in February and March. But the bias in the afternoon $T_x$ is small and positive with little dependence on season or cloud cover, completely different from the corresponding panel in Figure 7 for the warm season unstable BL. As a result the sign of the DTR bias changes from November to March.

Figure 9 picks up the seasonal cycle of the clear sky biases of $T_n$, $T_m$, $T_x$ and DTR (left) and (right) the corresponding terms in the clear-sky surface energy balance in ERAI. We see the discontinuities in the clear-sky biases that come from the fact that the $T_x$ bias changes sign from negative to positive with snow cover.

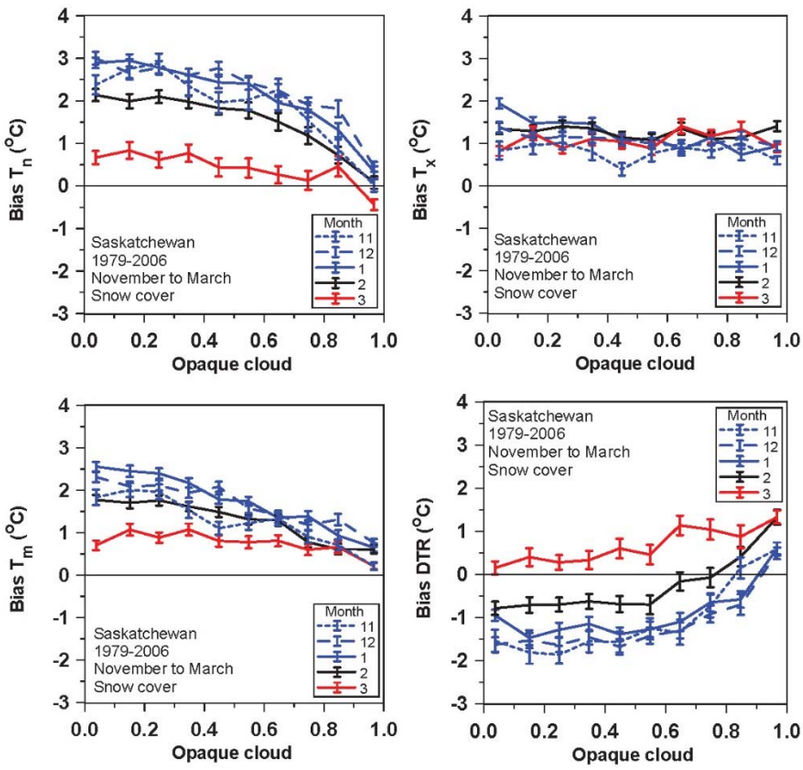


FIGURE 8. As Figure 7 for the cold season

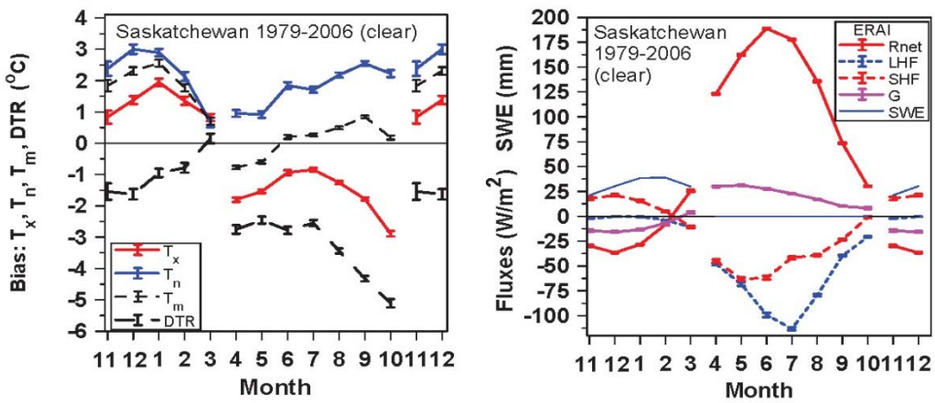


FIGURE 9. Seasonal cycle of clear-sky biases in Tx, Tn, Tm and DTR (left) and (right) seasonal cycle of clear-sky Rnet, LH, SH, G and SWE in ERAI.

## 5. CONCLUSIONS

This comparison between the Canadian Prairie data and corresponding gridpoints in the ERA-Interim reanalysis shows an interesting bias structure that is coupled

a. to the cloud radiative forcing
b. to the seasonal cycle

c. to surface snow cover and the summer/winter differences between unstable and stable BLs

However, interpreting these biases in terms of model structure and parameters requires further work. Betts et al. (JAMES 2017) suggested several possible model issues: too large a diurnal and seasonal amplitude of the ground heat flux, the lack of a diurnal cycle of LAI, possible errors in surface roughness for the unstable BL, and in the stable BL turbulent transports.

**What observations are needed to make meaningful progress in understanding and modeling global BLs? We need routine data that can be used in global data analysis.**

The central challenge is that we have few routine measurements of the surface fluxes and BL structure. Satellite observations poorly sample the near-surface BL, so that the coupled BL structure is modeled using parameterizations. Many of these were developed for homogeneous conditions (eg MO similarity theory for the profiles), and their applicability to real-world heterogeneous conditions are not well tested.

**Surface BL data is needed.** ECMWF suggests (Anton Beljaars, personal communication)

SYNOP stations could add Doppler lidar profilers, giving profiles to 100m (useful also for wind turbines).

SYNOP stations could measure net radiation, and add a temperature observation at the top of the 10 m wind mast. This would give the (2m-10m) temperature gradient, and give observational input to the model MO fit to the surface fluxes.

This workshop could suggest others that could be made routinely and cheaply.

# Marine Boundary Layers: Observations and Models

C.W. Fairall
NOAA/ESRL Physical Science Division

## BACKGROUND

Observations play a crosscutting role in the context advancing the science of weather and climate. At a fundamental level, it is observations that can be used to develop a basic understanding of physical processes that must be modeled within the land-ocean-atmosphere system. Observations are needed for initialization, assimilation, and verification of models and play a key role in improving parameterizations. In-situ observations are required to improve various aspects of satellite retrievals. Global cloud resolving models might cause the convective parameterization problem to, within a few years, evaporation in a puff of numerical smoke. But, with their predominance of small-scale processes, oceanic and atmospheric boundary layers (BLs) will likely remain a modeling battleground for decades. The future of BL observations is intimately tied up in the important science problems that can be practically addressed with existing observing technologies. But the priorities must also be considered in the context of the balance with numerical simulations – it makes no sense to field a new megadollar field program if the answers can be obtained with a carefully designed large eddy simulation (LES).

## SCOPE

Variables of observational interest include those associated with conservation equations for modeling environmental properties: standard meteorological, trace gas, and aerosols. We are interested in profiles of these variables: means and statistical moments associated with turbulent variability. Vertical fluxes (covariances with vertical velocity fluctuations) are premier, but $2^{nd}$ and $3^{rd}$ moments and cross-moments are important. Because parameterization of surface fluxes is critical, the measurement of surface fluxes alone has more limited value. Still, long time series measurements of surface fluxes have considerable values for evaluating coupled models and constraining closure of meteorological and bio-chemical processes. Effective parameterization development may require very accurate near-surface profiles of means and higher moments plus information on the surface and subsurface properties.

Parameterization of BL mixing (eddy diffusion vs mass flux-based non local schemes) are somewhat divorced from surface characterizations, but may depend on specification of properties (e.g., entrainment/detrainment of plumes) that are particularly intractable for today's observing technologies. BL clouds still present big problems for observations, simulations, and models. The classic stratocumulus topped BL has been continuously studied since the 1960's (Lilly, 1968) with most of the work done over the ocean. More recently attention has turned to shallow convectively driven cloudy BL's, often in the context of the transition from stratocumulus BL. Shallow convection has been identified as a key processes in representations of the MJO and in the difference in the CO2

forcing sensitivity of climate models. An amusing trend in this area has been the use of observations to constrain LES simulations of the field programs (e.g., McGibbon and Bretherton, 2017). The scope of this talk will be principally limited to marine BL, although many of the issues are not dependent on the nature of the surface. The topic is too vast to cover comprehensively in 30 minutes, so I will fall back to the tried and true approach of talking about what I actually know about.

## DIGRESSION TO LAND BLS

Before focusing more on marine issues, I want to briefly discuss the overwhelming problem of representing fluxes over real surfaces. The ocean is complicated (waves, breaking waves, surfactants, bubbles, biology), sea ice is more complicated (fractional coverage, ice thickness, freeboard, snow cover, melt ponds, open leads, and refrozen leads), but land surfaces are mind-numbingly complex. It is essentially impossible to characterize the subsurface properties in most locations and even if we had the data we likely would not know what to do with it. Soil moisture variability is a big problem (and can change significantly every time it rains) and the nature of the plant canopy and its interaction with soil and atmosphere is basically unsolvable from first principles. Besides the strong diurnal cycle, we have the hydrological cycle and the plant growing cycle. And don't get me started on 'complex terrain'. Much of the research on this problem has been based on a few point observations from fixed towers. The classic approach of trying to improve models by comparing their outputs to accurate observations is uniquely poorly posed because of the sampling/representation/aggregation problem. Here we really need a revolution in acquiring/applying area-averaged direct and remote observations combined with re-thinking the parameterizations in more observable variables. Direct measurement of area-average fluxes is still a confounding problem. Small UAS and tomographical methods hold great (but so far unfulfilled) promise.

## GENERAL THOUGHTS ON TECHNOLOGY

Before launching into more discussion, it is of interest to ponder instruments and measurement systems that have really changed things in BL observations: fast compact computer DAS with vast/cheap digital storage, sonic anemometers, Doppler mm-wavelength cloud radars, GPS, reanalysis, ARGO floats, fast low-noise H2O/CO2. Are there any recent technologies that might add to this list in the near future? How about fast pressure sensors, air launched UAS, affordable Doppler lidars, …? Here are a few buzz words to consider in designing future observation programs:

Big data. Here we are referring to collecting lots of data to span multiple parameter space, seasons, locations. Still room for narrowly focused, short duration field programs, but the idea here is massive amounts of observations to beat down sampling uncertainty or to cover longer-scale evolution.

Comprehensive: Collect all the ancillary observations to complete the parameterization space.

Accuracy: A balance between application, practicality, cost, etc.

Complementary: Blending information from simulations, NWP, etc.

## SOME SPECIFIC PROBLEMS

- Air-sea fluxes at high wind speeds (U>30) and how to characterize the surface. This includes interactions within the wavy BL (WBL). The question of the wind speed dependence of drag coefficient and a hypothesized fundamental change in the nature of the interface at hurricane wind speeds is still unresolved. Parameterizations of gas transfer and aerosol production involve arguments about role of bubbles and sea spray. The basic forcing parameter for gas transfer and spray production is not known: wind speed, stress, whitecap fraction, energy dissipated by wave breaking. It is not clear how to determined sea spray production flux (see Fig. 1 for an example) from observations. Observations over the ocean at high wind speeds are difficult. Ships are impractical. Fixed platforms have very long (decades) return periods. Airborne platforms cannot fly low enough. So, aircraft-based remote sensors are the obvious approach. There are methods to measure wave spectra, sea spray, whitecaps, and wind speed profiles for aircraft but they have yet to be applied together. Another interesting approach is the use of air-launched UAS. NOAA is experimenting with launching Coyote UAS in hurricanes from the NOAA P-3.
- Stable SL/BL. There is a big difference in arctic 'near-equilibrium' vs midlatitude 'diurnally driven' stable BL. Much about Arctic was learned in SHEBA but only the near-surface layer was measured effectively. The MOSAIC project is an opportunity to add information on the rest of the BL. This information is necessary for linking surface and upper layer, role of waves, intermittency, KH overturning, etc. Taller towers and high resolution surface-based remote sensors are required. Overland, sloping terrain adds another confusing factor. This is another situation where observations and simulations may be combined (e.g., see Fig. 2).
- Important properties of clouds are still a problem: liquid water, cloud droplet and precipitation microphysics are a major challenge for remoted sensing approaches. Some success in simplest cases – stratus with no drizzle. The has been a lot of progress in retrieval algorithms. Separation of particle gravitational settling velocity and turbulent motions is a critical need. Multi-wavelength Doppler spectral methods show promise. Stratocumulus clouds are the obvious targets, but shallow cumulus is also possible. A lot of work has been done on estimating cloud top entrainment rate (see Figs. 3 and 4). I think this is still a problem. Model radars can measure profiles of vertical velocity variance, skewness, and TKE dissipation rate with 10-m resolution near cloud top. Aircraft methods have improved significantly in the last decade with better drop measurements, better liquid water, fast humidity, DMS, and ozone sensors.
- Turbulent pressure terms. With the recent development of commercial fast pressure sensors with full one-atmosphere dynamic ranges will allow a major step forward in the measurement of turbulent pressure correlation terms in the atmospheric BL. It isn't obvious where this needs to be applied and how it balances with LES simulations. Turbulent pressure correlations with surface wave slop also provide a measurement of the wave component of stress over the ocean. Today's parameterizations (there are many) are based on laboratory measurements and one or two old field programs. The observations have yielded data on the pressure-slope correlation at the wave peak while the parameterization is applied spectrally. To do these measurements properly will require mounting fast sensors on a mechanical wave follower. Another approach to measuring turbulence in the WBL is with Particle Imaging Velocimetry (PIV). This has been done

with considerable success in the laboratory and applications over the ocean are on the horizon.

- Characterization of vertical mixing in shallow cumulus/broken clouds via so-called mass flux and stochastic parameterizations. Can we use direct measurements from combined Doppler lidar and radar to determine the important variables? Some exploratory work has been done on measuring profiles of mass flux, but it isn't clear how to apply this. Does this really add to LES approaches?

## REFERENCES

Albrecht, B.A., M. Fang, and V. Ghate. 2016. Exploring stratocumulus top entrainment processes and parameterizations by using Doppler cloud radar observations. *Journal of the Atmospheric Sciences* 73: 729-749.

Lilly, D.K. 1968. Models of cloud-topped mixed layers under a strong inversion. *Quarterly Journal of the Royal Meteorological Society* 94: 292-309.

McGibbon, J. and C. S. Bretherton. 2017. Skill of ship-following large-eddy simulations in reproducing MAGIC observations across the northeast Pacific stratocumulus to cumulus transition region. *Journal of Advances in Modeling Earth Systems* 9: 810-831.

Sorbjan, Z. 2017. Assessment of gradient-based similarity functions in the stable boundary layer derived from a Large-Eddy Simulation. *Boundary Layer Meteorolory* 163: 375-392.

Sullivan, P. P, J. C. Weil, E. G. Patton, H. J. J. Jonker, and D. V. Mironov. 2016. Dynamics and intermittent temperature fronts in large-eddy simulations of the stable atmospheric boundary. *Journal of the Atmospheric Sciences* 73: 1815-1840.

Veron, Fabrice, 2015: Ocean spray. A*nnu. Rev. Fluid Mech.,***47**, 507-538.

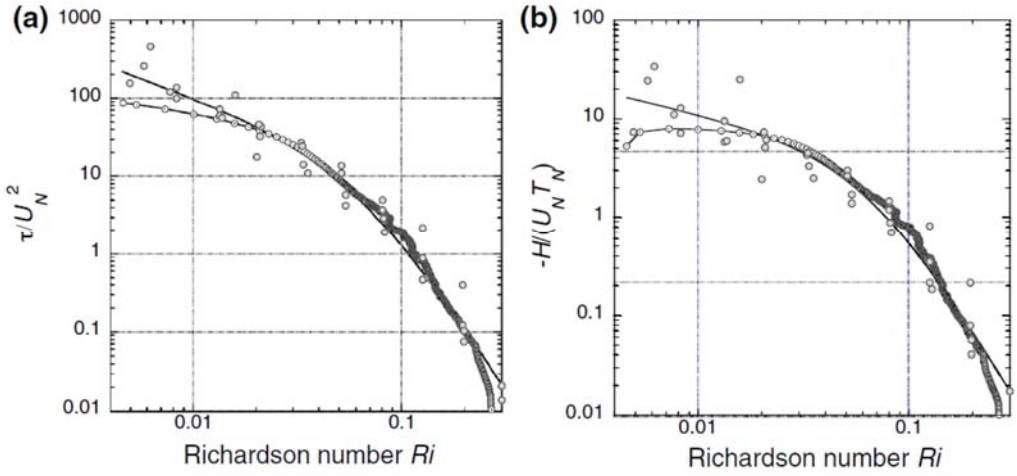


FIGURE 1. The explicit similarity functions for: **a**, momentum flux, and **b**, temperature flux. The solid line is a parameterization, lines with open circles are from the LES model of Sullivan et al. (2016), and the shaded circles are observations from the SHEBA project. Figure from Sorbjan (2017).

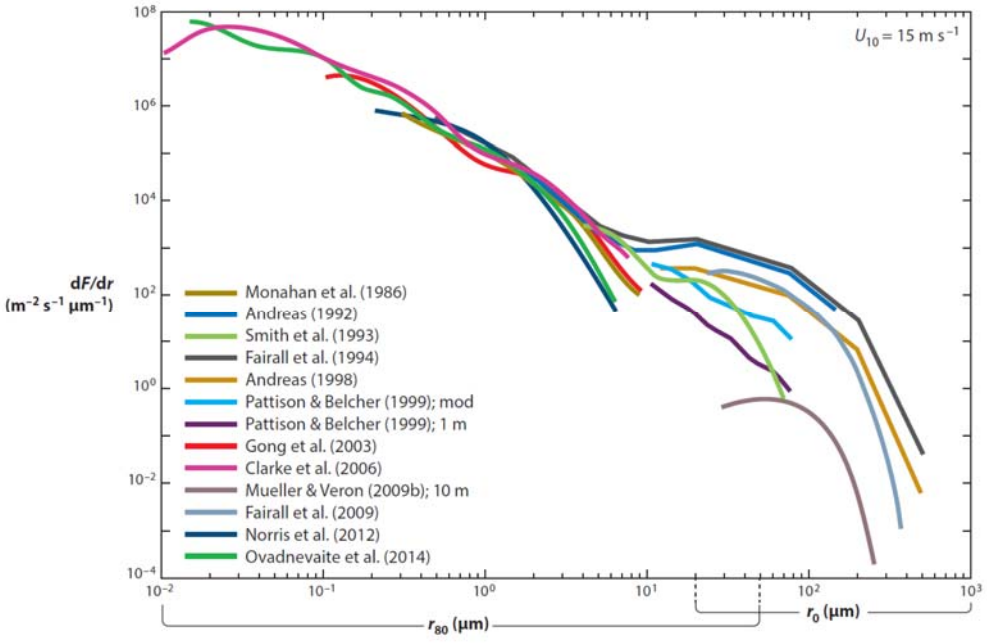


FIGURE 2. Size-dependent sea spray generation functions (# drops/area/sec/dr) for a wind speed of 15 m/s as reported by various authors (from Veron 2015). Note this disparity in estimates for larger droplets.

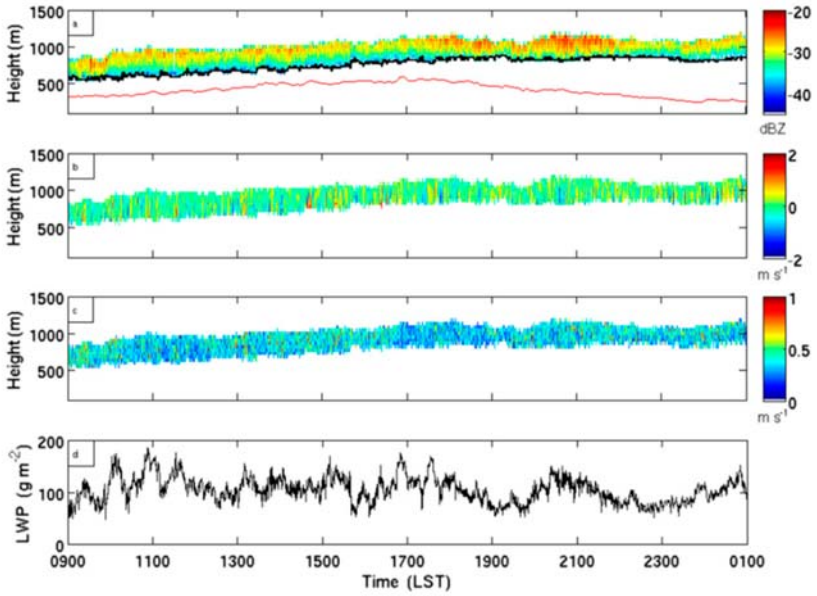


FIGURE 3. Time-height display of (a) reflectivity factor, (b) mean Doppler velocity, and (c) Doppler spectrum width recorded by a mm-wave cloud radar, and (d) liquid water path from a microwave radiometer. The ceilometer-recorded cloud-base height (black) and the LCL calculated from the surface observations (red) are also shown in (a). From Albrecht et al. 2016.

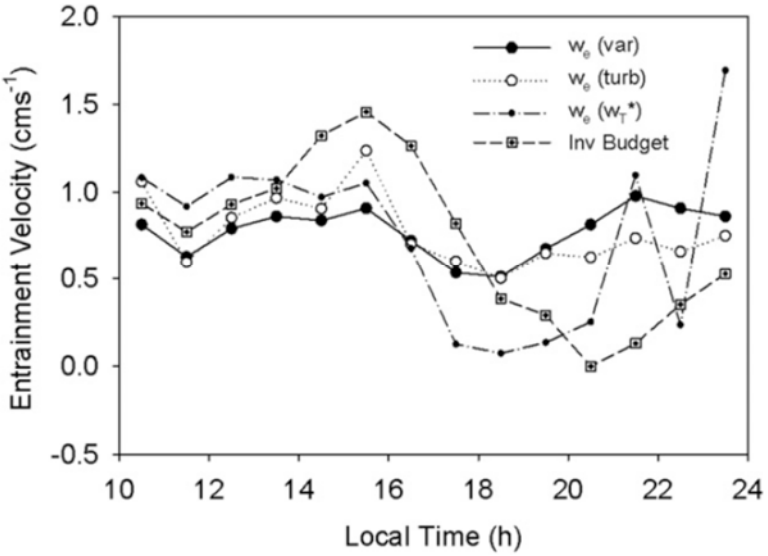


FIGURE 4. Entrainment velocities as a function of time from several estimation methods: Variance and dissipation (solid circle), dissipation (open circle), convective velocity scale (dots), and the height budget (Albrecht et al. 2016).

Figure 1. The explicit similarity functions for: **a**, momentum flux, and **b**, temperature flux. The solid line is a parameterization, lines with open circles are from the LES model of Sullivan et al. (2016), and the shaded circles are observations from the SHEBA project. Figure from Sorbjan (2017).

Fig. 2. Size-dependent sea spray generation functions (# drops/area/sec/dr) for a wind speed of 15 m/s as reported by various authors (from Veron 2015). Note this disparity in estimates for larger droplets.

Fig. 3. Time-height display of (a) reflectivity factor, (b) mean Doppler velocity, and (c) Doppler spectrum width recorded by a mm-wave cloud radar, and (d) liquid water path from a microwave radiometer. The ceilometer-recorded cloud-base height (black) and the LCL calculated from the surface observations (red) are also shown in (a). From Albrecht et al. 2016.

Figure 4. Entrainment velocities as a function of time from several estimation methods: Variance and dissipation (solid circle), dissipation (open circle), convective velocity scale (dots), and the height budget (Albrecht et al. 2016).

# Modeling and Observation of Atmospheric Boundary Layers: Advancing Together

Christopher S. Bretherton
Departments of Atmospheric Sciences and Applied Mathematics, University of Washington

**Note**: This draft version does not yet include any references, which will be added later!

The atmospheric boundary layer (ABL) forms where the atmosphere turbulently couples to the underlying land or ocean surface. Our lives and civilization play out in the ABL. Accurate modeling and forecasting of the ABL are important to our everyday lives, as well as to simulation of past, present and future climate.

The ABL contains a rich spectrum of turbulent eddy motions which transport heat, moisture, momentum and chemical constituents. These range in vertical scale from millimeters up to the ABL depth, which itself can be as little as a few meters or as deep as a few km. The ABL often has substantial horizontal variability on mesoscales (10-100 km) that sometimes is strongly tied to corresponding variability in the underlying surface properties or orography. The ABL must be represented in regional and global numerical models. No contemporary numerical model can afford to simulate this entire range of scales; parameterization of unresolved ABL circulations and associated transport and cloud-formation processes is unavoidable.

## HIGHER-RESOLUTION MODELS

For regional and global models, the challenge of representing the ABL and of making effective use of the diverse observations we can take within the ABL is rapidly evolving. Global weather prediction models, and soon climate models, are employing 10-25 km grid resolution and sub-100 m vertical grid spacing in the lower troposphere. Such models start to explicitly resolve mesoscale circulations, land-surface heterogeneity and flow around and over topographic obstacles that previously had to be fudged into ABL and gravity-wave drag parameterizations.

NOAA runs the nonhydrostatic HRRR model, a WRF derivative, operationally several times daily with 3 km horizontal grid spacing over a domain spanning the contiguous U. S. At the University of Washington, the WRF model has been nested down to a 300 m grid over the complex terrain of the Columbia Gorge. This grid starts to resolve large ABL turbulent eddies and cumulus updrafts. To better represent cloud processes, an ‘ultraparameterized’ global climate model runs a cloud-resolving model with 250 m horizontal by 20 m vertical grid spacing in the lower troposphere in every grid column of the climate model, in place of conventional

physical parameterizations. At such resolutions, yesterday's ABL parameterizations may become inappropriate or at a minimum require retuning.

## NEW OPPORTUNITIES FOR MODEL-DATA FUSION

A finer model grid provides exciting new opportunities for better using observations within the ABL. A model that better resolves local land surface features can be more confidently compared with a point observation. One hopes to better assimilate satellite observations of quantities such as skin temperature and clouds over complex land surfaces into models, or to improve simulations of ABL vertical structure of winds (e. g. for wind power or aviation), stability, humidity and pollutant transport. Are ABL vertical profile observations effective for data assimilation and model improvement?

Model-data fusion will be a central challenge for future ABL observations. Analyses based on high-resolution models will be increasingly important context for necessarily limited boundary layer observations, both for field experiments and for long-term measurements. More generally, could we develop an improved, cost-effective ABL observing system that would improve forecasts and simulations of near-surface meteorological parameters such as temperature, humidity and wind, and/or better forecasts of boundary layer wind, temperature and cloud profiles? Could such an observing system function even with an imperfect (but tunable and finely spatially resolved) land surface scheme? Could sparse surface remote sensing instruments such as ABL wind profilers, RASS, or Doppler lidars play a role? Observing system simulation experiments and clear performance metrics would be required to design such a system.

## ENDURING ABL PARAMETERIZATION CHALLENGES

Most long-term PBL parameterization challenges remain even with 1-25 km grids:

- Boundary-layer cloud and its feedbacks on vertical structure and surface energy budget
- Stable BL – surface temperature and fluxes
- Vertical structure (for wind power, chemistry, aerosols, clouds)
- Complex land surfaces, e. g. canopies, urban areas, steep terrain defy the assumptions of traditional M-O theory (e. g. where is the effective surface height?)

Extensive field studies have tackled all of these issues and improving parameterizations is challenging because they must work well across a range of conditions – are we using the existing observations well enough to this end? New ABL field studies should target clearly documented ABL biases in current forecast and climate models, and detailed comparison of the new observations with space-time collocated forecasts by such models should be a central analysis strategy.

ABL parameterizations are particularly important in air pollution models, but uncertainties in chemistry and sources also induce large errors in those models. Simulating the correct vertical structure of the ABL under both stable and unstable conditions over the complex surfaces in and around many urban areas is challenging – are there particular targets for model improvement?

Over the ocean, surface flux parameterization in high wind conditions remains uncertain due to the difficulty of making reliable observations and also the possible role of sea state. This is particularly important for tropical cyclone prediction.

## METRICS

To improve ABL predictions, we must have reliably measurable metrics for errors in salient ABL quantities. Errors in such quantities may reflect the characterization of the underlying surface or the overlying atmosphere as well the the ABL. Commonly-used metrics are surface air temperature, humidity and 10 m winds, cloud cover and type, surface downwelling longwave and shortwave radiation, and surface sensible and latent heat fluxes. These can be sampled at specific sites, e. g. buoys or ARM-like supersites which also provide vertical profiles of cloud and ABL structure, or based on space-time gridded observational estimates. The history of precipitation at a natural land site is also very important to its vegetation and land-surface characteristics, and hence to the skill of a forecast model in predicting near-surface temperature, humidity and surface turbulent and radiative fluxes at that site.

Ideally, global and regional models should be compared with observations in a short-range forecast mode, which better isolates ABL errors from those in the weather and surface state, Climatological evaluation of a model against the seasonal and geographical variability of an observed metric such as surface air temperature or the partitioning of the surface energy budget is also a helpful and time-honored approach, but throws away much of the information content of the observations and the biases can sometimes be difficult to attribute.

Should we be looking more at metrics of vertical structure within the ABL, e. g. based on vertical wind shear or low-level temperature structure? Do we have enough data to usefully do this?

## LARGE-EDDY SIMULATION (LES)

Another important class of ABL models is ‘process’ models optimized to elucidate particular ABL phenomena such as coherent eddy structures interacting with the surface, flow in urban canyons or forest canopies, or turbulent mixed layer evolution. These can span a wide range of complexity and idealization. Perhaps the most broadly used is LES, which simulates ABL turbulence, often coupled to other processes such as clouds, aerosols, chemistry or a complex surface. LES uses a three-dimensional grid sufficient to resolve those eddy scales that contribute most to fluxes of heat, moisture and momentum, and use a combination of subgrid turbulence parameterization and numerical diffusion to remove eddy kinetic energy and scalar variance at an affordable grid scale much larger than the Kolmogorov scale. A typical LES domain is several times as wide as the ABL depth, with a horizontal grid spacing of a few percent of the ABL depth and a comparable vertical grid spacing, often refined near the surface or near sharp inversions.

LES has proved useful in studies of all types of ABL, especially stable, convective and cloud-topped boundary layers, in the development of ABL-related parameterizations in large-scale models, and in mixed applications such as flow through wind farms. As with other modeling approaches, applications of LES must be rigorously observationally tested. For instance, for cloud-topped boundary layers, LES intercomparisons have exposed modeling uncertainties, e. g. due to parameterizations of microphysics and precipitation

processes, and entrainment through sharp inversions. Nevertheless, LES with computationally affordable grid resolution have shown impressive skill in replicating many types of observations in diverse boundary layer types. Remote sensing observations such as Doppler lidar and cloud radars that can provide time-dependent estimates of profiles of turbulent statistics such as vertical velocity variance or turbulent dissipation rate are particularly useful for comparison with LES. Routine, day-in, day-out LES at ARM-like observational supersites, forced by time-varying boundary conditions from large-scale forecast models, should be run and analyzed to gain a fuller appreciation of the strengths and limitations of LES as a bridge between observations and large-scale models with parameterized ABL processes. ARM's LASSO pilot study on shallow cumulus convection at the SGP site is a first step in that direction.

## REGIONAL AND GLOBAL BOUNDARY LAYER EDDY-PERMITTING MODELS

Developmental models combine regional scale and LES-like O(100 m) boundary-layer eddy resolving horizontal resolution. These may be a useful window into the performance of boundary-layer parameterizations to the extent they can be shown to have enhanced skill compared to 1-25 km models with PBL parameterizations.

Perhaps the biggest promise of such models is improved simulation of clouds and vertical structure of unstable boundary layers. Is there any observational evidence supporting this promise? How do they handle transitions between stable and unstable ABLs? Do we have adequate routine or IOP observations of vertical profiles of boundary-layer turbulence or vertical wind structure to test whether that is better simulated by such models than is captured in parameterizations?

# Atmospheric Boundary Layer over Land, Ocean, and Ice

Xubin Zeng, Michael Brunke, Josh Welty, and Patrick Broxton
University of Arizona

In this talk, I will briefly review our work related to atmospheric boundary layer (ABL) processes over land, ocean, and ice:

1) Over oceans, field campaign and cruise observational data are used to evaluate ABL clouds and ABL height from satellite remote sensing and climate modeling (Zeng et al. 2004; Brunke et al. 2010). These results demonstrate the importance of measurements over a seasonal cycle and the need of more model vertical layers in ABL (Zeng et al. 2004) as well as the importance of surface-based measurements for the evaluation of both satellite products and climate models (Brunke et al. 2010).

2) Over land, the surface-ABL-cloud (radiation, precipitation) interaction is analyzed using in situ observations over the southern Great Plains (Welty et al. 2017, manuscript under preparation). In particular, the importance of measuring turbulent and radiative fluxes as well as precipitation and thermodynamic variables (e.g., ABL height versus lifting condensation level) is emphasized.

3) Over polar regions, the humidity inversion is documented (Brunke et al. 2015). Specific humidity inversion over polar regions is one difference in ABL between polar regions and lower latitudes. This is primarily contributed by horizontal moisture advection, and hence horizontal wind measurements are needed. More measurements of the humidity vertical profiles are also needed to reduce reanalysis differences.

4) The snow impact on seasonal prediction during the spring-summer transition season (April-June) is quantified (Broxton et al. 2017). This illustrates the importance of measuring snow water equivalent globally and suggests that snow water equivalent affects other variables (e.g. 2-m air temperature) over mid- and high-latitude land in April-June more strongly than do sea surface temperatures, whose influence is mostly felt on the edges of continents.

5) Finally, observational needs for understanding and modeling ABL are presented. ABL horizontal wind, temperature, and humidity measurements need to combine satellite remote sensing with ground-based and aircraft measurements. ABL measurements need to resolve the diurnal cycle and cover the seasonal cycle. Various observations need to be brought together in a dynamically consistent way through data assimilation.

References

Broxton, P., X. Zeng, and N. Dawson. 2017. The impact of a low bias in SWE initialization on CFS seasonal forecasts. *Journal of Climate* doi: 10.1175/JCLI-D-17-0072.1

Brunke, M. A., S. P. de Szoeke, P. Zuidema, and X. Zeng. 2010. A comparison of ship and satellite measurements of cloud properties with global climate model simulations in the southeast Pacific stratus deck. *Atmospheric Chemistry and Physics* 10, 6527-6536. doi:10.5194/acp-10-6527-2010.

Brunke, M., S. Stegall, and X. Zeng. 2015. A climatology of tropospheric humidity inversions in five reanalyses. *Atmospheric Research* 153, 165-187. doi: 10.1016/j.atmosres.2014.08.005.

Zeng, X., M. Brunke, M. Zhou, C. Fairall, N. A. Bond, and D. H. Lenschow. 2004. Marine atmospheric boundary layer height over the eastern Pacific: data analysis and model evaluation. *Journal of Climate* 17, 4159-4170.

# Addressing Biases in Earth System Models: Role of Atmospheric Boundary Layer Processes

L. Ruby Leung
Pacific Northwest National Laboratory

The Earth system is determined by coupled processes of the atmosphere, land, ocean and cryosphere. The atmospheric boundary layer plays a critical role in the exchange of energy, water, and biogeochemical fluxes across the various interfaces of the atmosphere with the underlying surfaces. Therefore, gaps in observing, understanding, and modeling atmospheric boundary layer processes, including their interactions with clouds and convection, have limited advances in climate science ranging from climate predictions at sub-seasonal-to-seasonal time scale to quantifying cloud feedback and climate sensitivity. Earth system models are developed from bottom-up to represent myriads of processes with many degrees of freedom and connected in models for the atmosphere, land, ocean, and ice, which are then coupled to represent their interactions. Besides capturing individual processes, parameterizations must also work together to reproduce the overall behaviors of the Earth system as measured by top-down global and large-scale metrics such as top-of-the-atmosphere energy balance, general circulation of the atmosphere and ocean, and global and seasonal distribution of precipitation. Detailed observations used to develop and evaluate parameterizations are often not used to constrain their behaviors in Earth system models because of the scale mismatch. Despite multiple ways to evaluate models using uncoupled and coupled short forecast simulations, isolating the contributions from a specific parameterization to the overall model biases and demonstrating process fidelity remains difficult. Model development is largely an under-constrained problem, leading to equifinality of model outcomes.

I will show a few practical examples of how common biases in Earth system models involving surface and boundary layer processes are diagnosed and addressed using uncoupled and coupled simulations of Energy Exascale Earth System Model (E3SM) and Community Earth System Model (CESM).

## 1. DRY BIAS IN THE TROPICAL WESTERN PACIFIC

The atmospheric component of E3SM has a notable dry bias in the north tropical west Pacific (NTWP). The dry bias has important implications to ENSO variability in the model through its impacts on salinity and mixing in the upper ocean, and hence the ocean response to wind stress in the equatorial tropical Pacific. Including convective gustiness, a missing subgrid process in the current model version, is shown to reduce the bias through an increase in the surface winds and hence a net increase in surface evaporation (Harrop et al. 2017). Convective gustiness favors increased precipitation in regions where the resolved surface winds are weak and convection is present. Using a Normalized Gross Moist Stability (NGMS) framework, it is found that the increased moist static energy forcing from the enhanced evaporation amplifies the increase in precipitation to exceed the increase in the evaporative flux. Consistency of the model response to the convective gustiness parameterization with the predicted response from the NGMS framework and the use of LES simulations and TOGA COARE observations to constrain the parameterization (Redelsperger et al. 2000) lend some confidence in our approach to addressing the NTWP dry bias in the model.

## 2. AMAZON DRY BIASES

Like many CMIP5 models, both E3SM and CESM exhibit dry biases over the Amazon during the wet season. Since the Amazon is also a region where precipitation is dominated by convection and weak winds, convective gustiness may also have a positive impact on addressing the Amazon dry biases. Numerical experiments with E3SM show that this is indeed the case (Po-Lun Ma et al. manuscript in preparation), but the gustiness parameterization is not well constrained over land. It remains unclear how increasing evapotranspiration (ET) due to the gustiness parameterization increases precipitation while numerical experiments with CESM show little sensitivity in the Amazon wet season precipitation to two versions of the land models that differ quite significantly in simulating ET (Sakaguchi et al. 2017). Furthermore, the role of surface versus tropospheric forcing in Amazon convection remains unclear as different datasets point to different land-atmosphere coupling strengths in the Amazon. Modeling land-convection-troposphere coupling in which the atmospheric boundary layer plays a key role remains challenging over the Amazon, but it has important consequences to the global energy, water, and biogeochemical cycles. Besides convective gustiness, turbulence and shallow convection schemes such as CLUBB (Golaz et al. 2002) that better capture the transition from shallow to deep convection improves the simulation of diurnal timing of rainfall and reduces the dry biases in the wet season, but the dry bias in the dry season has been rather insensitive to numerous changes in parameterizations used in climate models (Zhang et al. 2017). Co-located measurements of processes from the subsurface to the top-of-the-atmosphere are needed to quantify the roles of multiple inter-related processes and diagnose and address model biases. Boundary layer measurements are particularly important to pin down the role of surface fluxes in shallow and deep convection.

## 3. LOW BIAS IN STRATOCUMULUS CLOUDS

ES3M also exhibits significant low bias in stratocumulus (SC) along the coast of western North and South America, leading to a shortwave cloud forcing bias of 40 $W/m^2$. A doubling of the vertical resolution from v0 to v1 was suspected to be a reason for the increased low bias in SC, but numerical experiments to systematically isolate the changes from v0 to v1 eliminated the higher vertical resolution as the culprit (Shaocheng Xie and Wuyin Lin, personal communication). Sensitivity experiments with E3SM suggest significant impacts of several parameters in the CLUBB parameterization for boundary layer clouds on simulations of SC in the model. Most importantly, parameters that enhance turbulence and reduce the skewness of vertical velocity can significantly increase the areal extent of coastal SC and improve the transition from SC in the subtropical region towards trade cumulus in the tropical region in the eastern Pacific Ocean. Improving coastal SC through parameter tuning of CLUBB also has significant positive effect in reducing the liquid water path biases at high latitudes. While these outcomes obviously improve model skill, observations and large-eddy simulations (LES) should be used to understand the behavior of CLUBB to support the parameter changes in reflecting processes operating in SC.

Model bias in boundary layer processes and their interactions with clouds can have significant implications to model simulations of regional precipitation, cloud feedback and aerosol indirect forcing, top-of-atmosphere energy balance, and climate sensitivity. Two key challenges are how to develop confidence in the boundary layer processes represented in the models and to isolate biases from multiple processes that are strongly coupled (e.g., boundary layer processes with clouds, convection, and surface processes). As model resolution continues to increase both horizontally and vertically, the challenge in constraining parameterizations of boundary layer and its interactions with clouds and convection does not go away as these processes will not be explicitly resolved even for models capable of utilizing exascale computers in the coming years. Unifying turbulence parameterizations for different regimes and cloud types is likely important for a smooth transition from current models to global cloud resolving models in the future. Both observations and LES simulations are useful for continued development of boundary layer parameterizations, with a stronger focus on unifying representations of strongly interactive

processes (turbulence, cloud microphysics, shallow and deep convection) and developing long term observations of the interactive processes in regions with common biases in climate and Earth system models. Metrics of boundary layer processes should be adopted in addition to top-down metrics for evaluation of climate models and diagnosis of model biases. Innovative use of observations and LES modeling in combination through short-term forecasting experiments, model-data fusion, machine learning and uncertainty quantification should be explored along with development of new measurement techniques and strategies.

## REFERENCES

Golaz, J.-C., V. E. Larson, and W. R. Cotton. 2002. A PDF-based model for boundary layer clouds. Part I: Method and model description. *Journal of the Atmospheric Sciences* 59(24), 3540–3551.

Harrop, B. E., P.-L. Ma, P. J. Rasch, R. B. Neale, and C. Hannay. 2017. The role of convective gustiness in reducing seasonal precipitation biases in the tropical west Pacific. *Journal of Climate* (in review).

Redelsperger, J. L., F. Guichard, and S. Mondon. 2000. A parameterization of mesoscale enhancement of surface fluxes for large-scale models. *Journal of Climate* 13: 402–421, doi:10.1175/1520-0442(2000)013<0402:APOMEO>2.0.CO;2.

Sakaguchi, K., L. R. Leung, C. D. Burleyson, H. Xiao, and H. Wan. 2017. Role of troposphere-convection-land coupling in the southwestern Amazon precipitation bias of the Community Earth System Model version 1 (CESM1). *Journal of Geophysical Research* (in review).

Zhang, K., R. Fu, M.J. Shaikh, S. Ghan, M. Wang, L.R. Leung, J. Marengo, and R.E. Dickinson. 2017. Influence of super-parameterization and a higher-order turbulence closure on rainfall bias over Amazonia in Community Atmosphere Model Version 5 (CAM5). *Journal of Geophysical Research* 122, 9879-9902. doi: 10.1002/2017JD026576.

# The Enigmatic Arctic Boundary Layer: A Key Modulator of Multi-scale Variability and Change

Ola Persson
Senior Research Scientist, CIRES/UColo and NOAA/ESRL/PSD

The atmospheric boundary layer modulates the exchange of heat, moisture, momentum, aerosols and other constituents between the surface and the free troposphere, and hence has a significant impact on weather and climate. Because forcings in the Arctic differ significantly from lower latitudes and because the remoteness and harsh environment hamper direct observations, the structure of and processes within the Arctic atmospheric boundary layer (AABL) are poorly understood in comparison with those in other parts of the globe. Unfortunately, they are arguably perhaps even more important for modulating weather and climate variability and change on a variety of space and time scales. This presentation will summarize what is known about the structure of and processes within the AABL and how they are forced, briefly discuss the observations that have provided this current understanding, and highlight key gaps in both understanding and observational capabilities, including examples of significant model errors. The discussion will include examples of how the AABL impacts Arctic weather and climate.

## 1. STRUCTURE, PROCESSES, AND VARIABILITY OF THE AABL

The Arctic (areas north of 68· N) consists of maritime areas, approximately comparable in extent to the contiguous United States, and surrounding land areas. With the exceptions of the Nordic seas, the maritime areas (Arctic Ocean) are entirely covered by sea ice during ~8 months of the year, while the land areas include northern portions of forested regions, bare tundra, flat terrain and significant orography, glaciers and large ice caps (including Greenland), and a very extensive coastline. Not only does the extent and thickness of the sea ice vary greatly during the annual cycle, but there is also a significant temporal and spatial variability to the snow cover over all surfaces. The snow distribution and depth over sea ice is especially poorly known. Retreat of the sea ice extent near the end of the summer melt season over the last 30 years has also produced significant areas of open water allowing for increased wave activity (e.g., Thomson et al 2016).

The overall northerly latitude, characteristics, and processes associated with all of these surface types impact the structure and variability of the AABL. The northerly latitude means that surface buoyancy from solar radiation is limited throughout the year and entirely absent during part of the year, producing a tendency for surface cooling and low-level stability. It also means that the lower free troposphere just above the AABL often is affected by thermal and moisture advection from lower latitudes. The combination of effects from local surface processes and the larger-scale latitudinal effects produces a unique structure to the AABL.

The AABL's role as a resistant buffer between sea ice and the bulk of the atmosphere is facilitated by the presence of a general Arctic inversion (AI), whose top is typically between 500 and 1500 m above the surface and marks the base of the unaffected free troposphere (Fig. 1). The

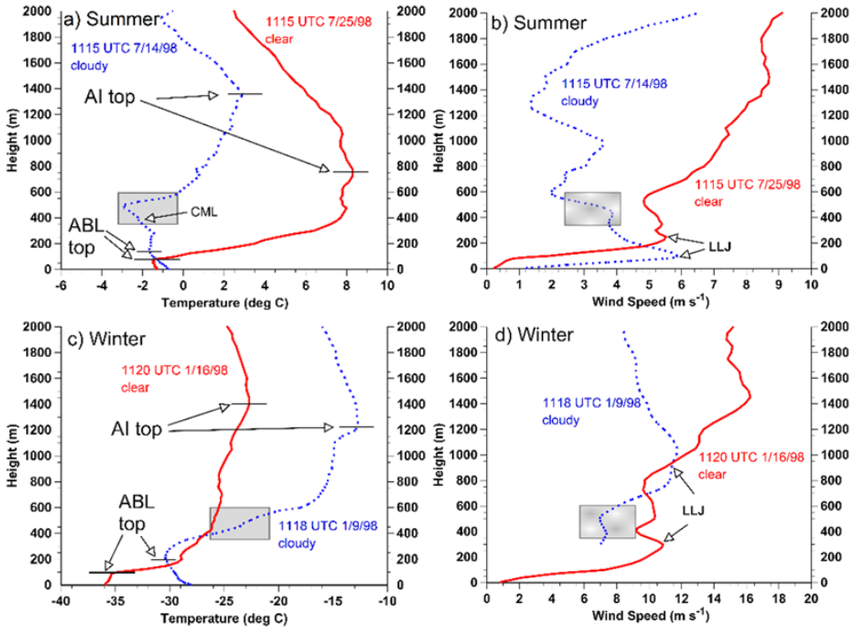


FIGURE 1. Sample temperature and wind profiles in the lowest 2 km at the SHEBA site for a), b) summer and c), d) winter for clear (solid) and cloudy (dotted) conditions. The shaded grey region represents the observed clouds for the respective soundings. The Arctic inversion tops (AI), the atmospheric boundary layer tops (ABL), the cloud mixed layer (CML), and the low-level jets (LLJ) are given for each profile. (Persson and Vihma, 2017).

base, depth, and magnitude of the AI has significant variability on synoptic to annual time scales and on regional spatial scales (e.g., Kahl et al., 1992, 1996; Tjernström and Graversen 2009). Surface cooling is likely the dominant mechanism for maintaining the AI during winter and warmair advection is likely dominant in summer (e.g., Persson et al 2002; Tjernström et al 2015), when the surface temperature is fixed at the sea-ice melting point. However, numerous warm-air advection events have been documented in winter as well, and produce significant impacts on the lower troposphere and the sea-ice (e.g., Persson et al 2016) as well as reinforce the AI. However, the mechanisms involved in forming and maintaining the AI aren't fully understood.

Significant structural variability occurs within this larger-scale AI due to surface mixing, clouds, and other features and processes between the surface and the AI (e.g., low-level jets), and these processes may be involved in forming the AI. If clouds are sufficiently dense, mixing due to cloud-top radiative cooling produces cloud mixed layers (CML) that can extend below cloud base and intermittently couple with the local surface-forced mixed layer (called ABL in Fig. 1) (Shupe et al., 2013; Sotiropoulu, et al., 2014; Brooks et al., 2017). The CML and ABL in Fig. 1a are not coupled, as a shallow isothermal (stable) layer of ~150 m depth exists between the two. While this coupling process is not yet well understood (e.g., the modulation mechanism is unknown), aerosols and potentially heat, moisture and momentum may be transported from cloud top to near the surface when such coupling occurs. Through long-wave radiation, clouds also tend to produce the surface-based mixed layers, even during the Polar Night (Persson et al., 2002). Hence, clouds within the AI and their associated processes are clearly a major component of the AABL and AI. Most studies on Arctic clouds have focused on these low-level stratocumulus clouds.

Note, however, that cloud top is generally below the AI top, so mixing by clouds does not provide a complete conduit for turbulent transport from the free troposphere to the surface. We know very little about turbulent mixing processes between cloud top and the top of the AI and,

above the local ABL under clear-sky conditions. We can speculate that mixing may occur from shear produced by frequently observed low-level jets (LLJs) (e.g., Tjernström et al 2004; Jakobsen et al 2013). The role of the AABL as an inhibitor to vertical mixing between the surface and the free troposphere hinges on understanding these intermittent mixing processes.

The structure of the local ABL at the base of the AI is influenced by the local surface type and roughness through classical mechanical and buoyant forcing. The latter primarily occurs through shortwave and longwave radiative fluxes, which are the primary forcing on the surface energy budget over sea ice, while the turbulent sensible and latent heat fluxes, as well as the conductive flux, tend to respond to the radiative forcing through changes in the surface temperature during the non-melt season (e.g., Persson 2012; Persson et al. 2016; Miller et al. 2017). Wintertime surface heating by longwave radiation and springtime surface daytime solar heating over sea ice can produce well-mixed ABLs reaching to 50-250 m, especially when combined with significant mechanical mixing by strong winds (Persson, et al 2002; Tjernström et al 2005). Solar radiation during the summer melt season (June-July-Aug) does not affect the ABL stability and structure because it can't warm the ice surface temperature above the melting point. Hence, all the summer excess surface energy flux, including solar, is used for melting sea-ice rather than warming the surface (Persson 2012). Mechanical mixing alone may produce ABLs between a few tens of meters to over 200 m deep. Fig. 2b shows the annual surface energy budget over sea ice during the Surface Heat Budget of the Arctic Ocean (SHEBA) experiment, a one-year deployment following a multi-year ice floe in the Beaufort/Chukchi Seas. The $SW_{net}$ is significant during the summer but is strongly damped by the high surface albedo from what it could be over less reflective surfaces. Long-wave cooling occurs throughout the year, and turbulent heat fluxes are relatively small. The atmosphere weakly warms the surface through turbulent sensible heat flux (negative $H_s$) during winter, a response to the surface longwave cooling. Mechanical mixing of the local surface ABL dominates through most of the year, except during daytime in spring, as suggested by Figs. 1a and c. Time series of daily mean surface energy budget terms (Persson 2012) show significant variability (10-80 W $m^{-2}$) on the 3-5 day time scale in all terms, suggesting significant forcing and responses from processes related to synoptic variability, especially clouds.

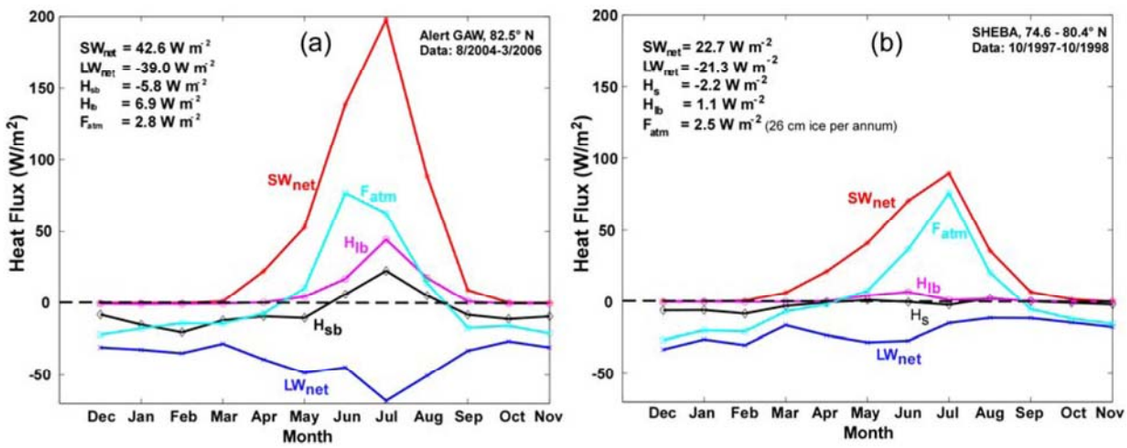


FIGURE 2. Annual cycle of the various terms of the SEB at a) Alert GAW and b) SHEBA. The annual mean values of the terms are shown in the upper left of each panel.

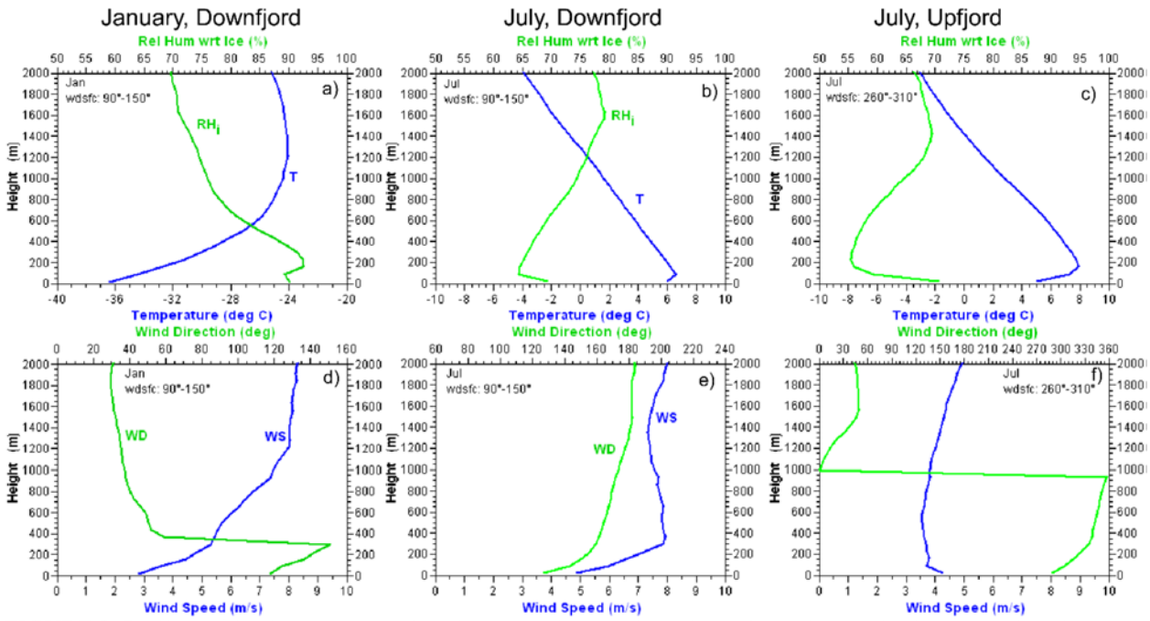


FIGURE 3. Profiles of (top) temperature (blue) and relative humidity (green) and (bottom) wind speed (blue) and wind direction (green) for downfjord surface flow in January, downfjord surface flow in July, and upfjord surface flow in July at Eureka, Ellesmere Island. Twice daily sounding data from January 1998 through December 2004 were used.

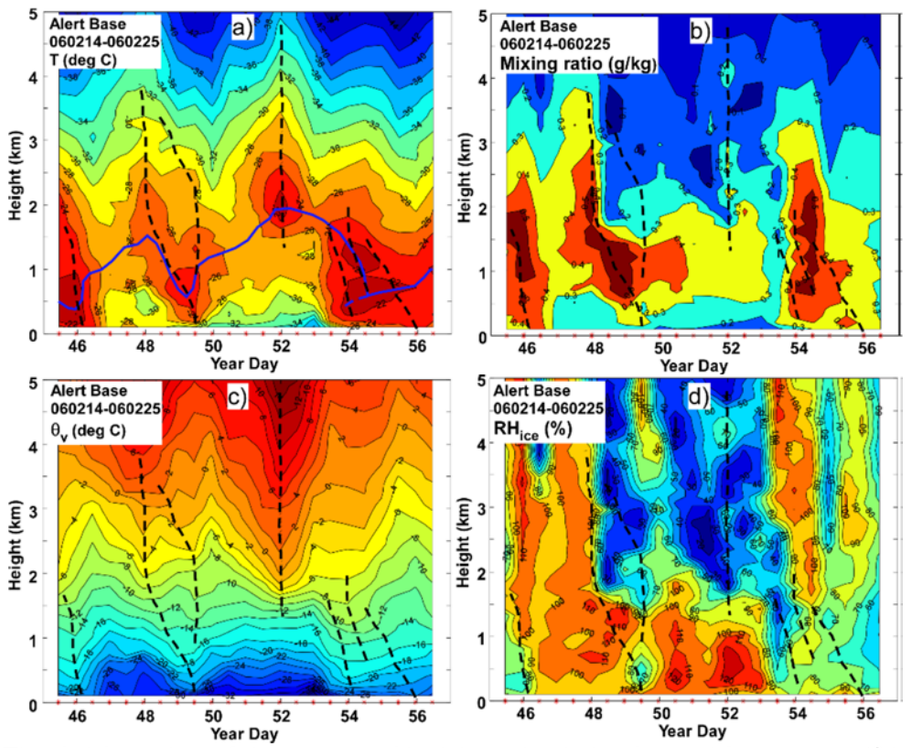


FIGURE 4. Time-height sections of a) temperature, b) mixing ratio, c) virtual potential temperature ($\theta_v$), and d) relative humidity with respect to ice from serial rawinsonde ascents at Alert CFS during Feb. 14-25, 2006 (YD 45-56). The erratic blue line in a) marks the top of the Arctic inversion, while the dashed lines in all panels mark locations of "trough lines" (warm axes) in the $\theta_v$ field. The red stars on the abscissa show the times of the rawinsonde launches.

A well-defined AI is also found over Arctic terrestrial sites during non-summer months, (e.g., Fig. 3a), with variability below AI top due to clouds and mesoscale processes, including orographic processes. However, during the summer after the snow has melted and surface temperatures can continue to warm, an AI is often no longer present or very weak. Instead, a well-mixed atmospheric boundary layer is often present (Fig. 3b,c) with some variability due to local mixed atmospheric boundary layer is often present (Fig. 3b,c) with some variability due to local topographic or surface effects. The Eureka rawinsonde site in Fig. 3 is located on the shore of a WNW-ESE oriented fjord on the interior of Ellesmere Island, near the southern end of a broad NS oriented valley. The effects of the fjord can be seen at the lowest levels in the temperature, humidity, and wind profiles. At Alert on the north side of Ellesmere Island, downslope wind events (mountain waves) from an upwind mountain range allow descent of warm air near the AI top down towards the surface (Fig. 4). Hence, topographic effects can strongly modulate the vertical structure of the AI, and regional surface heating over summer land can eliminate it. Figure 2a provides evidence for the latter, since the sensible and latent heat fluxes at Alert become positive (upward heat flux, cooling of the surface) in summer in response to the strong net shortwave radiation resluting from the small surface albedo after the snow has melted. Warm surface summer temperatures (~ 15° C or higher) also lead to enhanced outgoing longwave radiation and a stronger net longwave energy loss than over sea ice. Wintertime surface energy budget terms are similar over sea ice and land, except that the frequent downslope wind events at Alert produce stronger downward sensible heat fluxes and surface warming. The annual modulation of the diurnal cycle over high-latitude terrestrial surfaces leads to long-lived stable boundary layers during winter and long-lived turbulent boundary layers during summer (Grachev et al., 2017), which generally don't occur in other parts of the globe.

Sharp transitions between surface types that provide sharp gradients in energy fluxes also produce transitions in ABL structure and surface temperature. Important examples of this in the Arctic are along the summer coastlines and the non-summer ice edge. The difference in surface energy fluxes across an ice edge, even for thin ice, is substantial, leading to significant gradients in the ABL height (Fig. 5). Over thin, new sea ice (< 40 cm thick) with the reduced but still significant heat flux from the warm ocean below, significant but reduced upward turbulent heat flux produces a well-mixed ABL layer to ~100-400 m height (Fig. 5b). Over the nearby open water with much greater upward turbulent heat flux, the well-mixed ABL reaches 900-1200 m. Furthermore, clouds tend to be more prevalent near the low-level baroclinic zone at the ice edge and over the nearby open water rather than over the ice (not shown). These low-level, ice-edge, baroclinic zones can produce low-level jets that potentially feed back on surface conditions near the ice edge and the ice evolution, including winds, ice movement, and ocean upwelling/downwelling (e.g., Guest et al., 2017).

## 2. Past, current and future direct observations of the AABL

The above results are primarily dependent on a few Arctic research campaigns over limited time periods, especially over the sea ice. Only one campaign (SHEBA, conducted over multi-year sea ice from Oct 1997 to Oct 1998) obtained year-round measurements of the AABL using a 18- m tower, twice daily rawinsondes, surface-based remote sensing of clouds, and thorough characterization of the structure and evolution of the ice surface. Unfortunately, SHEBA had fairly poor measurements of the ABL structure, especially its turbulent structure, above the surface layer (though at times the top of the surface layer was below the top of the tower), and its evolution other than for clouds. Other campaigns (e.g., AOE-2001, Tjernström et

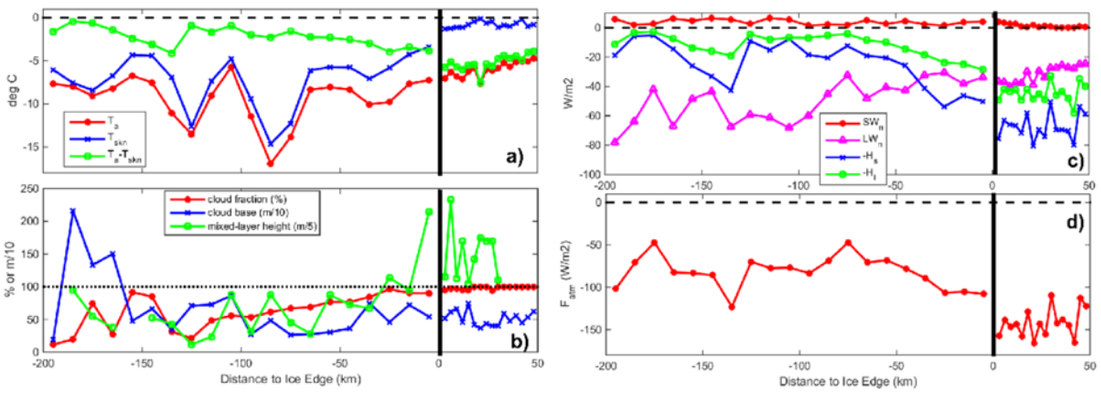


FIGURE 5. Mean values of various parameters from Sea State ship measurements as a function of distance from the nearest ice edge, marked by the heavy vertical black bar. Shown are a) 16-m air ($T_a$) and skin ($T_{skn}$) temperature, and their difference; b) cloud fraction, cloud base, and mixed-layer height from ceilometer and radiosondes; c) surface energy budget terms; and d) net atmospheric heat flux (negative is from the surface to the atmosphere) (Persson et al, 2017).

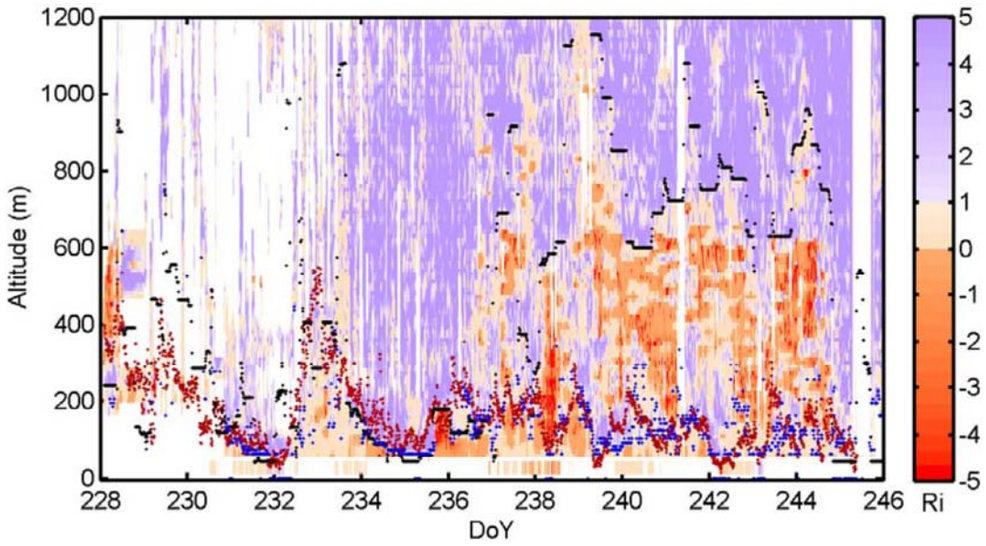


FIGURE 6. Time-height cross section of Richardson number derived from a suite of remote sensors and frequent radiosondes during ASCOS in 2008. Data below 35m derive from the mast profiles. Also included are the SML depth from the analytical formula $H_{CN} = 1.36\ u_* (fN)^{-1/2}$ (red dots), SML depths from an analysis of Ri ($H_{Ri}$ blue dots), and observed top of upper-most mixed layer ($z_i$, black dots). The colour scale is broken at Ri = 0 and Ri = 1 to make distinct the regimes of turbulent convection, stratified non-turbulent flow, and stable but turbulent (or potentially turbulent) flow (from Brooks et al 2017).

al 2004; ASCOS in 2008, Tjernström et al 2012; and ACSE in 2014 (Tjernström et al 2015) had more frequent soundings and more extensive remote sensing of the AABL, but for limited time periods and typically during late summer. The extensive suite of remote sensors deployed for 3 weeks during ASCOS was sufficiently complete to derive a 18-day time-height series of the bulk Richardson number in the lowest 1200 m with nominally 10-minute temporal resolution and 10-m vertical resolution (Fig. 6; Brooks et al., 2017). Examination of the CML and local ABL coupling was possible with this data set, though spatial observations were inadequate to define the processes modulating the coupling. The Sea State campaign in 2015 (Thomson et al., 2015)

had frequent radiosoundings and very good surface-layer measurements in the evolving AABL during autumn freezeup in October until early November, a very undersampled environment, but remote sensing of the AABL thermal and kinematic structure and associated clouds was mostly missing.

An international network of terrestrial sites include measurements of the structure of the AABL, and especially the local ABL. The sites are primarily coastal, and in areas of both flat tundra and significant orography (e.g., Uttal et al 2016). Observational capabilities have recently been added to many sites, and new analyses and understanding are likely to result.

## 4. MODEL DEFICIENCIES

The unique structure and processes of the AABL, lead to modeling deficiencies that have significant impacts. Using observations from the above field campaigns and terrestrial sites, a number of studies have highlighted problems in both regional and global climate models, and in reanalyses, for reproducing observed downwelling radiation (e.g., Tjernström et al 2008; deBoer et al., 2012, 2014; Karlsson and Svensson 2013; Pithan et al 2014). Mean errors and intermodel discrepancies are particularly large for cloudy skies (Fig. 7). It is believed that the model errors result from the inability of the models to accurately reproduce the supercooled mixed-phase clouds that occur during the Arctic winter, leading to too little downwelling longwave radiation. The errors in representing the cloud macro and microphysical structure is combined with additional errors in representing the surface turbulent and conductive heat fluxes, resulting in significant errors in several surface energy budget terms, all of which can impact key validation parameters, such as surface temperature. Process validation techniques are currently being used to better understand the error sources and how the errors interact to produce the errors in the near-surface characteristics. Figure 8 shows that the ERA-40 reanalysis (black dots) is incapable of producing the bimodal clustering of net surface longwave radiation fluxes and the responding turbulent sensible heat fluxes that are observed at the SHEBA site (red +) during the polar night. The observed clusters near -0 W $m^{-2}$ and -42 W $m^{-2}$ are due to the occurrence of super-cooled low-level startocumulus clouds or not, respectively, with the observed turbulent sensible heat fluxes responding to counteract the longwave surface forcing. However, ERA-90 does not produce a cluster near $LW_{net}$ = 0 W $m^{-2}$ because of being unable to maintain the supercooled liquid in the clouds, while the ERA-90 cluster near -55 W $m^{-2}$ is at a lower flux value because the clear-sky incoming LW radiation is slightly too small while the outgoing LW radiation is too large. The latter results from the representation of a fixed-thickness ice slab with no snow cover, resulting in a too strong conductive heat flux from the ocean. Hence, multiple errors impact the surface temperature with different signs. These and other process-relationship diagnostics (e.g., Persson 2012; Sterk et al 2013; Pithan et al 2014; Miller et al., 2017a,b) illustrate the complexity of the model error propagation for the interconnected AABL processes, and are crucial for understanding the error sources.

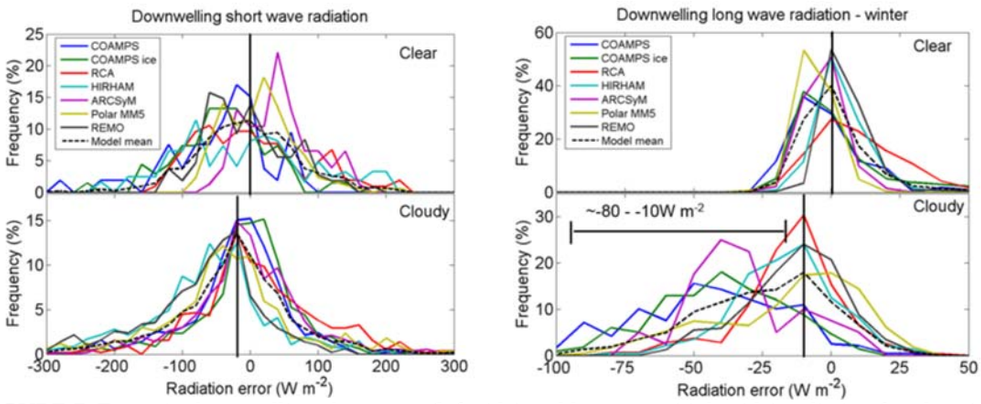


FIGURE 7. Errors in downwelling shortwave (left side) and longwave (right side) radiation for clear (top row) and cloudy (bottom row) conditions from a number of regional climate models. SHEBA data is used for validation (from Tjernström et al 2008).

FIGURE PERMISSION PENDING

FIGURE 8. Scatterplot of the turbulent sensible heat flux as a function of the net longwave radiation during the polar night at SHEBA (Nov 7, 1997 - Feb 8, 1998) from the in-situ observations (red "+") and ERA-40 reanalysis (black ".") Only coincident 6-h values are used from each source. The blue ovals show the observed clusters near -42 W $m^{-2}$ and 0 W $m^{-2}$ (from Persson et al 2008).

## 5. KEY GAPS IN OBSERVATIONS AND UNDERSTANDING OF AABL

The key gaps for understanding the structure and main processes important for modeling the evolution of the Arctic boundary layer and understanding its impacts on weather and climate include:

a) better understanding of the formation and evolution of the AI and how its stability structure is affected by clouds, LLJs, and other mixing events
b) formation of low-level clouds within the AI. Cloud maintenance once formed is reasonably well known, but the processes associated with the initial formation are only speculations at this point. Longwave radiation, aerosol concentrations and types, as well as atmospheric dynamics, likely play significant roles.
c) turbulent structure/mixing processes throughout AI, especially during clear skies and in regions above clouds. This would include formation and evolution of LLJs, and their roles in producing turbulent mixing, and roles of non-MOST mixing processes, such as low-frequency gravity waves. The temporal and spatial variability of these mixing processes will greatly help the understanding the efficacy of the stable AABL for inhibiting interactions between the surface and the free troposphere in the Arctic.
d) quantification and parameterization of the relative roles of MOST and non-MOST mixing processes in the stable local ABL

e) impacts of synoptic storms on the AABL
f) quantify impacts of ABL processes, including low-level baroclinic zones, on evolution of Arctic storms. There are some examples of possible of Petterssen type B cyclone developments in the Arctic (e.g., Inoue and Hori 2011), where ABL diabatic processes in the presence of a low-level baroclinic zone produce low-level circulations that phase with upper-tropospheric disturbances (e.g., a PV anomaly) and strengthen.
g) improve understanding and parameterizations of surface fluxes in Arctic-specific heterogeneous surface environments, such as evolving sea-ice, open ocean, and waves. This needs to occur for both stable and unstable atmospheric surface layers.

Key observations for overcoming some of these gaps are exemplified in the planned observations for the upcoming Multidisciplinary drifting Observatory for the Study of Arctic Climate (MOSAiC) campaign (Shupe et al., 2015; http://www.mosaicobservatory.org/index.html). This campaign should again provide year-round measurements over the now thinner sea ice in the Central Arctic, and should provide much more extensive measurements of the entire AI through the use of a large suite of surface based remote sensors. All measurements made during SHEBA will again be made, including an instrumented ~20 m (possibly 30 m) tower on the ice Thermodynamic and kinematic profiles within the AI will be characterized with Doppler lidars, Doppler sodars, microwave profilers, and cloud and precipitation radars. Some turbulence measurements will also be available from these systems and through occasional tethersonde deployments. Scanning lidars and radars will provide some observations of horizontal structure in the AI to complement the extensive profiles to be collected. Unmanned aerial vehicles have also been proposed to provide spatial (vertical and horizontal) thermodynamic and possibly turbulence structure, though their presence is not yet certain. Some planned manned aircraft campaigns during spring and summer of the MOSAiC year will include low-level flights within the AI and lower, and will supplement the above year-round measurements. This suite of sensors should fill many of the gaps in previous measurements of the Arctic boundary layer structure and processes. The one exception may be the lack of a wind profiler for high temporal resolution wind and turbulence profiles within the entire AI and into the free troposphere. The wind profiler would be the only system for deducing the high temporal evolution of wind and turbulence structures within and above the clouds; wind and turbulence profiles from the lidars will only be available up to cloud base. Another key component of the planned MOSAiC deployment is to coordiante the air, ice, ocean, and biological observations to provide data on the various interdisciplinary processes that are highly coupled to the AABL processes. Observations such as these are necessary to address the key gaps in understanding outlined above.

## REFERENCES

Brooks, I. M., M. Tjernström, P. O. G. Persson, M. D. Shupe, R. A. Atkinson, G. Canut, C. E. Birch, T. Mauritsen, J. Sedlar, and B. J. Brooks, 2017: The turbulent structure of the Arctic summer boundary layer during ASCOS. *J. Geophys. Res. - Atmos.*, 122. https://doi.org/10.1002/2017JD027234.

de Boer, G., W. Chapman, J. Kay, B. Mederos, M. Shupe, S. Vavrus, J. Walsh, 2012: Characterization of the present-day Arctic atmos in CCSM4. *J. Clim.*, **25**, 2676-2695.

de Boer, G., and Coauthors, 2014: Near-surface meteorology during ASCOS: Evaluation of reanalyses and global climate models. *Atmos. Chem. Phys.*, **14**, 427-445

Grachev, A. A., P. O. G. Persson, T. Uttal, E. A. Konopleva-Akish, C. J. Cox, S. M. Crepinsek, C. W. Fairall, R. S. Stone, G. Lesins, A. P. Makshtas, and I. A. Repina, 2017: Seasonal and latitudinal variations of surface fluxes at two Arctic terrestrial sites. *Clim. Dyn*., accepted.
Guest, P., P. O. G. Persson, S.Wang, M. Jordan, B. Blomquist, C. Fairall and D. Price, 2017: Low-level baroclinic jets over the New Arctic ocean. *J. Geophys. Res.-Oceans*, Sea State special issue, In preparation.
Inoue, J. and M. E. Hori, 2011: Arctic cyclogenesis at the marginal ice zone: A contributory mechanism for the temperature amplification? *Geophys. Res. Lett.*, **38**, L12502, doi:10.1029/2011GL047696
Jakobson, L., Vihma, T., Jakobson, E., Palo, T., Männik, A., & Jaagus, J. (2013) Low-level jet characteristics over the Arctic Ocean in spring and summer. *Atmospheric Chemistry and Physics*, **13**, 11089-11099, doi:10.5194/acp-13-11089-2013.
Kahl JD, Serreze MC, Schnell RC. 1992. Tropospheric low-level temperature inversions in the Canadian Arctic. *Atmos.–Ocean* **30**: 511–529.
Kahl JDW, Martinez DA, Zaitseva NA. 1996. Long-term variability in the low-level inversion layer over the Arctic Ocean. *Int. J. Climatol.* **16**: 1297–1313.
Karlsson, J., and G. Svensson, 2013: Consequences of poor representation of Arctic sea-ice albedo and cloud-radiation interactions in the CMIP5 model ensemble. *Geophys. Res. Lett.*, **40**, 4374- 4379.
Miller, N. B., M. D. Shupe, C. J. Cox, , D. Noone, P. O. G. Persson, and K. Steffen, 2017a. Surface energy budget responses to radiative forcing at Summit, Greenland, *The Cryosphere*, **11**, 497-516, doi:10.5194/tc-11-497-2017.
Miller, N.B. and Coauthors, 2017b: Process-based evaluation of ERA-Interim, CFSv2, and CESM in central Greenland. *J. Geophys. Res*., in review.
Persson, P. O. G., 2012: Onset and end of the summer melt season over sea ice: Thermal structure and surface energy perspective from SHEBA. *Clim. Dynamics*, **39**, 1349-1371, DOI: 10.1007/s00382-011-1196-9.
Persson, P. Ola G., C. W. Fairall, E. L. Andreas, P. S. Guest, and D. K. Perovich, 2002: Measurements near the Atmospheric Surface Flux Group tower at SHEBA: Near-surface conditions and surface energy budget. *J. Geophys. Res.* **107**(C10), 8045, doi:10.1029/2000JC000705.
Persson, P. O. G., M. Shupe, D. Perovich, and A. Solomon, 2016: Linking atmospheric synoptic transport, cloud phase, surface energy fluxes, and sea-ice growth: Observations of midwinter SHEBA conditions. *Clim. Dyn*., DOI: 10.1007/s00382-016-3383-1.
Persson, P.O.G., and T. Vihma, 2017: The Atmosphere Over Sea Ice. Chapter 6 in Sea Ice, 3rd Edition. Edited by David N. Thomas, Wiley-Blackwell, London. 652 pp., 160-196 ISBN: 9781118778388
Persson, P. O. G., B. Blomquist, P. Guest, I. Brooks, S. Stammerjohn, G. Björk, M. Tjernström, J. Sedlar, G. Sotiropoulu, M. Shupe, and C. Fairall, 2017: Ice begets ice: Observations of the Arctic Ocean autumn freezeup process. *J. Geophys. Res.-Oceans*, Sea State special issue, In preparation.
Persson, P. O. G., J.-W. Bao, M. Shupe, C. Wheeler, A. A. Grachev, and C. W. Fairall, 2009: Process relationships useful for evaluating model performance in the Arctic. Presentation 14.4, *10th Polar Meteorology and Oceanography Conference*, Madison, WI, May 18-21.

Pithan, F., B. Medeiros, T. Mauritsen, 2014: Mixed-phase clouds cause climate model biases in Arctic wintertime temperature inversions. *Clim. Dyn*., **43**, 289-303.
Shupe, M. D., P. O. G. Persson, I. M. Brooks, M. Tjernström, J. Sedlar, T. Mauritsen, S. Sjögren, and C. Leck, 2013: Cloud and boundary layer interactions over the Arctic sea-ice in late summer. *Atmos. Chem. Phys.*, **13**, 9379-9399.
Shupe, M, D. Barber, K. Dethloff, S. Gerland, J. Inoue, C. Lee, B. Loose, A. Makshtas, W. Maslowski, M. Nicolaus, D. Notz, I. Peeken, D. Perovich, O. Persson, J. Schmale, M. Tjernström, T. Vihma, and J.-P. Zhao, 2015: Multidisciplinary Drifting Observatory for the Study of Arctic Climate (MOSAiC): Science Plan and Experimental Design., July 2015, IASC Report.
Sotiropoulu, G., J. Sedlar, M. Tjernström, M.D. Shupe, I.M. Brooks, and P.O.G. Persson, 2014: The thermodynamic structure of summer Arctic stratocumulus and the dynamic coupling to the surface. *Atmos. Chem. Phys.*, **14**, 12573-12592, doi:10.5194/acp-14-12573-2014
Sterk, H., and Coauthors, 2016: Clear-sky stable boundary layers with low winds over snowcovered surfaces. Part II: Process sensitivity. *Q. J. Roy. Met. Soc*., **142**, 821-835.
Thomson, J., Y. Fan, S. Stammerjohn, J. Stopa, W. E. Rogers, F. Girard-Ardhuin, F. Ardhuin, H. Shen, W. Perrie, H. Shen, S. Ackley, A. Babanin, Q. Liu, P. Guest, T. Maksym, P. Wadhams, C. Fairall, O. Persson, M. Doble, H. Graber, B. Lund, V. Squire, J. Gemmrich, S. Lehner, B. Holt, M. Meylan, J. Brozena, J.-R. Bidlot, 2016: Emerging trends in the sea state of the Beaufort and Chukchi Seas. *J. Ocean Modelling*, **105**, 1-12, DOI: 10.1016/j.ocemod.2016.02.009.
Thomson, J., M. Doble, B. Lund, B. Blomquist, E. Rogers, J. Anderson, O. Persson, M. Smith, A. de Klerk, P. Guest, T. Maki, A. Kohout, R. Clancy, P. Wadhams, G. Williams, H. Shen, T. Maksym, S. Stammerjohn, S. Ackley, B. Holt, B. Weissling, B. McKiernan, R. Ziegenhals, 2015: ONR Sea State Cruise Report (SKQ201512S), 11 Nov 2015. Available at http://www.apl.washington.edu/project/project.php?id=arctic_sea_state
Tjernström, M. (2005) The summer Arctic boundary layer during the Arctic Ocean Experiment 2001 (AOE-2001). *Boundary-Layer Meteorology*, **117**, 5–36, DOI 10.1007/s10546-004- 5641-8
Tjernström, M., C. E. Birch, I. M. Brooks, M. D. Shupe, P. O. G. Persson, J. Sedlar, T. Mauritsen, C. Leck, J. Paatero, M. Szczodrak, and C. R. Wheeler, 2012: Meteorological conditions in the central Arctic summer during the Arctic Summer Cloud Ocean Study (ASCOS). *Atmos. Chem. Phys.*, **12**, 6863-6889, doi:10.5194/acp-12-1-2012.
Tjernström, M., and Graversen, R. G. (2009), The vertical structure of the lower arctic troposphere analysed from observations and the ERA-40 reanalysis. *Quarterly Journal of the Royal Meteorological Society*, **135**(639), 431-443. doi:http://dx.doi.org/10.1002/qj.380
Tjernström, M., Leck, C., Persson, P.O.G., Jensen, M.L., Oncley, S.P., & Targino, A (2004) The summertime Arctic atmosphere: Meteorological measurements during the Arctic Ocean Experiment 2001 (AOE-2001). *Bulletin of the American Meteorological Society*, **85**, 1305- 1321.
Tjernström, M., M. D. Shupe, I. M. Brooks, P. O. G. Persson, J. Prytherch, D. Sailsbury, J. Sedlar, P. Achtert, B. J. Brooks, P. E. Johnston, G. Sotiropoulou, D. Wolfe, 2015: Warm-air advection, air mass transformation and fog causes rapid ice melt, *Geophys. Res. Lett*., **42** (13), 5594-5602, doi:10.1002/2015GL064373.
Uttal, T., S. Starkweather, J. Drummond, T. Vihma, C. J. Cox, E. Dlugokencky, J. Ogren, B. McArthur, L. Schmeisser, V. Walden, T. Laurila, L. Darby, A. P. Makshtas, J. Intrieri, J. F. Burkhart,T. Haiden, B. Goodison, M. Maturilli, M. Shupe, G. de Boer, R. Stone, A. Saha, A. Grachev, L. Bruhwiler, O. Persson, G. Lesins, S. Crepinsek, C. Long, S. Sharma, A. Massling,

D. D. Turner, D. Stanitski, E. Asmi, M. Aurela, H. Skov, K. Eleftheriadis, A. Virkkula, A. Platt, E. Forland, J. Verlinde, I. Yoshihiroo, I. E. Nielsen, M. Bergin, L. Candlish, N. Zimov, S. Zimov, N. O'Neil, P. Fogal, R. Kivi, E. Konopleva, V. Kustov, B. Vasel, Y. Viisanen, V. Ivakhov, 2015: International Arctic Systems for Observing the Atmosphere (IASOA): An International Polar Year Legacy Consortium. *Bull. Amer. Meteor. Soc*., 6, 1033-1056, DOI: 10.1175/BAMS-D-14-00145.1.

# Interactions between biodiversity and the atmosphere – lessons from the Neotropics

Ana Carolina Carnaval
Department of Biology, City College of CUNY
With Jason Brown, Andrea Paz, Maria Strangas, Fabian Michelangeli, André Freitas, Cristina Miyaki, Miguel Rodrigues, Mike Hickerson, Ashfaq Khan, Kyle McDonald

Observation, modeling, and data assimilation all demonstrate that the distribution of biodiversity on Earth is intimately linked to atmospheric processes. Species vary in the way they relate to the environment (a process largely defined by their evolutionary history, and strongly shaped by natural selection), yet their ability to survive, to disperse, and to reproduce are largely dictated by the availability of energy, water, water-energy dynamics, productivity, environmental stress, environmental suitability, stability, and heterogeneity. These constraints, or relationships, are in turn reflected in patterns of distribution of biodiversity on the planet. The biosphere is organized in a way that responds to atmospheric processes – and in turn provides input to the Earth's atmosphere through respiration, photosynthesis (in the case of plants), and the organization and decomposition of biomass. Because some of these processes are essential to other living systems, they are often referred to as the ecosystem services of biodiversity.

In this talk, I discuss how the integration of novel tools in the fields of ecology, evolution, and environmental sciences is key to advance our understanding of these interactions between the biosphere and the atmosphere, at multiple spatial and temporal scales. For that, I use the Atlantic Forest as a study system and buildi on data, models and new products developed in association with a Dimensions of Biodiversity program jointly funded by NASA and the National Science Foundation. I divide the talk into three major parts. First, I focus on studies of the present-day spatial patterns of biodiversity in this region, discussing i) what they tell us about the relationships between the Earth's biota and the Earth's environment, and ii) the challenges and gaps that the scientific community must address to further advance the field. In a nutshell, these studies provide support for strong correlations between environmental conditions (largely precipitation and temperature patterns) and the accumulation of species diversity in space. Whether one is interested in species richness (that is, the number of species in a given area), in the diversity of evolutionary lineages, and, often times, in the diversity of ecological functions provided by biodiversity, it is now clear that they can be successfully predicted based on the amount and distribution of energy and water. There is, however, ample room for improvement in this realm of biodiversity prediction. I will argue that novel frontiers in remote sensing can significantly advance the way we describe and model biosphere/atmosphere interactions in this system and others globally by allowing i) for more efficient ways to remotely quantify and monitor biodiversity and ii) for more accuracy and complexity in the way we describe shifts in temperature and humidity in natural systems.

In the second part of my talk, I move from insights from pattern-based studies to process-based studies of biodiversity and its interaction with the atmosphere. By processes, here, I discuss the historical changes witnessed by biodiversity, throughout the evolution of biotas and biomes. History matters when it comes to explaining the distribution of narrowly restricted components of the biosphere – or endemic species. It also explains much of the way in which

genetic diversity is distributed across geography within species. In this part of the talk, I present how genetic information can be combined with knowledge about the distribution of biodiversity and environmental descriptors (both currently and in the past) to improve our ability to understand the distribution of diversity on Earth – both at the species and the lineage level. Novel methods to infer the historical demography of natural populations, when coupled with information about past environmental changes, provide a promising new way to predict the future interactions between the biosphere and atmosphere.

In the third and last portion of the talk, I move from the historical processes to the ecological mechanisms that define species responses to environmental shifts. Using data from physiological experiments with endemic species in the Atlantic Forest, I discuss the extent to which species-specific tolerances to temperature extremes explain their distribution. I end with a discussion of additional knowledge gaps and challenges that we face, particularly in respect to the mechanisms that drive biosphere/atmosphere interactions. These include 1) the need to improve our ability to describe microenvironments occupied by species on the ground, and 2) the grand challenge of efficiently monitoring and documenting species interactions.

# Boundary Layer Science Challenges in the Context of Wind Energy

William J. Shaw
Pacific Northwest National Laboratory

## OVERVIEW

Boundary layer science challenges are often framed by specific applications of boundary layer meteorology. A significant emerging application is wind energy, which now exceeds 5% of U.S. electrical power production and continues to grow rapidly. The U.S. Department of Energy (DOE 2015) has published plausible scenarios in which wind energy provides 20% of U.S. electrical power by 2030 and 35% by 2050. Boundary layer winds are the fuel for this energy source. Errors or uncertainty in wind forecasts raise the cost of energy in power markets. Uncertainty in the local wind speed climate raises the risk-based financing costs for wind plants, and uncertainties in the local shear and turbulence climate of the turbine-layer (~50–150 m above the ground) can result in fatigue failure from mechanical loads or unnecessary costs from over-engineered turbines.

Wind power plants are commonly located in complex terrain, which poses particularly stringent challenges to our ability to treat the boundary layer. In contrast to flat terrain, complex terrain:

- Through diurnal heating, channeling, and blockage, significantly modulates winds and enhances turbulence on spatial scales comparable to the ~10-km horizontal extents of industrial scale wind plants
- Creates cold pools, whose erosion creates large vertical wind shears and is difficult to forecast
- Creates gravity waves, which generate hard-to-predict intermittent turbulence in nocturnal stable boundary layers
- Creates wakes downstream of significant geographic features with strong variability on scales of 10 km
- Violates conventional scaling assumptions that focus on the role of vertical gradients
- Can require model resolution to adequately account for the terrain that extends from the mesoscale well into Wyngaard's (2004) "terra incognita" where subgrid-scale parameterizations that do not account for horizontal gradients are no longer adequate

Improving the representation of model physics at scales between the traditional mesoscale and scales of large-eddy simulation will require fundamental advances in subgrid-scale parameterization, particularly in the treatment of horizontal gradients. A path to progress will entail an integrated observational and modeling approach. LES models, for example, can provide detailed insights into processes dominating force and energy balances at varying resolutions in complex terrain, and those insights can be used to inform improved larger-scale parameterizations. Observations can confirm both that the LES results are realistic and that models using consequent parameterizations are actually improved.

The required resolution of simulations and the variability of observations across scales has historically represented a daunting challenge. High-resolution simulations over broad domains have required costly CPU cycles and massive data storage. Validation of such simulations in complex terrain really requires an effective way to measure fields of atmospheric variables. Happily, recent years have seen remarkable advances (and lower costs) for both high-performance computing and observational capabilities of remote sensing systems, and both observational and numerical resources promise to continue to improve.

## NEEDS FOR NEW OBSERVATIONS FOR MODEL VALIDATION

The synergistic use of atmospheric modeling and observations will be a primary path toward progress in understanding complex terrain boundary layers in the next decades. However, complex terrain poses particular challenges to model validation in at least two ways. First, local errors in inner model nests may reflect errors in larger-scale simulations that form the boundary conditions for these nests. Thus, observations to validate models in complex terrain need to include observations on scales large enough to evaluate errors associated with outer model domains, or at least, through assimilation, to constrain the outer domains. Second, because of the non-linear interactions of the atmosphere with arbitrary topography, horizontal gradients can be large and variable, and there really are not representative conditions in complex terrain. As a result, conventional in situ observations carried out over the short term have limited value in validating models in this environment.

The need for data for physical insights and model validation over multiple scales has been progressively addressed in the meteorological community since the 1970s. [The GARP Atlantic Tropical Experiment (GATE) being the archetype for multi-scale studies.] Most recently, in the wind energy context in complex terrain, the U.S. Department of Energy and NOAA have supported the second Wind Forecast Improvement Project (WFIP 2), which has used a nesting of observations from the mesoscale to the microscale in an effort to improve 100-m wind forecasts by improving the treatment of subgrid-scale physics in NWP models in complex terrain. The field component of the study, which is just completed, nested increasing densities of in situ and remote sensing instrumentation from an outer domain covering much of the states of Oregon and Washington through successively smaller scales to an inner site approximately 2 km on a side devoted to observing horizontal and vertical variability of in situ flux measurements. A significant feature of the study is that the field instrumentation, including scanning Doppler remote sensing systems, were designed to operate unattended for a full year. This was made possible by advances in communications and system controls. The resulting sampling of the spectrum of atmospheric conditions over a full annual cycle is expected to generate a more robust validation of model improvements. It also points the way toward possibilities for long-term deployments of sophisticated, integrated measurement systems that can provide validation data for increasingly detailed models.

## OBSERVATION SYSTEM DEVELOPMENT

In the last decade in particular, significant advances have been made in understanding how information from multiple measurement systems may be combined to gain significantly more information about the atmosphere that if the individual systems were operating independently. This is particularly the case for Doppler lidars and radars. While the dual Doppler concept has been implemented for many decades, it is relatively recently that control systems have been available to coordinate sampling in space and time, opening the prospect of routine sampling of atmospheric fields. Examples of this sort of sampling include the use of three lidars to calculate the stress tensor at arbitrary points in space to heights of 150 m (Mikkelsen, 2014). Another example is the concept of using multiple lidars to create multiple virtual towers for wind measurements [e.g., Calhoun et al. (2006), Newsom et al. (2015), Newman et al. (2016)]. More recently, the Experimental PBL Instrumentation Assessment (XPIA) was carried out in 2015 to explore the capabilities of lidars, radars, and microwave radiometers, used individually and in combination, to map the structure of the planetary boundary layer's winds, turbulence, and thermodynamic variables (Lundquist, et al., 2017). Using the 300-m Boulder Atmospheric Observatory (BAO) tower with multiple levels of sonic anemometers as a reference, this study was able to quantify the uncertainty associated with several approaches to mapping atmospheric fields, including dual-Doppler radar, moving point stares with multiple systems, virtual towers, and novel scanning patterns such as the "large checkerboard pattern" to map wind fields. Detailed results of this study have been published in a 2017 special issue of Atmospheric Measurement Techniques, with articles by [Bianco et al.; Choukulkar et al.; Debnath et al. (a,b); McCaffrey et al. (a,b,c); and Newsom et al.]. Studies such as XPIA that can

establish uncertainties for observational techniques with developing instrument systems will be an essential component of model validation and, consequently, advances in complex terrain meteorology.

## REFERENCES

Bianco, L., K. Friedrich, J. M. Wilczak, D. Hazen, D. Wolfe, R. Delgado, S. P. Oncley, and J. K. Lundquist. 2017. Assessing the accuracy of microwave radiometers and radio acoustic sounding systems for wind energy applications. Atmospheric Measurement Techniques 10(5):1707-1721. DOI: 10.5194/amt-10-1707-2017.

Calhoun, R., R. Heap, M. Princevac, R. Newsom, H. Fernando, and D. Ligon. 2006. Virtual towers using coherent Doppler lidar during the Joint Urban 2003 dispersion experiment. Journal of Applied Meteorology and Climatology 45(8):1116-1126. DOI: 10.1175/Jam2391.1.

Choukulkar, A., W. A. Brewer, S. P. Sandberg, A. Weickmann, T. A. Bonin, R. M. Hardesty, J. K. Lundquist, R. Delgado, G. V. Iungo, R. Ashton, M. Debnath, L. Bianco, J. M. Wilczak, S. Oncley, and D. Wolfe. 2017. Evaluation of single and multiple Doppler lidar techniques to measure complex flow during the XPIA field campaign. Atmospheric Measurement Techniques 10(1):247-264. DOI: 10.5194/amt-10-247-2017.

Debnath, M., G. V. Iungo, W. A. Brewer, A. Choukulkar, R. Delgado, S. Gunter, J. K. Lundquist, J. L. Schroeder, J. M. Wilczak, and D. Wolfe. 2017. Assessment of virtual towers performed with scanning wind lidars and Ka-band radars during the XPIA experiment. Atmospheric Measurement Techniques 10(1215-1227). DOI: 10.5194/amt-10-1215-2017.

Debnath, M., G. V. Iungo, R. Ashton, W. A. Brewer, A. Choukulkar, R. Delgado, J. K. Lundquist, W. J. Shaw, J. M. Wilczak, and D. Wolfe. 2017. Vertical profiles of the 3-D wind velocity retrieved from multiple wind lidars performing triple range-height-indicator scans. Atmospheric Measurement Techniques 10(431-444). DOI.

Lundquist, J. K., J. M. Wilczak, R. Ashton, L. Bianco, W. A. Brewer, A. Choukulkar, A. Clifton, M. Debnath, R. Delgado, K. Friedrich, S. Gunter, A. Hamidi, G. V. Iungo, A. Kaushik, B. Kosovic, P. Langan, A. Lass, E. Lavin, J. C. Y. Lee, K. L. McCaffrey, R. K. Newsom, D. C. Noone, S. P. Oncley, P. T. Quelet, S. P. Sandberg, J. L. Schroeder, W. J. Shaw, L. Sparling, C. St Martin, A. St Pe, E. Strobach, K. Tay, B. J. Vanderwrwende, A. Weickmann, D. Wolfe, and R. Worsnop. 2017. Assessing State-of-the-Art Capabilities for Probing the Atmospheric Boundary Layer the Xpia Field Campaign. Bulletin of the American Meteorological Society 98(2):289-314. DOI: 10.1175/Bams-D-15-00151.1.

McCaffrey, K., L. Bianco, and J. M. Wilczak. 2017. Improved observations of turbulence dissipation rates from wind profiling radars. Atmospheric Measurement Techniques 10(7):2595-2611. DOI: 10.5194/amt-10-2595-2017.

McCaffrey, K., L. Bianco, P. Johnston, and J. M. Wilczak. 2017. A comparison of vertical velocity variance measurements from wind profiling radars and sonic anemometers. Atmospheric Measurement Techniques 10(3):999-1015. DOI: 10.5194/amt-10-999-2017.

McCaffrey, K., P. T. Quelet, A. Choukulkar, J. M. Wilczak, D. E. Wolfe, S. P. Oncley, W. A. Brewer, M. Debnath, R. Ashton, G. V. Iungo, and J. K. Lundquist. 2017. Identification of tower-wake distortions using sonic anemometer and lidar measurements. Atmospheric Measurement Techniques 10(2):393-407. DOI: 10.5194/amt-10-393-2017.

Mikkelsen, T., 2014: Lidar-based Research and Innovation at DTU Wind Energy–A Review. Journal of Physics: Conference Series, 524, doi:10.1088/1742-6596/524/1/102007.

Newman, J. F., T. A. Bonin, P. M. Klein, S. Wharton, and R. K. Newsom. 2016. Testing and validation of multi-lidar scanning strategies for wind energy applications. Wind Energy 19(12):2239-2254. DOI: 10.1002/we.1978.

Newsom, R. K., L. K. Berg, W. J. Shaw, and M. L. Fischer. 2015. Turbine-scale wind field measurements using dual-Doppler lidar. Wind Energy 18(2):219-235. DOI: 10.1002/we.1691.

Newsom, R. K., W. A. Brewer, J. M. Wilczak, D. E. Wolfe, S. P. Oncley, and J. K. Lundquist. 2017. Validating precision estimates in horizontal wind measurements from a Doppler lidar. Atmospheric Measurement Techniques 10(3):1229-1240. DOI: 10.5194/amt-10-1229-2017.

# Complex Terrain Atmospheric Boundary Layer

H.J.S. Fernando
University of Notre Dame

More than 70% of the Earth's land surface and the majority of world's largest cities are in complex terrain, which affects weather in general as well as related 'quality of life' indicators such as air pollution, energy production, noise, transportation and security of cities. As a result, extensive work has been done on mountain meteorology, with particular focus on weather prediction and air quality in urban valleys. Nevertheless, meteorology in the proximity of mountains themselves, mountain clusters or very complex terrain with little human habitation has received only little consideration. High gradients and large heights of terrain are associated with a host of important phenomena, for example, gravity waves, wind gusts, canyon and gap flows, Venturi effects, flow stagnation, rotors, cold air pooling, up/down drafts, slope and valley flows, skewed shear, fog, snow/ice, convective clouds and lightning, which are highly variable and defy reliable forecasting. While traditional complex-terrain Atmospheric Boundary Layer (ABL) studies have foci on mesoscale phenomena (~ 1-100km), recent demands from the energy industry and increased focus on unmanned aerial vehicle operations in complex terrain, security applications (e.g., contaminant dispersion) and recreational and sporting industry (e.g., skiing, Olympics) have provided impetus for prediction of weather at microscale (<500 m).

FIGURE 1 Characteristics ABL processes in complex terrain, overlaid on a 3D topographic map of Mexico City as an example. Blue represents nocturnal processes and red the daytime phenomena associated with convection. Meso to microscale phenomena are shown. Their interactions may lead to entirely new phenomena and scales.

Complex terrain ABL is strikingly different from its flat terrain counterpart. The latter is essentially driven by synoptic pressure gradients, balanced by turbulent shear stresses governed by ABL stability. In complex terrain, however, there are two main types of flows: synoptic flow perturbed by terrain and thermally driven flows, as schematized in Figure 1. These two types of flow often interact and enhance thermodynamic complexity of ABL. Synoptically driven flows take the form of rising flow above or deflected around the mountains and flow channeling (speeding) through canyons and gaps. The nature of these flows depends on the stability of ABL, for example, lee and propagating internal waves over mountains and upstream blocking during stable periods and recirculation zones and synoptically modified convection during daytime. Thermally driven flows (thermal circulation) include up slope and up valley winds (daytime) and downslope and downvalley (nighttime) winds, with slope winds driven by buoyancy forces and valley winds by pressure gradients introduced by horizontal temperature gradients. Interesting flow transitions occur in the morning and afternoon when thermal circulation changes from one to another following diurnal cycle. Microscale circulations are driven by horizontal temperature gradients introduced by shadowing or land cover variation.

**Fundamental Process Studies:** Since the early 1950's, remarkable progress has been made on the theoretical understanding of stably stratified flow past topography, for example, on linear and nonlinear (trapped) lee waves, dividing streamline, upstream flow blocking, internal hydraulics and propagating low-frequency modes. Progress has also been made on up and down slope flows, morning and evening transition as well as orographic convection and precipitation. Theoretical work has been complemented by numerical and laboratory modeling of idealized geometries, providing impressive insights on atmospheric and ocean flows and impetus for numerous field studies. There are areas needing further attention, for example, flow through gaps and canyons, orographic drag, flow over multiple topographic features, interactions between slope/valley flow systems or synoptic flow and thermal circulation, hydraulic phenomena, and fog and ice formation in complex terrain.

**Field Campaigns:** A large number of field campaigns have been conducted since the mid-1950's, but since the early 2000's field campaigns have had enhanced scope and sophistication, prompted in part by novel high space-time resolution instrumentation; some examples are VTMX, T-REX, MAP, COLPLEX, TRANFLEX, BLLAST, MATERHORN and Perdigão campaigns. Much of the nocturnal phenomena in Figure 1 have been addressed in previous campaigns, yet some phenomena of consequence such as rapid synoptically driven downslope winds, hydraulic jumps at slope breaks, canyon and gap flows with and without synoptic effects, convective up slope/valley winds and flow separation await detailed field investigations. It has also been noted that field experiments have not focused on model relevant parameters such as the influence of soil parameters and energy budgets. New measurement technologies for rapid measurement of soil moisture and surface properties need to be encouraged, for example, RF polarization radars and instrumented UAVs with remote sensing capabilities.

**Numerical Modeling:** Mesoscale numerical models have made leaps of progress in predicting complex-terrain weather, nevertheless, many vexing problems remain. Some bottlenecks concern poor prediction of near-surface (e.g., 2m) temperature and winds, mainly attributed to the lack of understanding of surface properties and energy budgets, high sensitivity of (arid climate) temperature forecasts to soil moisture, and fragility (lack of robust performance) of PBL schemes under stable conditions. Conduct of ultra-high resolution simulations (~50m) over reasonable periods of time still remains a problem. Further work is required on the use of variable resolution in models, selection of optimal coordinate systems (terrain following, Cartesian or other) and grid nesting. In very complex topographies, surface elements (trees, isolated buttes) introduce problems, much the same way as buildings in urban canopies. These elements may protrude beyond the first or first few grid layers, whence often-used similarity theories (e.g., Monin-Obukhov) for specifying boundary conditions become invalid. Steep terrain is bane for nesting, as there are reflections from lateral boundaries. Nesting of microscale LES and RANS models with mesoscale models is becoming commonplace, and studies to ensure compatibility of nesting (e.g., spin up of two models) are needed. Land Surface Models and Planetary Boundary Layer schemes used in mesoscale models are based on flat-terrain research, and their validity to complex terrain remains to be verified. This is especially important because the structure and production mechanisms of turbulence are different for the two cases. For example, complex terrain stable boundary layer is in a continuous state of weak turbulence whereas in flat terrain turbulence is highly intermittent both spatially and temporally. In addition, hydrologic models for complex terrain need to include gravity driven flow.

It is useful to promote modeling systems that can handle all terrain types, from flat to very complex terrain and from global to micro scales. While one-way nesting (down scaling) is common, the preponderance of energy production in small scales in mountainous terrain may lead to upscale transfer, requiring two-way nesting (up-scaling). The conditions that require upscaling need to be identified. Vertical nesting, in addition to horizontal nesting, must to be considered. The models are usually calibrated and evaluated for mid latitudes, and thus data from low and high latitudes will be welcome additions to model calibration studies. With the emergence of unified models, parameterizations valid across the nests are needed.

# Intricacies of Coupling Numerical Modeling and Field Observations for Stable Boundary Layer Simulations over Complex Terrain

Fotini Katopodes Chow
University of California, Berkeley

Predictions of weather, wind energy resources, and air quality under stable conditions rely on sparse observations and poorly resolved numerical models. For example, turbulence intermittency is expected under stable conditions and is triggered by mechanisms such as breaking of critical internal waves and strong near-surface shear. The intermittency is dependent on a myriad of factors (e.g., terrain, energy content, generating mechanism), which are almost always under-resolved by models and need to be better studied using both modeling and field measurements.

Models continue to be pushed to higher resolution, and field observations in atmospheric boundary layer campaigns also increasingly focus on fine-scale turbulence information. How can this be leveraged to create better turbulence closure models, for instance, when the assumptions about turbulence are often fundamentally different in the field (e.g. use of the Taylor hypothesis)? Improving observations and models also relies on linking the meso-scale and the micro-scale. How can, for example, point observations in the field be used to inform large-scale models, and how can model results inform detailed sensor placement in the field? Furthermore, how can measurements help in the *terra incognita*, or model resolution gray zone, which describes the range of resolutions in between those classically used for mesoscale models and fine-scale large-eddy simulations where traditional turbulence parameterizations may fail?

Detailed field observations must be intricately woven together with numerical simulation output to improve understanding of the stable boundary layer. There are also, however, many modeling issues which need to be separately addressed to create a high-fidelity simulation. Some questions to consider include: What are the best methodologies for nesting micro-scale models within meso-scale models? Which turbulence models remain scale-aware across the terra incognita (model resolution gray zone)? How can steep terrain or urban geometries be included accurately as resolution increases? What vertical coordinate system works best for mountainous terrain?

## TURBULENCE CLOSURES AND THE TERRA INCOGNITA

Traditional closure models continue to be widely used in ABL modeling despite their shortcomings. Under stable stratification, these models tend to be over-dissipative, and cannot predict intermittency of the turbulence. For example, previous work over rolling hills in the CASES-99 field campaign found that gravity waves and intermittently stable flow could only be represented in LES using non-eddy viscosity closures which allow backscatter such as the dynamic reconstruction model (DRM) (see Fig. 1, Chow et al. 2005, Zhou and Chow 2014). Recent studies of the convective boundary layer and the stratocumulus topped boundary layer also show unique abilities of the DRM within the terra incognita, with better representation of high-order turbulent statistics. Other more sophisticated turbulence modeling approaches include

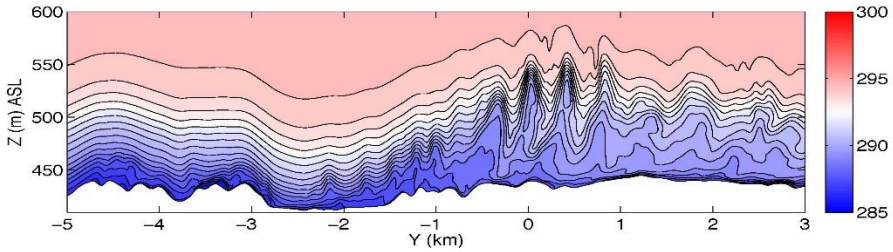


FIGURE 1. Potential temperature contours from CASES-99 field site using DRM turbulence closure model for LES at 25 m horizontal resolution show breaking internal waves responsible for intermittent turbulence. (Zhou and Chow, 2014)

Reynolds-stress closures such as those proposed by Ramachandran and Wyngaard (2011) and Enriquez et al. (2014). Atmospheric LES codes must use recent success of new turbulence closure models to expand their use and eventually inform new models in the terra incognita and coarser scales.

## TERRAIN REPRESENTATION

Numerical errors due to terrain-following coordinate systems are non-negligible for moderate or steep slopes, which are increasingly resolved at the higher grid resolutions used in LES, especially needed for the stable boundary layer. Alternative grids include immersed or embedded boundary methods, or shaved cell techniques. While potentially transformative, these alternative gridding approaches are complex and difficult to implement in a robust manner.

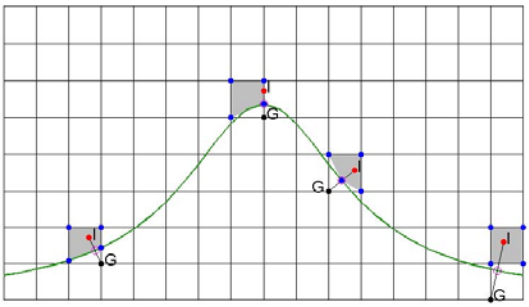


FIGURE 2. Schematic of an immersed boundary method showing background Cartesian coordinates and terrain surface (green) (Lundquist et al. 2010)

The immersed boundary method (IBM) was implemented into WRF to mitigate terrain slope errors and also enable simulation over very steep slopes (Lundquist et al. 2010, 2012). In this approach, the model topography is “immersed” within a Cartesian grid, and interpolation techniques are used to enforce boundary conditions on the immersed surface (see Fig. 2). The IBM approach has the ability to represent complex mountainous terrain with ~10 m resolution even when terrain slopes approach 90 degrees (which cannot be handled using traditional WRF coordinates). Further development of WRF-IBM must fully include surface roughness and vegetation effects and other physics schemes. In addition there is need for a robust nesting procedure to enable mesoscale to microscale nesting (Daniels et al. 2016). This requires development of new coupling strategies to address grid discontinuities when transitioning from

terrain-following to IBM coordinates. The ultimate goal is to create a modeling system that can handle all terrain types, including flat, hilly or mountainous terrain and urban terrain.

## LINKING FIELD MEASUREMENTS AND MODELS

Field measurements and models should be intricately coupled so that progress in one is linked to the other. Observational strategies have advanced to the point where over 20 lidars are used simultaneously in a field campaign, generating vast amounts of data (for example in the recent Perdigão field campaign, Fernando et al. 2017). To take full advantage of these datasets, new paradigms for model comparisons with observations need to be developed. Integration of lidar and LES data, for example, could be used in nowcasting for optimal control of wind turbine blades. Yet current model resolutions are barely able to resolve the turbulent features seen in lidar and other field instruments, making comparisons difficult.

Strategies to address this might involve: having multiple rigorous, collaborative modeling teams participate in field programs with targeted code development and validation tasks, performing field trials of new data-model comparison techniques, developing nowcasting methods where LES output is combined with lidar scanning techniques and data assimilation, analyzing spatially distributed point measurements from sensors in a fashion compatible with model output, and many other ideas that may arise from this workshop.

## EDUCATION AND TRAINING

There is an urgent need to create a new generation of atmospheric turbulence modelers with solid scientific and physical foundation. These modelers should be integrated into interdisciplinary teams where high-risk new algorithms and components are combined to create an “ultra”-capability model with top-notch components in all areas. Such a model might include, for example, the latest turbulence closure models for LES, RANS and the terra incognita, the best surface terrain representation, sophisticated grid nesting techniques, scalar transport capabilities, wind turbine wake models, grid nesting capabilities, and data assimilation capabilities, to name a few. In addition the code could leverage GPU acceleration to enable simulations running at 5-10 m resolution over complex terrain, which may just barely reach the minimum resolution required under stable conditions. This “ultra”-capability model must be developed in a way that is also closely connected with field observations, as discussed above.

## REFERENCES

Chow, F. K., Street, R. L., Xue, M., and J. H. Ferziger. 2005. Explicit filtering and reconstruction turbulence modeling for large-eddy simulation of neutral boundary layer flow. *Journal of the Atmospheric Sciences* 62:2058-2077.

Daniels, M. H., Lundquist, K. A., Mirocha, J. D., Wiersema, and F. K. Chow. 2016. A new vertical grid nesting capability in the Weather Research and Forecasting (WRF) model. *Monthly Weather Review* 144(10):3725-3747.

Enriquez, R. M. and R. L. Street. 2014. Large-eddy simulation of the stable boundary layer: Revisiting GABLS with a linear algebraic subgrid-scale turbulence model. *21st Symposium on Boundary Layers and Turbulence, AMS,* Paper 14.B3, 7 pp.

Fernando, H. J. S., J. K. Lundquist, and S. Oncley. 2017. Monitoring wind in Portugal’s mountains down to microscales. *Eos.* 98. DOI: 10.1029/2017EO074745.

Lundquist, K. A., F. K. Chow, and J. K. Lundquist. 2010. An immersed boundary method for the Weather Research and Forecasting model. *Monthly Weather Review* 138 (3):796–817.
Lundquist, K. A., F. K. Chow, and J. K. Lundquist. 2012. An immersed boundary method enabling large-eddy simulations of flow over complex terrain in the WRF model. *Monthly Weather Review* 140 (12):3936–3955.
Ramachandran, S., and J. Wyngaard. 2011. Subfilter-scale modelling using transport equations: Large-eddy simulation of the moderately convective atmospheric boundary layer. *Boundary-Layer Meteorology* 139:1-35.
Zhou, B. and F. K. Chow. 2014. Nested large-eddy simulations of the intermittently turbulent stable atmospheric boundary layer over real terrain. *Journal of the Atmospheric Sciences* 71:1021-1039.

# The Marine Atmospheric Boundary Layer: a view from the surface.

William Drennan
RSMAS, University of Miami

Improved understanding of the Marine Atmospheric Boundary Layer (MABL) is closely tied to that of the underlying surface waves. The 1990s saw the winding down of the very successful WAve Modelling (WAM) project which developed much of the framework for wave modelling still used today (Komen et al. 1996). That same decade saw significant improvements in our capabilities to measure both surface waves and turbulent fluxes. In particular, the introduction of inexpensive rate gyros, along with algorithms to account for motion correction (e.g. Anctil et al. 1994), opened the possibilities of making high resolution wave and air-sea flux measurements from nonstationary platforms, namely buoys and ships. By the late 1990s the increasingly widespread use of ultrasonic anemometers and infrared gas analysers revealed a growing consensus of on the behaviour of momentum, sensible heat and humidity fluxes, at least in the moderate windspeed ranges typically encountered. By the following decade, attention was turning to the more challenging low- and high-wind regimes. The high-wind regime, in particular, became increasing relevant in the aftermath of the busy hurricane seasons of the early 2000s (and again this year). Here we look at some of the remaining challenges, and of our prospects for further advances in the coming years. In particular, we focus on i) high wind regime, ii) high latitude regimes and iii) wave growth and dissipation. We end with a brief discussion of flow distortion.

Air sea fluxes at high winds are important, especially for tropical cyclone modelling. Over the past decade, several field data sets have reported air-sea flux measurements in the wind speed range 20 - 30 m/s. The summary curve of Potter et al (2015) is shown in Figure 1, with the various data sets described in the caption. While this figure highlights the field data from cyclones, high latitude high wind data sets include Peterson and Renfrew (2009), Cook and Renfrew (2015). There is now considerable support that the air-sea momentum flux changes behaviour at higher winds, with the drag coefficient leveling off and possibly decreasing. Several mechanisms have been proposed (wave sheltering, spray drag...), but much work remains to be done on understanding the details. It is also important to keep in mind that we should not necessarily expect universal CD-type scaling (as in Fig. 1) at high winds. The various environments of the high wind regime (Southern Ocean, North Atlantic, cyclones, and wave tanks) all have different fetches, durations and (therefore) waves.

We will also summarise recent progress with high wind measurements of latent heat and enthalpy fluxes. While sea spray has been proposed to significantly increase these fluxes at high winds, this has yet to be demonstrated. We will discuss some of the challenges of making measurements in these conditions. New autonomous platform technologies will likely be significant in the near future, but deployments are risky in boundary layer.

The high latitude MABL regime is characterised by strong winds and high waves (Southern hemisphere) along with seasonal sea ice, strong thermal gradients, and high inhomogeneity among other factors. While the region is now a focus of increasing attention, including by the remote sensing and modelling communities, many challenges remain, due both to the remoteness of the areas and the factors above. Here we draw attention to the recent recommendations of the US Clivar/Seaflux Working Group on High latitude Surface Fluxes (Bourassa et al 2013).

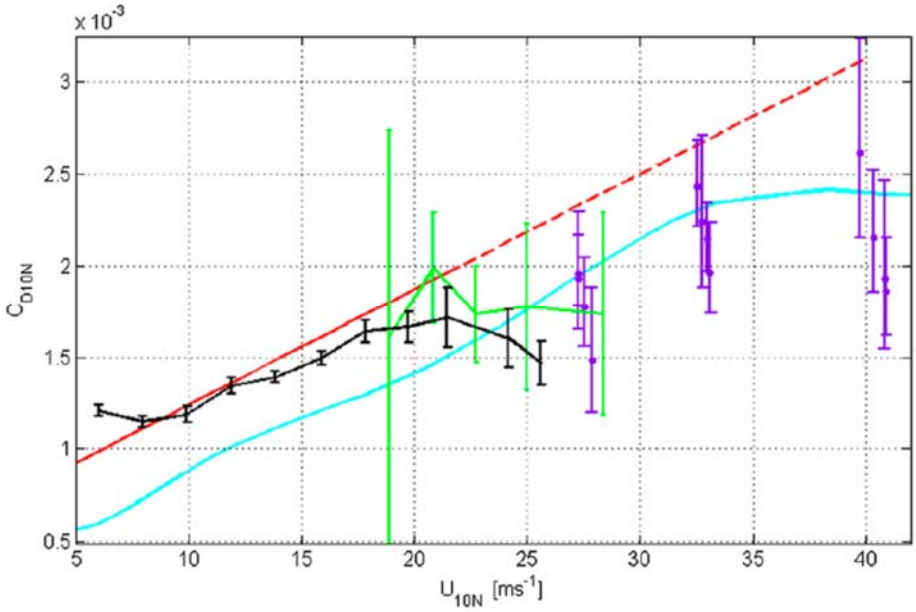


FIGURE 1 (from Potter et al 2015). CD10N as a function of U10N from Potter et al. 2015 (black; buoy measurements in typhoons), French et al. 2007 (green, 2.5m/s bins; aircraft measurements in hurricanes), Donelan et al. 2004 (blue; laboratory measurements), and Powell et al. 2003 (purple, drop sonde measurements in hurricanes). Error bars denote 95% confidence intervals of the means. The Smith 1980 bulk coefficient curve is shown in red solid, with the dashed lines shows the curve extended beyond original measurements.

One of the most challenging measurements in air-sea interaction remains that of pressure fluctuations over waves. The measurements are key to understanding wave growth, yet little real progress has been made since the Bight of Abaco experiments in the mid 1970s (Snyder et al. 1981). Our results published last year on wave growth/decay over swell waves (Kahma et al. 2016) were based on measurements made in 1987 ! These measurements are very challenging, in that *static* pressure fluctuations are small compared to background dynamic pressure fluctuations, are strongly impacted by flow distortion, and decay exponentially away from the surface. Though difficult, these measurements are crucial to improving our understanding of the impact of swell waves on air-sea transfer, and to improve wave models which rely on growth parameterisations (source functions, e.g. Plant 1982) based on the limited available data from the 1970's and 1980's.

## REFERENCES

Anctil, F., M. A. Donelan, W. M. Drennan and H. C. Graber. 1994. Eddy correlation measurements of air-sea fluxes from a Discus buoy. *Journal of Atmospheric and Oceanic Technology* 11:1144-1150.

Bourassa, M. A, S. T. Gille, C. Bitz, D. Carlson, I. Cerovecki, C. A. Clayson, M. F. Cronin, W. M. Drennan, C. W. Fairall, R. Hoffman, G. Magnusdottir, R. T. Pinker, I. A. Renfrew, M. Serreze, K. Speer, L. Talley, and G. A. Wick. 2013. High-Latitude Ocean and Sea-Ice Surface Fluxes: Challenges for Climate Research. Bulletin of the American Meteorological Society 94: 403–423.

Cook, P. A. and I. A. Renfrew. 2015. Aircraft-based observations of air–sea turbulent fluxes around the British Isles. *Quarterly Journal of the Royal Meteorological Society* 141:139–152.

Donelan M. A., B. K. Haus, N. Reul, W. J. Plant, M. Stiassne, H. C. Graber, O. B. Brown, and E. S. Saltzman. 2004. On the limiting aerodynamic roughness of the ocean in very strong winds. *Geophysical Research Letters* 31:L18306.

French, J. R., W. M. Drennan, J. A. Zhang, and P. G. Black. 2007. Turbulent fluxes in the hurricane boundary layer. Part I: Momentum flux. *Journal of the Atmospheric Sciences* 64:1089–1102.

Kahma, K.K., M.A. Donelan, W.M. Drennan and E.A. Terray, 2016: Evidence of energy and momentum flux from swell to wind. *Journal of Physical Oceanography* 46, 2143 – 2156

Komen, G. J., L. Cavaleri, M. Donelan, K. Hasselmann, S. Hasselmann, and P. A. E. M. Janssen. 1996. Dynamics and Modelling of Ocean Waves. Cambridge, UK: Cambridge University Press.

Petersen, G. N., and I. A. Renfrew. 2009. Aircraft-based observations of air-sea fluxes over Denmark Strait and the Irminger Sea during high wind speed conditions. *Quarterly Journal of the Royal Meteorological Society* 135:2030–2045.

Plant, W. J. 1982. A relationship between stress and wave slope. *Journal of Geophysical Research* 87:1961–1967.

Powell, M. D., P. J. Vickery, and T. A. Reinhold. 2003. Reduced drag coefficient for high wind speeds in tropical cyclones. *Nature* 422:279–283.

Smith, S. D. 1980. Wind stress and heat flux over the ocean in gale force winds. *Journal of Physical Oceanography* 10:709–726,

Snyder, R. L., F. W. Dobson, J. A. Elliot, and R. B. Long, 1981. Array measurements of atmospheric pressure fluctuations above gravity waves. *Journal of Fluid Mechanics* 102:1–59.

Zhang J. A., P. G. Black, J. R. French, and W. M. Drennan. 2008. First direct measurements of enthalpy flux in the hurricane boundary layer: The CBLAST results. *Geophysical Research Letters* 35:L14813.

# Marine boundary layer cloud observations needed to address interactions across scales

Simon P. de Szoeke
Oregon State University

Marine boundary layer clouds strongly increase the planetary albedo while changing the Earth's thermal radiance little. The climate is sensitive the change of boundary layer clouds in a climate warmed by increased greenhouse gases, and this sensitivity is a leading cause of uncertainty in climate change projections. Boundary layer clouds depend on subtle microphysical, turbulent, diurnal, synoptic, and regional processes. The scales of the processes, from molecular (1 nm) scales to scales of 1000s of km, encompass 15 orders of magnitude. Processes that have opposing effects buffer marine clouds against changes. Observations of key processes in isolation, as well as observations of how they interact within the variability of conditions across its wide range of scales, are needed.

Long deployments of high-resolution observations provide simultaneous sampling of boundary layer processes and variability at multiple scales. Below I provide examples of the results of such observations from field experiments: 1) turbulence measurements in the vicinity of entrainment at cloud top; 2) remotely-sensed covariability of cloud optical depth, macrophysics, and droplet number concentration; and 3) resolving the effects of convective downdrafts on the boundary layer.

1. *Diurnal cycle of stratocumulus cloud top turbulence*. Turbulence at the top of stratocumulus clouds is responsible for entrainment, which dries clouds, yet maintains the depth of the boundary layer (BL) against mean subsidence. Remarkably persistent southeastern Pacific stratocumulus clouds were observed for 2 months during VOCALS in 2008. The vertically pointing 3-mm NOAA Doppler cloud radar sampled reflectivity and vertical velocity at 3.5 Hz for 19 days ($5.7 \times 10^6$ samples). Near cloud top, where entrainment takes place, settling velocity is small and the Doppler velocity represents turbulent air velocity. From this, turbulence kinetic energy (TKE) and its dissipation rate were estimated. Net upward radiation from cloud top drives positive convective buoyancy flux, maintaining a steady heat balance. The net positive buoyancy flux is the main source of TKE for the cloud. Entrainment of warmer air into the cloud from above the inversion represents a negative buoyancy flux and sink of TKE.

   The BL depth, stratocumulus cloud, and cloud-top turbulence undergo a distinct diurnal cycle. Figure 1 shows the average diurnal cycle of TKE dissipation rate estimated from the cloud radar relative to cloud top. During the day, solar warming offsets longwave cooling, reducing cloud-top buoyancy flux and TKE dissipation by a factor of 3. Dissipation reduces by a factor of 30 in the decoupled stratified layer at the receding cloud base.
2. *Cloud microphysical interactions*. The effect of tiny ($10^{-9}$ m) aerosol particles on the amount, microphysics, and albedo of clouds involves many interactions that are highly uncertain. This uncertainty hampers our ability to constrain climate model predictions of historical radiative heat budgets and projections of climate feedbacks due to clouds. Cloud amount, microphysics, precipitation, and albedo respond to cloud droplet number concentration $N$, which is modulated by cloud coalescence and precipitation processes,

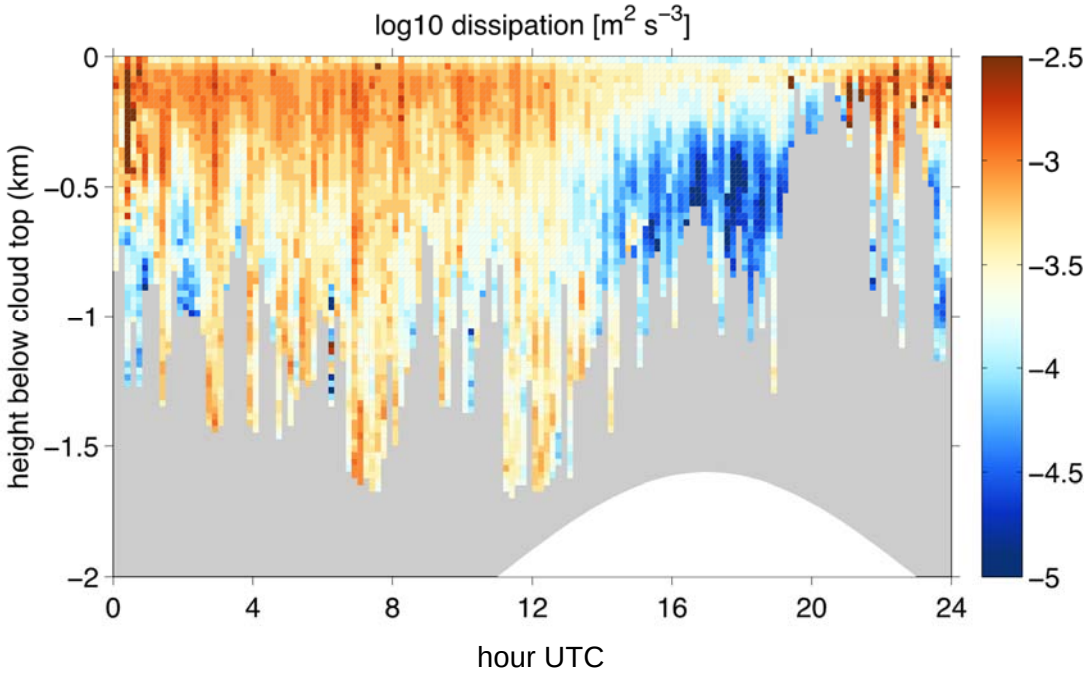


FIGURE 1. Diurnal composite of turbulence kinetic energy (TKE) dissipation in VOCALS southeastern Pacific marine stratocumulus clouds from Doppler cloud radar vertical velocity spectra.

and by sources of cloud condensation nuclei. Statistically stationary observations of the internal and forced variability of the boundary layer must be diligently integrated with detailed observations of the microphysical processes. A suite of remote sensors on a ship simultaneously measured cloud optical depth, liquid water path (LWP), and cloud thickness, enabling an optical retrieval of average cloud droplet number concentration in VOCALS. Almost all the joint variability of the logarithms of LWP, cloud height, and optical depth describing the clouds is described by a macrophysical mode (68% variance) and by a microphysical mode (28%) that projects onto drop number concentration *N*. LWP is anticorrelated with *N*, consistent with drizzle at higher LWP scavenging cloud droplets, and counter to drizzle suppression increasing cloud lifetime. The strong sensitivity of *N* to LWP suggests cloud dynamic and thermodynamic forcings drive macrophysical variability that controls *N* in southeastern tropical Pacific stratocumulus clouds. Measurements of the interactions between cloud micro- and macrophysical properties suffer from sampling noise due to the different fields of view of the remote sensors employed in the retrieval. We can improve them by better characterizing random and correlated sampling error among instruments.

2. *BL-cumulus interaction.* Feedbacks reinforcing intraseasonal precipitation anomalies depend on interactions between the atmospheric boundary layer and free tropospheric cumulus convection, including exchange of moist static energy (MSE) between the atmospheric boundary layer and the cumulus ensemble. In boundary layer quasi-equilibrium, the surface source of MSE to the boundary layer must be balanced by import of low MSE air by entrainment, cumulus downdrafts, and horizontal advection. The convection scheme of Arakawa and Schubert (1974) proposed a balance in the boundary layer largely between surface fluxes and boundary layer entrainment. Raymond (1995) proposed downdrafts as the primary sink of MSE from the boundary layer. Entrainment

appears to be the larger sink of boundary layer MSE in eddy flux calculations from recent large eddy simulations (LES, Thayer-Calder and Randall 2015).

Observations show that in this region, downdrafts are a slightly stronger sink of MSE than turbulent entrainment. The observed MSE fluxes from the surface, entrainment, and downdrafts are distinguished by conserved properties $\theta$ and $q$ of the boundary layer and three end members: 1) the ocean surface, 2) air entrained from the boundary layer top, and 3) nearly saturated downdrafts cooled by evaporation of rain, observed in the DYNAMO field campaign of 2011 (Figure 2). Downdrafts are colder than air above the boundary layer, distinguishing them from entrainment. The exact ratio of downdraft to entrainment MSE flux varies with the strength of convection. The overall dominance of downdrafts is due to the increased frequency of downdrafts entering the BL during the convectively active phase of the MJO.

Advances in reliable small, low-cost, low-power, fast-response sensors, and fast mobile-generation data-logging hardware—suitable for autonomous platforms—and scientifically integrated suites of remote sensing measurements will improve observations of the marine boundary layer at multiple scales.

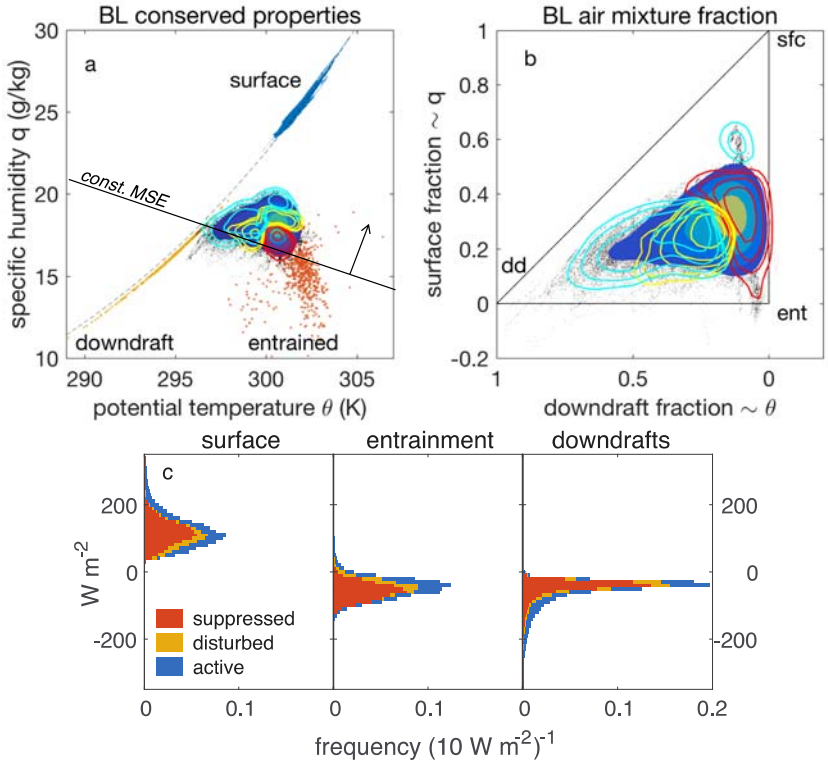


FIGURE 2. Conserved properties (a) specific humidity $q$ and potential temperature $\theta$, estimate (b) mixing fraction of BL air properties due to downdrafts (dd), entrainment (ent), and surface (sfc). Entrained air and downdrafts reduce moist static energy. Dashed line shows saturation humidity. (c) MSE fluxes to the boundary layer due to these sources in convectively suppressed, disturbed, and active phases defined by a global MJO index. Open contours show probability density (positive) anomalies for convectively suppressed (red), disturbed (yellow), and active (cyan) conditions.

# Observational needs for the cloudy marine boundary layer

Robert Wood
Atmospheric Sciences
University of Washington

## OVERARCHING SCIENCE QUESTION

What observations are needed (over land, ocean, and ice) to make meaningful progress in our understanding and modeling of the global atmospheric boundary layer?

Within this umbrella, I will focus primarily on the following aspects:

- *Discuss key observing and modeling gaps and the science that could be accomplished by filling those gaps;*
- *Consider how new observing capabilities (including targeted field campaigns) can leverage the existing surface and boundary layer observational networks and where advances in satellite remote sensing could be most beneficial;*
- *Discuss ways to foster communication between user and technology development communities to develop increased collaboration opportunities that could help rapidly advance the science.*

## 1. MOTIVATING FACTORS

- MBL clouds shape the transports of energy, moisture and momentum in the marine PBL
- MBL clouds are central to the cloud feedback problem and therefore climate sensitivity
- MBL clouds are a primary mediator of aerosol forcing on climate (indirect effects)

## 2. KEY CLOUD CONTROLLING PROCESSES, CURRENT MEASUREMENT, MEASUREMENT GAPS

- The presentation will begin with a brief review of key processes controlling MBL cloud properties
- Brief review of the spatial and temporal scales that these processes need to be measured on to provide transformative science advances.
- Thoughts about what we currently observe and at what scales (field studies, fixed ground sites/networks, satellites)
- Identify critical measurement gaps, which include:

- Vertically resolved PBL thermodynamic and dynamic structure, including vertical motions that drive entrainment mixing and turbulent transports
- Vertically resolved condensate and its partitioning into precipitation and cloud
- Cloud base height poorly constrained from space

## 3. HOW CAN EXISTING MEASUREMENTS BE BETTER LEVERAGED?

- How do we aggregate and assimilate existing MBL cloud observations for comparison and improvement of model forecasts (e.g. through data assimilation)? Take advantage of NWP model developments that now allow assimilation of cloud information (e.g. column cloud condensate)
- How do we better combine, package and distribute datasets from disparate sources to provide more user-friendly datasets? Examples from ARM, NASA MEaSUREs program.
- Underused measurements for MBL research (e.g. GPS Radio Occultation to probe MBL moisture structure.

## 4. NEW MEASUREMENTS

- Point to new technologies that can potentially fill some gaps in the near (<decade) and longer timescales (>decade). Examples include
  - *Decadal* : improvements and miniaturization of millimeter radar technology for surface and airborne research platforms.
  - *Multi-decadal*: wide/multiple-field of view lidar to constrain vertical extinction profile; multi-wavelength radar for differential attenuation for vertically resolved condensate.
- Show how intensive field observations can be used synergistically with satellite and surface sampling to help meet MBL sampling needs in the near or longer time horizon.

# Coupling Observations and Large Eddy Simulations to Advance Boundary Layer Science

Peter P. Sullivan
National Center for Atmospheric Research

The development and ready access of large massively parallel computing machines has altered the landscape of turbulence simulations in geophysical flows. For example, “Cheyenne” housed at the NCAR Wyoming Super Computer Center is a 5.34-petaflop machine featuring more than 145,000 computational cores. Recent large eddy simulations (LES) of a canonical stable boundary layer on a similar petascale machine utilized a grid mesh of $1024^3$ points in a computational domain (400, 400, 400) m with an isotropic spacing of $\Delta$=0.39 m (Sullivan et al., 2016). The LES utilized 4096 cores and required nearly 900,000 time steps to simulate nine physical hours. An example of the output is shown in Figure 1 where we found, surprisingly, ubiquitous sharp temperature fronts populating the stable boundary layer. Heavy time and space averaging of the 4-D fields produced smooth vertical profiles of winds and temperature as might be observed from a vertical tower under nighttime conditions. The second example shown in Figure 2 presents results from an LES of a marine boundary layer where a spectrum of moving waves is imposed as its lower boundary condition (Sullivan et al., 2014). The simulations highlight the coupling between large-scale convective rolls in the outer boundary layer with wave induced fluctuations in the wavy surface layer.

As an LES developer and practitioner, I believe that a frontier for boundary-layer research lies in coupling LES and observations for flow regimes similar to those shown in Figures 1 and 2. LES is a powerful tool for helping to interpret and guide observations in addition to building databases of idealized flows to tune and evaluate 1-D column models used in climate and weather forecasts. LES can also ingest time and space varying measurements of geostrophic winds and surface fluxes to forecast fine scale boundary-layer motions. However LES codes do contain empiricism. When the scale of the resolved flow dynamics shrinks compared to the LES filter width, $\ell$<$\Delta$, there is an undue reliance on the subfilter scale model used. And rarely are LES solutions tested for grid convergence (Sullivan and Patton, 2011). Thus both subfilter scale models and outputs from LES need to be tested and calibrated using observations, see discussion by Wyngaard (1998) and Sullivan et al. (2003). An example showing measurements of subfilter scale variances $\tau_{ii} = \overline{u_i u_i} - \overline{u}_i \overline{u}_i$ obtained from sonic anemometers is provided in Figure 3; the overbars ( $\overline{\ }$ ) denote 2-D spatial filtering. These SFS variances and fluxes are modeled in LES codes.

Enclosed is a wish list of observational targets and possible outcomes that can potentially advance the present understanding of boundary-layer dynamics in LES and larger scale models.

1. Measure the correlation between pressure and waveslope ($p'\partial h/\partial x$, $p'\partial h/\partial y$) over the sea surface for varying wind speed and wave state down to centimeter resolution

- Fundamental drag of the sea surface
- Wind input source term in spectral wave models

2. Collect continuous space-time maps of the sea surface elevation $h(x, y, t)$ for varying surface wind speeds and wave state. For example, covering an area of (20×20) m down to (0.05 × 0.05) m

- LES of turbulent flow over an imposed wave surface to diagnose drag mechanics, e.g., Miles critical layer mechanism versus airflow separation, and address what wave scales support wind stress
- Identify the role of wave groups for drag unsteadiness

3. Collect an extensive database of breaker statistics as function of wave age, wind speed, and wind direction

- Identify what scales dominate the exchange of momentum between the atmosphere and ocean (e.g., Kleiss and Melville, 2010)
- Development of stochastic breaker models

4. Measure surface fluxes over a wide range of spatial areas and vertical heights with and without surface heterogeneity

- Develop scale aware parameterizations that work seamlessly over the “Terra Incognita” (Wyngaard, 2004) for WRF/MPAS style models
- Investigate relationships between resolved and sub-filter scale fluxes for LES, e.g., between the subfilter-scale momentum flux $\tau_{ij} = \overline{u_i u_j} - \overline{u}_i \overline{u}_j$ and the resolved wind $\overline{u}_i$ for varying spatial resolution D (e.g., Sullivan et al., 2003; Hatlee and Wyngaard, 2007)

5. Measure vertical profiles of temperature and wind speed with fine resolution $\Delta z < 1$m in stable conditions

- Intermittent temperature fronts in LES (e.g., Sullivan et al., 2016)
- Mixing rules and Richardson number dependence for stable boundary-layer paameterizations (e.g., Balsley et al., 2008)

References

Balsley, B. B., G. Svensson, and M. Tjernstro¨om, 2008: On the scale-dependence of the gradient Richardson number in the residual layer. Boundary-Layer Meteorol., 127, 57–72.

Hatlee, S. C. and J. C. Wyngaard, 2007: Improved subfilter-scale models from the HATS field data. J. Atmos. Sci., 64, 1694–1705.

Kleiss, J. M. and W. K. Melville, 2010: Observations of wave breaking kinematics in fetch-limited seas. J. Phys. Oceanogr., 40, 2575–2604.

Sullivan, P. P., T. W. Horst, D. H. Lenschow, C.-H. Moeng, and J. C. Weil, 2003: Structure of subfilter-scale fluxes in the atmospheric surface layer with application to large-eddy simulation modeling. J. Fluid Mech., 482, 101–139.

Sullivan, P. P., J. C. McWilliams, and E. G. Patton, 2014: Large eddy simulation of marine boundary layers above a spectrum of moving waves. J. Atmos. Sci., 71, 4001–4027.

Sullivan, P. P. and E. G. Patton, 2011: The effect of mesh resolution on convective boundary-layer statistics and structures generated by large-eddy simulation. J. Atmos. Sci., 68, 2395–2415.

Sullivan, P. P., J. C. Weil, E. G. Patton, H. J. J. Jonker, and D. V. Mironov, 2016: Turbulent winds and temperature fronts in large-eddy simulations of the stable atmospheric boundary layer. J. Atmos. Sci., 73, 1815–1840.

Wyngaard, J. C., 1998: Boundary-Layer modeling: History, philosophy, and sociology. Clear and Cloudy Boundary Layers, A. A. M. Holtslag and P. G. Duynkerke, Eds., Royal Netherlands Academy of Arts and Sciences.

Wyngaard, J. C., 2004: Toward numerical modeling in the Terra Incognita. J. Atmos. Sci., 61, 1816–1826.

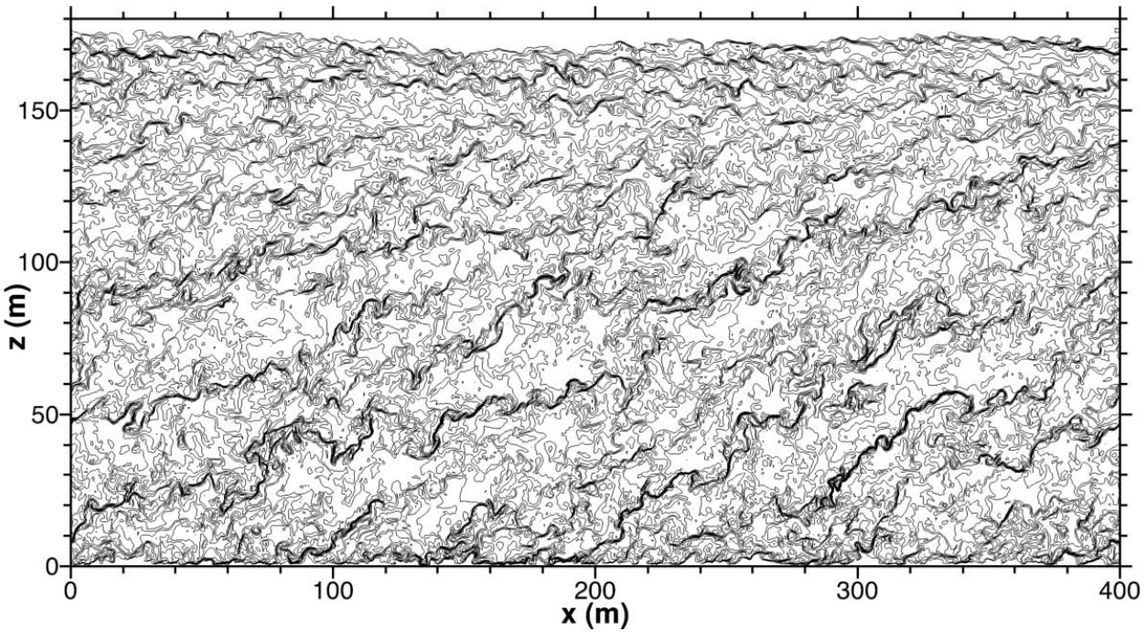


FIGURE 1. Contours of the temperature difference $\theta - \theta_o$ in an $x$-$z$ plane from an LES of a stable atmospheric boundary layer. Notice the intermittent temperature fronts that populate the boundary layer.

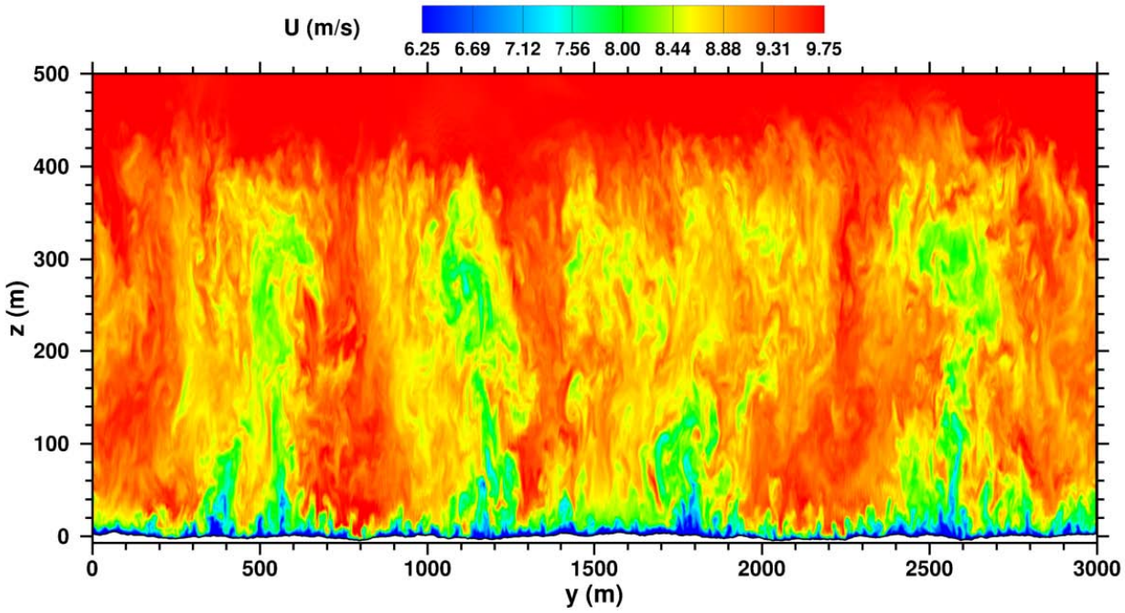


Figure 2: Results from an LES of a marine boundary layer above an imposed spectrum of moving waves at its lower boundary. Streamwise velocity contours are shown in a $y$-$z$ plane. Notice the large-scale shear-convective rolls and the eruption of low-speed fluid near the lower wavy boundary.

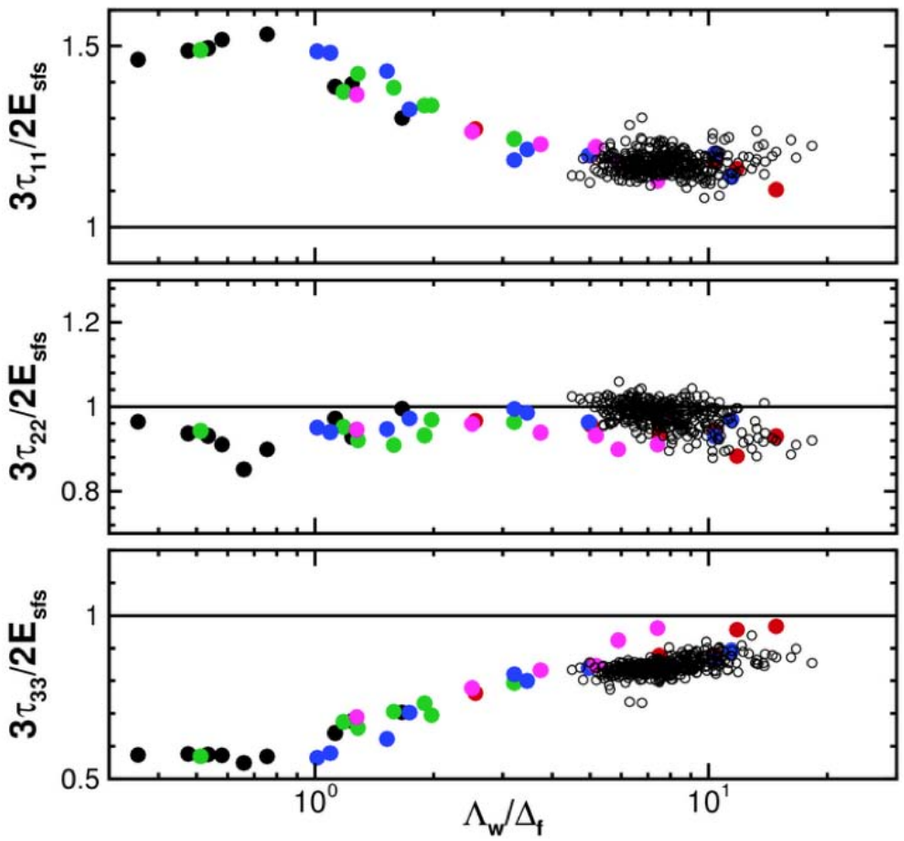


FIGURE 3. Measured subfilter scale variances normalized by the SFS energy $E_{sfs}$ for varying spatial filter $\Delta_f$ in the atmospheric surface layer (solid bullets) and in the marine surface layer (open dots). $\Lambda_w$ is the scale of the peak in the vertical velocity spectrum. The variances are isotropic when $3\tau_{ii}/2E_{sfs} = 1$.

# Organized Large Eddies and Tropical Cyclone Boundary Layers

Ralph Foster
Applied Physics Laboratory
University of Washington, Seattle, WA

## INTRODUCTION

A basic characteristic of the PBL, at least for near-neutral to convective conditions, is turbulent flow. Implicit in most turbulence parameterization is the assumption that the flow is homogeneous, which is why down-gradient diffusion modeling is at the core of most PBL parameterizations. In contrast, it is well-known that the PBL is often, perhaps usually, characterized by embedded organization. The organized part of the turbulence can induce fluxes of heat, water vapor and momentum that are essentially advective in nature and are not necessarily down the local mean gradient. Some ad hoc means of characterizing the non-gradient fluxes have been incorporated in some PBL parameterizations (e.g. Hong et al., 2006; Witek et al, 2011ab). However, at least for the case of PBL roll vortices, the form of the non-gradient flux models often does not reflect the mechanism. In order to improve parameterization of these non-gradient fluxes, it seems clear that there is a need to combine means of flow visualization with flux measurements in order to best quantify how the non-gradient PBL transport is related to the local fluxes measured by towers, buoys and aircraft. Two promising visualization methods are Doppler wind lidar (DWL) and satellite synthetic aperture radar (SAR). I will present some examples using SAR in tropical cyclones and DWL in the coastal marine atmospheric boundary layer (MABL) with a focus on roll vortices. As a caveat, shallow boundary layer convection, which is common in very unstable conditions, is likely just as important a process. However, its incorporation into PBL parameterization is a fairly mature subject in comparison to that of PBL rolls.

## TROPICAL CYCLONE BOUNDARY LAYER

Tropical cyclone boundary layers (TCBLs) present unique measurement and parameterization challenges. The environment is harsh and the mean structure is complex in ways that are not conducive to the use of standard parameterizations. For example, nonlinear mean flow “curvature” and vertical advection are leading order contributions. The mean temperature profile in the upper TCBL is strongly affected by latent heating. Inertial stability effects due to the swirling flow induce an upward slope in boundary layer depth with increasing radius. Hence, even defining the TCBL top is problematic. One defined by a bulk Richardson number will often be significantly shallower than one defined more classically as the depth through which turbulent flow dominates. Applied to the TCBL, PBL parameterizations such as the YSU model (Hong et al., 2006), which prescribe a specific, arbitrary cubic profile of eddy viscosity based on the PBL depth, can easily be fooled.

Furthermore, the basic TCBL conditions are nearly ideal for the formation and maintenance of organized large eddies (OLEs) in the form of roll vortices (rolls). Even though the surface buoyancy flux is large, the near-surface wind shear is extreme and this combination results in nearly-neutral stratification near the surface. Consequently, the roll generation mechanism is primarily related to dynamic instability of the mean flow (Foster, 2005; Morrison et al., 2005; Zhu 2008; Lorsolo et al., 2008; Zhang et al., 2008; Nakanishi and Niino, 2013; Wang and Jiang, 2017). The strength of TCBL roll circulation is significant, e.g., as much as $\pm 10 - 20\ ms^{-1}$ in the along-wind direction depending on the strength of the storm and the scale of the rolls. The first observations of rolls were obtained after landfall of hurricane Fran (1996) using the Doppler on Wheels (Wurman and Winslow, 1998). They found relatively small-scale rolls, with wavelengths of approximately 600 m. The importance of rolls to the overall transport of momentum and scalars is not well-characterized. Estimates range from 5% to 25% of the total fluxes (e.g. Zhu, 2008; Zhang et al., 2008). This is important because their contribution is not consistent with the gradient-diffusion PBL parameterization formations that are commonly used in weather and climate modeling. For example, see Figures 6 and 9 in Zhu (2008). Zhu used a five-domain WRF model in which the inner-most domain approximately resolved the turbulent fluxes. In this domain, the TCBL was highly organized and the contribution to the total fluxes of momentum, heat and water vapor, due to organized part of the TCBL are all large. The vertical profiles of these fluxes are larger than and look nothing like the parameterized fluxes in the outer domains.

## PBL ROLLS

Rolls are a very common feature of the PBL in general (Kuettner, 1959; Brown, 1980, Mikhaylova and Ordanovich, 1991; Etling and Brown, 1993; Young et al., 2002). In fact, the characteristics of the TCBL rolls follow essentially the same scaling as for “normal” PBLs (Foster, 2005). The large magnitude of roll-induced variability in the TCBL near-surface wind speed primarily reflects the fact that near-surface wind speeds are large in hurricane conditions. Hence, what we learn about rolls is most likely broadly applicable across a wide range of PBL conditions. Most basically, a clear understanding of why (or why not) rolls form in a particular region and how their basic characteristics depend on the local mean state of the PBL has not been firmly established by observations. A comprehensive PBL roll climatology has not been completed. This is largely because the primary flow visualization for rolls is the formation of PBL-top “cloud streets” in the linear updraft regions associated with the rolls flanked by clear air in the broader associated linear downdraft regions. Rolls can, and often do, form in cloud-free regions (e.g. Reinking et al., 1981). Climatologies from cloud imagery have been performed in limited regions (e.g. Walter 1980; Walter and Overland 1984; Miura, 1986; Brummer and Pohlmann, 2000). However, low-level cloud data sets have many limitations and there is no existing catalog (either basin-scale or global) of rolls and of their controlling environmental conditions. There is a clear-cut need for new satellite approaches to provide OLE data with significantly more detail and broader maritime coverage. It would be a significant parameterization error to either omit roll effects when they are expected to form or to include them when they should be absent. Analogous structures to rolls that form in the upper ocean boundary layer (OBL) are called Langmuir circulations (Leibovich, 1983; Mc Williams et al. 1997). It has been shown that the accuracy of OBL parameterizations is significantly improved

when their effects are included, although developing accurate parameterizations of the Langmuir contributions remains a challenge (e.g. Fan and Griffies, 2014).

## TCBL ROLL VISUALIZATION USING SAR

One of the primary uses for SAR in tropical cyclones is to produce fine-scale (*O(1 km)*) maps of the ocean vector winds (OVW). Empirical geophysical model functions describe the radar backscatter given the surface wind speed, radar incidence angle and the relative azimuth between the radar beam and the wind vector. Scatterometers obtain multiple, nearly-simultaneous backscatter measurements over the same wind vector cell at different incidence and azimuth angles, which allows OVW retrieval. SAR can only obtain a single backscatter measurement per cell, which means that the wind direction must be estimated by other means. OLE secondary circulations create distinctive ocean surface cm-scale modulation signatures that are observable using slight contrasts in SAR radar backscatter imagery (e.g. Gerling, 1986; Sikora et al., 1997; Vandemark et al. 2001; Young et al., 2000). The roll signatures are routinely extracted using image processing techniques in order to determine the wind direction (e.g. Horstmann 2013). They can also be detected using local FFT analyses (e.g. Zhang et al., 2008). Morrison et al. (2005), using Doppler radar observations, found that the basic TCBL rolls that correspond well to these routine SAR detections had aspect ratios (wavelength/TCBL depth) in the range 2.5 to 4. Note that these aspect ratios are larger than for the Doppler on Wheels observations. Losorlo et al. (2009) documented smaller-scale roll structures, more closely resembling the Wurman and Winslow (1998) observations, interacting with larger-scale rolls with scales resembling the Morrison et al. (2005) observations.

Interestingly, in all of the SAR images of TCBLs, there is a clear signature of much larger roll-like organized flow features, with aspect ratios around 10, in the surface wind divergence and wind stress curls (Figure 1). The divergence features are associated with local enhancement and reduction of the inflow (lower branch of hurricane secondary circulation) and the wind stress curl features are associated with local enhancement and reduction of the azimuthal flow (surface signature of the hurricane primary circulation). The phasing is consistent with the presence of very large aspect ratio rolls. Similar structures were reported by Gall et al. (1998) in the layer corresponding to the upper TCBL and lower troposphere. They noted the similarity to PBL roll vortices.

Hence, we have evidence of at least three classes of rolls that are most likely simultaneously present in the TCBL. The largest scale class would appear to provide a direct circulation that connects the sea surface and the lower troposphere. While this presents challenges for TCBL parameterizations, it does appear to provide a means by which parameterizations can be evaluated. Mourad and Brown (1990) developed a model for upscale energy transfer from fast-growing smaller scale 2-D neutrally-stratified PBL rolls into much slower growing large-scale 2-D rolls via resonant triad interaction. The interaction was limited to co-linear circulations and they did not provide selection criteria. Foster (2013, and unpublished work) has extended this model to 3-D, non-neutral stratification and to non-co-linear modes. A proposed selection criterion is that the full system seeks the combination that maximizes the downward flux of momentum. An example calculation is shown in Figure 2, which employed a specific eddy-viscosity parameterization similar to Hong et al. (2006) for the small-scale, down-gradient fluxes. The conditions that maximize the near-surface momentum transfer correspond to

triads that include the basic (e.g. “Morrison”) rolls, Small-scale, near-surface (e.g. “Wurman and Winslow”) rolls and large-scale rolls. This particular example predicts large aspect ratio roll orientations that are slightly off the observations. The predicted orientations depend on the assumed small-scale eddy-viscosity parameterization. Hence, a series of fairly straightforward calculations seeking to match predicted and observed multi-scale roll characteristics can place bounds on the vertical distribution of effective eddy viscosity (representing the local, down-gradient contribution to the total fluxes) in the TCBL. At present, observations can only place limits on an averaged effective eddy viscosity value (Zhang and Drennan, 2012).

The most unstable (basic) modes are the over-all most efficient structures at extracting energy from the mean flow, which is why they have the fastest growth rates are why they are predicted to be a persistent feature of the equilibrium mean state. It should be noted that the small-scale modes and the large-scale modes in the strong momentum transfer triad regime are both very slowly-growing in the classic instability analysis and would therefore not be expected to play a role in the nonlinear equilibrium condition. However, the small-scale modes actually are quite close in scale and orientation to what could be called the “most dangerous” modes that undergo short-term explosive “algebraic” growth that exceeds the exponential growth rate over finite time intervals (e.g. Foster, 1997). It can be shown that these small modes will attain amplitudes comparable to that of the basic modes while still in the linear growth phase. This allows the basic mode to transfer energy into the much slower large aspect ratio mode via the triad interaction in the quasi-linear regime that arises before the full nonlinear quasi-equilibrium is established.

The ubiquity of multi-scale TCBL rolls combined with various LES and LES-like modeling studies suggests that they make an important role that is not captured in parameterizations (e.g. Zhu, 2008; Nakanishi and Niino, 2014; Wang and Jiang, 2017). Simultaneous flux and structure measurements are needed. It is also necessary to obtain information about how the fluxes vary with respect to the branches of the OLE mean circulation. Observations suggest that in the case of rolls, the local fluxes in the linear updraft regions are higher than the surrounding regions. What is the representative mean flux for a region of typical numerical modeling scale? How long or how far should the high frequency data be averaged when calculating fluxes? These questions require a means of flow visualization coincident with the local flux measurements. A DWL has been installed on one of the NOAA P-3 aircraft (D. Emmitt, pers. comm.). Additionally, instruments like the Imaging Wind and Rain Profiler (IWRAP) can also detect rolls. However, the NOAA aircraft do not make TCBL flux flights and cannot fly near UAVs. New strategies (such as arrays of pre-deployed surface buoys, surface floats or undersea gliders or ???) are needed.

## MARINE BOUNDARY LAYER ROLLS

As mentioned above, the basic TCBL rolls appear to share the same scaling as rolls in more normal conditions. Hence, much can be learned from observations in more benign conditions. Satellite data is necessary for global coverage, but we must avoid a “cloudy conditions” sampling bias, which makes SAR an obvious choice as it is largely unaffected by clouds. An attempt to compile a dataset that catalogues OLE variability using full-swath SAR imagery was hampered both by the lack of global ocean data coverage and by image quality issues in the RadarSAT-1 imagery that was available at the time (Levy, 2001). Full SAR imagery

is quite limited and coverage is miniscule compared to the total sea surface. We are currently addressing the basic problem of no global assessment (not quite climatology) using the ESA Sentinel-1/2 SAR wave mode vignettes, which is the default mode of the Sentinel satellites over the world's oceans. Roughly 2700 vignettes are continuously collected at approximately 100 km spacing per satellite per day. The high quality and extensive coverage of Sentinel-1 WV vignettes presents the first opportunity to produce both a global catalog of maritime OLE data and one that can be used to test and quantify the mean conditions under which they do and do not form through co-location with ECMWF analyses.

An equally-important issue is the effects of shallow convection, loosely "cells", on PBL fluxes. Cloud imagery routinely shows a transition from rolls to cells, which presumably occurs as some combination of bulk Reynolds and Richardson numbers that define a regime boundary. SAR data are also useful for visualizing this transition, even in the absence of clouds. Shallow convection for moderate to strongly unstable stratification has been added to the conventional down-gradient modeling parameterizations (Bretherton et al., 2004, Wietek et al., 2011ab). However, roll effects, which may be just as important, are generally not included in the near-neutral stratification regime.

Figure 3 shows line of sight DWL winds obtained during MABL flights off-shore from Monterey, CA on Sep. 30, 2012 as part of an Office of naval Research directed research initiative that sought to improve PBL parameterization (PI: D. Emmitt). For these flights, the DWL was pointed forward and slightly downward, which allowed fine vertical resolution of a vertical slice through the MABL roughly perpendicular to the mean wind. Near the surface the MABL was about 300 m deep with a layer on top that may have moved in from onshore. This flight leg was roughly perpendicular to the local mean wind direction. Modulations of the near-surface line of sight wind are readily apparent at about twice the layer depth. The spectral width of the DWL signal broadens in these areas, which suggests increased level of turbulence associated with the rolls. This is consistent with the findings of LeMone (1976)Short-time averages of high-frequency measurements from a towed platform suggested that the fluxes were higher in the high turbulence bands associated with the features seen in the DWL. Co-location of data from the aircraft, the DWL sampling (~6 km ahead of the aircraft) and the towed platform (behind and downwind of the aircraft) has proven challenging. Furthermore, the averaging times were necessarily shorter than would ordinarily be used. However, these preliminary results provide a starting point for future investigations.

## PARAMETERIZING ROLLS

A means by which the eddy diffusivity/mass flux (EDMF) modeling paradigm could be expanded to include roll effects was suggested by Zhu (2008). Results from the DWL study were modeled using the nonlinear roll model and used to determine key terms for the non-local effects in a version of the EDMF model. There are significant differences between roll OLE and shallow convection. For example, rolls are, of course, far less skewed (0.3 to 0.45) than convection (0.1). One parameter of importance estimates the lateral entrainment between the ED-dominated environment and the non-local contribution (usually the MF, but in this case the rolls). In the standard EDMF model, this parameter is $\varepsilon \sim 0.001$. However, vertical profiles from the roll-modified EDMF using this value were far too efficient at mixing momentum downward. We found that $\varepsilon \sim 0.01$ produced good results. Zhu (2008) had examined the same parameter in his

nested WRF-LES study and estimated the same value. Fundamentally, however, incorporating rolls into such a parameterization is not so straightforward. In the normal EDMF framework, the non-local MF effects are convective and can be parameterized in terms of the surface conditions alone. Fundamentally, rolls depend on the full mean flow profiles, not surface values. In particular, the roll updraft regions do not have to align with the excess as convective updrafts do in the EDMF.

Gao and Ginis (2016) have experimented with simple super-parameterization of roll effects using embedded 2-D LES in idealized meso-scale hurricane studies. This presents its own set of problems since only the cross-wind roll contribution is included. Plus, rolls frequently form at angles relative to the mean wind (depending on stratification and baroclinicity). These effects are not be captured by the 2-D grids.

## SUMMARY

The near-neutral PBL frequently forms organized large eddies (roll vortices) that can have a significant effect on the fluxes of momentum, heat and water vapor between the surface and the lower troposphere. These OLE can form in a range of scales and these different scales can interact nonlinearly. The net effect of these OLE is an advective transport, as opposed to down-gradient flux, through the PBL. The particular OLE shapes that form and the fluxes that are induced in a given PBL depend primarily on the mean flow profiles rather than the surface conditions. This presents challenges to both observations and parameterization. Estimates of the OLE effect on fluxes range from 5% to 25%. Consequently, there is a need to combine flow visualization along with traditional flux measurements in order to place the fluxes in context. Similarly, averaging procedures may need to take the PBL mean state in consideration since the observations suggest that roll updrafts are regions of significantly higher fluxes.

## REFERENCES

Bretherton CS et al., 2004: A New Parameterization for Shallow Cumulus Convection and Its Application to Marine Subtropical Cloud-Topped Boundary Layers. Part I: Description and 1D Results, *Mon Wea Rev*, **132**, 864-882

Brown, RA 1980: Longitudinal instabilities and secondary flows in the planetary boundary layer: A review. *Rev. Geophys. Space Phys.*, **18**, 683–697.

Brummer B and S Pohlmann 2000: Wintertime roll and cell convection over Greenland and Barents Sea regions: A climatology, *J. Geophys. Rev*. **105**(D12) 15,559-15,566

Etling, D, and RA Brown, 1993: Roll vortices in the planetary boundary layer: A review. *Bound.-Layer Meteor.*, **65**, 215–248

Fan Y, SM Griffies 2014: Impacts of Parameterized Langmuir Turbulence and Nonbreaking Wave Mixing in Global Climate Simulations, J. Phys. Ocean., 27, 4752-4775.

Foster RC 1997: Structure and energetics of optimal Ekman layer perturbations, *J Fluid Mech*, **333**, 97-123.

Foster RC 2005: Why rolls are prevalent in the hurricane boundary layer, *J Atmos. Sci*, **62**, 2647-2661.

Foster RC 2013: Signature of large aspect ratio roll vortices in synthetic aperture radar images of tropical cyclones, *Oceanography*, **26** 58-67.

Gall R, J Tuttle and P Hildebrand, 1998: Small-scale spiral bands observed in hurricanes Andrew, Hugo and Erin, *Mon. Wea. Rev*, **126**, 1749-1766.

Gerling, TW: 1986, Structure of the Surface Wind Field from the Seasat SAR, *J. Geophys. Res*., **91**, 2308–2320.

Gao, K. and I. Ginis, 2016: On the equilibrium-state roll vortices and their effect in the hurricane boundary layer. *J. Atmos. Sci*., **73**, 1205-1222.

Hong, Song–You, Yign Noh, Jimy Dudhia, 2006: A new vertical diffusion package with an explicit treatment of entrainment processes. *Mon. Wea. Rev*., **134**, 2318–2341.

Horstmann, J et al. 2013: Tropical cyclone winds retrieved from synthetic aperture radars, *Oceanography*, **26**, 46-57.

Jones, CT, TD Sikora, PW Vachon, and JR Buckley, 2014: Ocean feature analysis using automated detection and classification of sea-surface temperature front signatures in RADARSAT-2 images. *B. Am. Meteorol. Soc*., **95**, 677-679.

Kuettner, JP, 1959: The band structure of the atmosphere. *Tellus*, **11**, 267–294.

LeMone, M 1976: Modulation of turbulent energy by longitudinal rolls in an unstable boundary layer. *J. Atmos. Sci.*, **33**, 1308–1320.

Leibovich, S, 1983: The form and dynamics of Langmuir circulations, *Ann. Rev. Fluid Mech*.,**15**, 391-427.

Levy, G, 2001: Boundary layer roll statistics from SAR, *J. Geophys. Res.*, **28**, 1993–1995

Losorlo, S et al. 2008: An observational study of hurricane boundary layer small scale coherent structures, *Mon. Wea. Rev.*, **136**, 2871-2893.

McWilliams, JC, PP Sullivan, C-H Moeng, 1997: Langmuir turbulence in the ocean, *J. Fluid Mech*., **334**, 1-30.

Mikhaylova, LA, and AY Ordanovich, 1991: Coherent structures in the atmospheric boundary layer (a survey). *Izv. Acad. Sci. USSR, Atmos. Oceanic Phys.*, **27**, 413–428.

Miura, Y, 1986: Aspect ratios of longitudinal rolls and convection cells observed during cold air outbreaks. *J. Atmos. Sci.*, **43**, 26–39.

Morrison I. et al., 2005: An Observational Case for the Prevalence of Roll Vortices in the Hurricane Boundary Layer, *J Atmos. Sci*, **62**, 2662-2673

Mourad, P.D., Brown, R.A.: 1990, On Multiscale Large Eddy States in Weakly Stratified Planetary Boundary Layers, *J. Atmos. Sci*. **47**, 414–438.

Nakanishi M and H Niino, 2012: Large-Eddy Simulation of Roll Vortices in a Hurricane Boundary Layer. *J. Atmos. Sci.*, **69**, 3558–3575.

Reinking, RF, R. JDoviak, and RO Gilmer, 1981: Clear-air roll vortices and turbulent motions as detected with an airborne gust probe and dual-Doppler radar. *J. Appl. Meteor.*, **20**, 678–685.

Vandemark, D, PD Mourad, SA Bailey, TL Crawford, CA Vogel, J Sun and B Chapron 2001: Measured changes in ocean surface roughness due to atmospheric boundary layer rolls, *J Geo. Phys*. **43**, 26-39.

Walter, BA, 1980: Wintertime observations of roll clouds over the Bering Sea. *Mon. Wea. Rev*., **108**, 2024–2031.

Walter BA and JE Overland, 1984: Observations of longitudinal rolls in a near neutral atmosphere. *Mon. Wea. Rev*., **112**, 200–208.

Wang, S. and Jiang, Q.: Impact of vertical wind shear on roll structure in idealized hurricane boundary layers, *Atmos. Chem. Phys.*, **17**, 3507-3524, https://doi.org/10.5194/acp-17-3507-2017, 2017.

Witek et al. 2011a: An Integrated TKE-Based Eddy Diffusivity/Mass Flux Boundary Layer Closure for the Dry Convective Boundary Layer, *J Atmos. Sci.*, **68**, 1526-1540.

Witek et al. 2011b: An Eddy Diffusivity–Mass Flux Approach to the Vertical Transport of Turbulent Kinetic Energy in Convective Boundary Layers, *J Atmos. Sci.*, **68**, 2385-2394.

Wurman, J. and J. Winslow, 1998: Intense sub-kilometer boundary layer rolls in Hurricane Fran. *Science*, **280**, 555-557.

Young GS, TD Sikora, NS Winstead 2000: Inferring Marine Atmospheric Boundary Layer Properties from Spectral Characteristics of Satellite-Borne SAR Imagery, *Mon Wea Rev.* **128**, 1506-1520.

Young GS, DAR Kristovich, MR Hjelmfelt, RC Foster, 2002: Rolls, Streets, Waves, and More: A Review of Quasi-Two-Dimensional Structures in the Atmospheric Boundary Layer (and electronic supplement), *Bull Amer Meteorol Soc* **83**, 997-1001.

Zhang J. A., K. B. Katsaros, P. G. Black, S. Lehner, J. R. French and W. M. Drennan, 2008: Effects of roll vortices on turbulent fluxes in the hurricane boundary layer. *Bound.-Layer Meteor.*, **128**, 173–189.

Zhang J, and W. Drennan, 2012: An Observational Study of Vertical Eddy Diffusivity in the Hurricane Boundary Layer, *J Atmos Sci*, **69**, 3223-3236

Zhu, P., 2008: Simulation and Parameterization of the Turbulent Transport in the Hurricane Boundary Layer by Large Eddies. *J. Geophys. Res.*, **113**, D17104

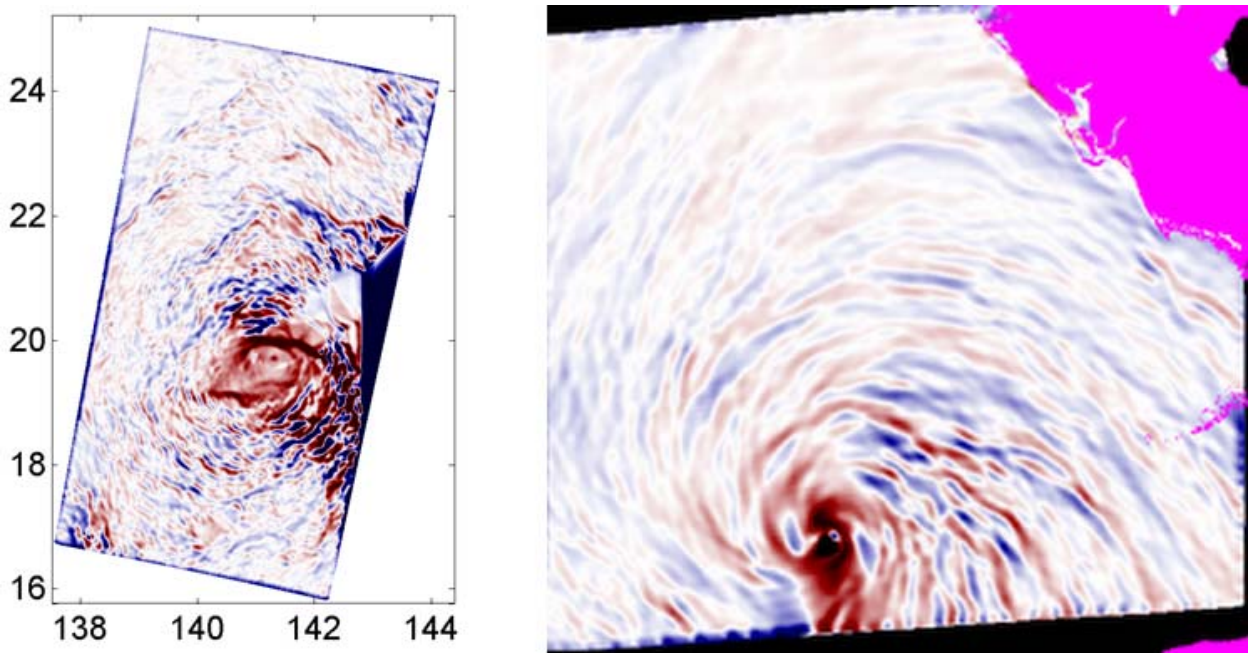


Figure 1: (a) Typhoon Malakas, 22 Sep, 2010 surface wind stress curl. (b) Hurricane Katrina, 29 August, 2005. Surface wind divergences.

Figure 2: (a) Momentum transfer index for resonant triads plotted against radial and azimuthal wave numbers. Hollow symbols represent less momentum transfer than a single roll mode. (b) Linear growth rates for the assumed mean flow. Cross shows most unstable normal

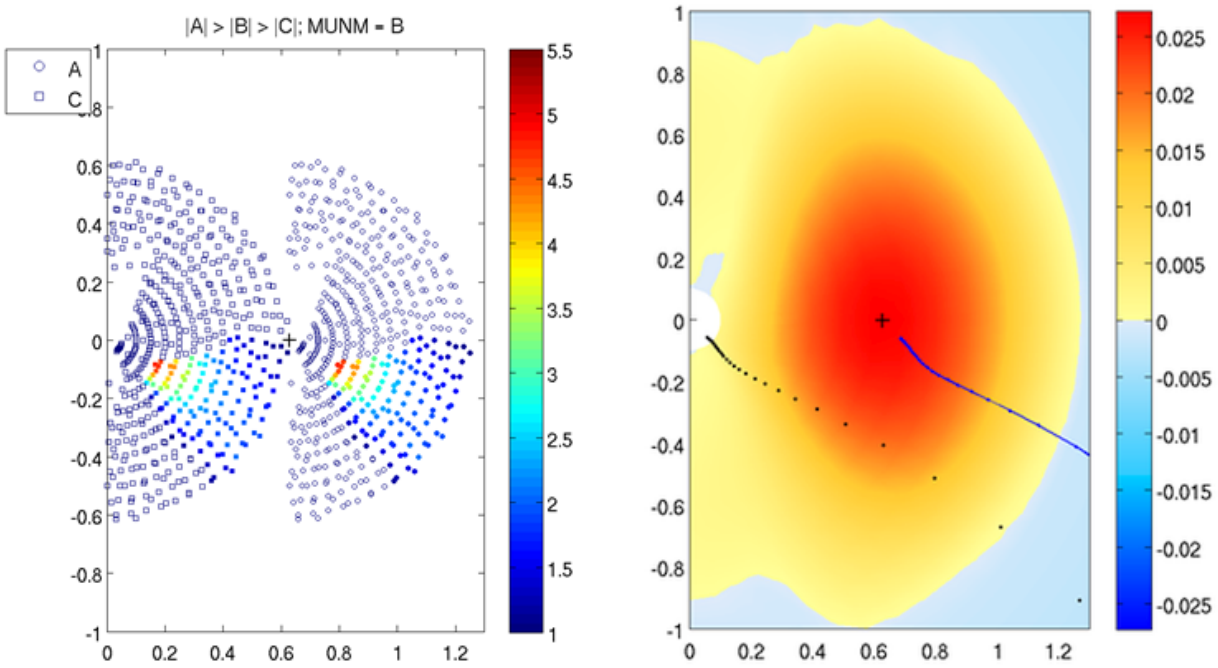


mode. Line of modes to the lower right are the most dangereous algebraic perturbations. Moodes to the lower left are the slowly-growing large-scale mode

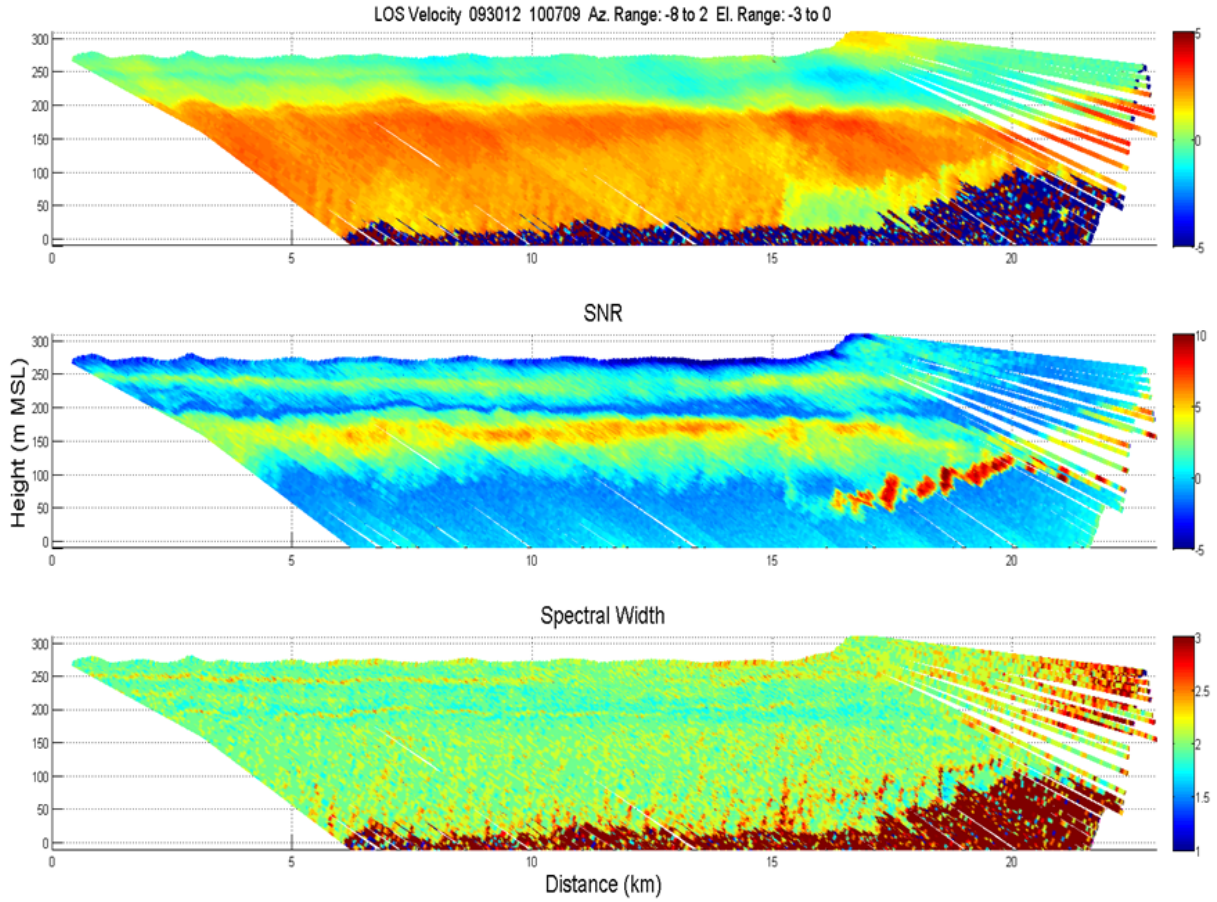


Figure 3: Airborne Doppler wind lidar line-of-sight winds in the MABL near Monterey, CA (D. Emmitt). Aircraft flew across the mean wind above the top of the shallow MABL staring forward and slightly down. (a)LOS winds. (c) Spectral width of the Doppler returns.

# Momentum Fluxes Over Land: A Difficult But Important and Neglected Issue

David Randall
Department of Atmospheric Science
Colorado State University

Since the 1970s, by far the most active area of boundary-layer research has dealt with boundary-layer clouds, especially stratocumulus and shallow cumulus clouds. Almost all of this large body of research deals with various thermodynamic and radiative aspects of buoyancy-driven circulations, primarily over the subtropical and tropical oceans. Relatively little attention has been paid to the momentum fluxes in such cloudy boundary layers.

The same 40-year period has seen the introduction and eventual operational use of radar-based satellite observations of surface momentum fluxes over the oceans, beginning with the 1978 launch of Seasat. Space-based scatterometers have now provided decades of accurate observations of surface momentum fluxes over the oceans.

Unfortunately, we have nothing comparable over land. Near-surface winds are generally weaker over land than over the oceans, but the momentum fluxes over land can be strong and arise from a wider variety of processes than momentum fluxes over the ocean. The only global climatologies for momentum fluxes over land are based on reanalysis. We don’t know how good those climatologies are, but there is plenty of reason to worry.

# Advancing Measurement Science for Atmospheric Trace Gas Flow Measurement and Estimation: Impact of the Atmospheric Boundary Layer

James Whetstone
Special Programs Office
National Institute of Standards and Technology

Atmospheric trace gases and particulates, e.g., greenhouse gases and a range of obnoxious to hazardous air pollutants, result in significant societal impacts and are manifest as the focus of a range of research and regulatory interests. Their evolution and dynamics from emission sources on or near the Earth's surface into and through the atmospheric boundary layer (ABL) to the troposphere are strongly influenced by ABL properties and dynamics. Quantification of their impact on a range of societal issues are strongly dependent upon atmospheric observations and analyses. The fidelity of these results is central to many discussions and the focus of research efforts in the air quality and greenhouse gas mitigation communities.

In the case of the greenhouse gases (GHG), mole fraction observations coupled with atmospheric transport models and statistical inference methods are being used to measure GHG flow to and from the atmosphere and to identify source and sink locations. National GHG emissions data and reports to the UNFCCC[1] are inherently flow quantification statements, i.e., number of tons of $CO_2$ equivalent per year per socio-economic sector. These are currently based primarily on a range of measurements and methods that utilize the properties and characteristics of the emission processes themselves. Examples are the measurement of both mole fraction and bulk flowrate of combustion products from electrical generation plants to determine flow of $CO_2$, $SO_2$, and $NO_x$ in smokestacks, or the use of transportation statistics and vehicle emission factors to estimate emissions associated with our transportation systems. Atmospheric observing methods have been applied to estimation of their concentration and movement within the global atmosphere. Recent research efforts have been focused on estimating GHG emissions from urban areas with the objective of source attribution. Because cities concentrate population and energy use, GHG emissions are intense from a small fraction of the total area of our country, and they are the source of a significant fraction of total U.S. emissions. Recent efforts by cities have focused on sustainable operations and growth and include greenhouse gas mitigation efforts. Reliable information on GHG emissions, and that of other trace gases, can significantly aid the effective and efficient management of such efforts.

Atmospheric observation and inversion methods applied to GHG emissions at urban scales, are derived from GHG mole fraction measurement networks located within and immediately outside urban domains. Mole fraction observations combined with atmospheric transport measurements and models provide a means to attribute sources to specific locations and estimate their flux to and from the atmosphere. Critical to improving the capabilities of these analyses are

[1] United Nations Framework Convention on Climate Change

advances in ABL dynamics knowledge and its accurate representation in transport models, such as the Weather Research and Forecasting (WRF)[2] and the Stochastic Time-Inverted Lagrangian Transport (STILT)[3] models.

NIST is engaged in measurement science research to advance measurement and estimation capabilities for GHG flows to and from the atmosphere at urban scales as a means of strengthening the technical quality of GHG inventory data and reports. The goal is to advance development and demonstrate measurement and analysis methods suitable for standardization that estimate GHG ($CO_2$ & $CH_4$) emissions for a range of city types. Specifically, to quantify trends & absolute values and uncertainties and to attribute emissions spatially, temporally, and by economic sector. With our collaborators, NIST pursues a strategy of developing city "laboratories" or testbed sites, investigating measurements with potential to positively impact determination of air quality, energy efficiency & utilization, traffic patterns, & urban planning. Through partnerships with universities, private industry organizations, and other Federal Agencies, NIST is developing the fundamentals upon which good practices & standards useful to others will result in accurate measurement and estimation methods for urban trace gas emissions.

This research, implemented in three cities and regions, Indianapolis, the Los Angeles Air Basin, and the Northeast Corridor from Washington, D.C to Boston, constitutes the NIST Urban GHG Measurements Testbed System. It is focused on both atmospheric observations and analyses, so-called top down approaches, and GHG emissions modeling or bottom up methods to strengthen both approaches. Emissions modeling utilizes a range of socio-economic and inventory data submitted to the EPA to determine emissions at spatial and temporal scales consistent with those of urban atmospheric observing methods. Atmospheric observations applied to urban spatial scales inherently emphasize the ABL influences in transporting GHG emissions, and of course, particulate materials occurring at trace levels, from their source to observing points and beyond. Mole fraction observing networks, composed of observing points located advantageously within and just outside cities, are mostly sited on communication towers, or at times on building roofs. These have sampling heights that range from 40 to 100 meters in the network's interior urban locations and at 100 meters or above at stations along the network periphery. These have spatial and temporal sensitivities that are strongly, perhaps completely, influenced by ABL dynamics. The current state of modeling capabilities limit analyses to times of day when the ABL is fully developed. Therefore, observation locations are fully immersed in the ABL and its dynamics largely determine network observing performance.

Recent efforts[4] in Indianapolis, the initial location of the NIST GHG Measurements Testbed System, have attempted to better represent ABL dynamics in WRF through data assimilation methods. Since surface-based meteorological observations reveal only limited insights into ABL behavior, this investigation used upper-air observational data taken from the Aircraft Communications Addressing and Reporting System (ACARS) program and continuous ground-based Doppler Lidar wind observations. In this limited study conducted for the months of September to November of 2013, wind direction mean absolute error (MAE) decreased from 26 to 14 degrees and wind speed MAE decreased from 2.0 to 1.2 m/sec relative to values obtained

[2] https://www.mmm.ucar.edu/weather-research-and-forecasting-model

[3] http://stilt-model.org/pmwiki/pmwiki.php

[4] Deng A, Lauvaux T, Davis KJ, Gaudet BJ, Miles N, Richardson SJ, et al.. Toward reduced transport errors in a high resolution urban CO2 inversion system. Elem Sci Anth. 2017;5:20. DOI: http://doi.org/10.1525/elementa.133

from WRF runs with no data assimilation. The bias remained small (< 6 degrees and 0.2 m/sec) over the range of the experiment. ABL depth MAE reduced by ~10%, with little bias reduction. These results indicate that although the spatial distribution of $CO_2$ fluxes obtained in the inversion analysis were positively impacted by transport model performance, the overall flux estimates were not significantly reduced across the several WRF simulation schemes used. Although the improvement in transport simulation performance alone did not translate significantly to improvement in inversion performance, one important component of a complex method is improved. Repetition of the experiment in another city of the testbed is warranted and planned. Continued improvements in performance of other components of this complex, multi-step observation and analysis process continues with the anticipation that advancements on several fronts will improve the overall performance.

# Densely spaced observations of trace gases: Constraints on the PBL

Ronald C. Cohen
Departments of Chemistry and of Earth and Planetary Science
University of California, Berkeley

Mixing within and across the top of the boundary layer affects exposure of humans, animals and plants to toxic chemicals and controls the lifetime of reactive chemicals within the atmosphere. The interactions are strong, and because some aspects of the chemistry are highly non-linear errors in representing boundary layer dynamics can induce errors of comparable (or larger) size in chemical concentrations. As a result, measurements of trace gas concentrations from the surface and from space can carry information about boundary layer mixing. This is true even if absolute values of emissions are known poorly, if the variability in emissions on the time scale of interest is small compared to variability in the boundary layer dynamics on that time scale.

I describe two emerging strategies for observing chemicals in ways that could be used to improve our understanding of the boundary layer and give some examples of a data assimilation approach to using the observations that provide constraints on the boundary layer. First, I describe observations of urban plumes using the OMI and TEMPO UV/Vis instruments. OMI is aboard the Aura satellite and observes reflected sunlight once a day at ~1:30 local time with a spatial resolution of 13 x 24 km. TEMPO will be launched into a geostationary orbit in 2-3 years with observations once an hour with a spatial resolution of ~3 x 3 km. The observations from both instruments can be used to retrieve column $NO_2$. The measurements will provide clear information on the emissions from major urban and power plant sources and their downwind evolution. Both the retrieval and the downwind evolution are sensitive to the PBL. Second, I describe an example of a dense network of surface observations, http://beacon.berkeley.edu/ , that provide point measurements at approximately 2km spacing of $CO_2$, NO, $NO_2$, $O_3$, CO, and PM. Such networks will provide information about emissions and boundary layer mixing. For many of these species, variation in the emissions can be small on some time scales (e.g., every Monday approximately the same) or some spatial scales (e.g. distance from a highway). To oversimplify, one might say that the first day of measurements tells us about emissions and the subsequent days have information that can be used to constrain the boundary layer. In both cases, the measurements are going to become widely available independent of the interests of the atmospheric boundary layer research community.

The third aspect of my presentation will be a description of one possible approach to using these types of observations. I will show how data assimilation with column $NO_2$ as a constraint can improve representation of boundary layer wind speed and direction and improve the representation of vertical mixing.

# Air Quality Predictions and Planetary Boundary Layer

Ivanka Stajner
NOAA/NWS/STI
with contributions from the air quality implementation team, especially
Jeff McQueen (NOAA/NCEP/EMC) and Amanda Sleinkofer, Millersville University

Air quality predictions of ozone, wildfire smoke, windblown dust and fine particulate matter (PM2.5) are provided by NOAA/National Weather Service for next 48 hours using models with 12km resolution. The predictions are displayed at http://airquality.weather.gov/ and web services for these predictions are available at https://idpgis.ncep.noaa.gov/arcgis/rest/services/NWS_Forecasts_Guidance_Warnings.

The planetary boundary layer (PBL) plays a key role in air quality. Pollutants and precursor species are emitted into the PBL and lost to wet and dry deposition to the surface. Pollutants are transported by the wind, mixed and diluted by atmospheric turbulence. Temperature and humidity conditions in the PBL affect chemical reactions and the rates of chemical formation. Diurnal cycling of the PBL from its day-time deep well-mixed state to a night-time shallow stable layer leaves behind pollutants that become incorporated into the free troposphere. Next morning, remnants of the previous day's PBL or a new air mass of pollutants transported into lowest free troposphere, sometimes from afar, may get incorporated into the PBL as its growth resumes.

The accuracy of air quality predictions depends on the understanding and accurate representation of PBL processes in prediction models. Some challenges for prediction of the diurnal cycle in the concentrations of pollutants may be related to the uncertainties in the prediction of PBL diurnal cycle. Diurnal range of NOAA's ozone predictions tends to be smaller than observed and the night time ozone depletion is underestimated (Fig. 1a). Both, the previously operational version of the modeling system and the currently operational system overestimate predicted PM2.5 concentrations at night (Fig. 1b). Additional challenges affect prediction in coastal areas where underestimated PBL height over water can lead to overestimated ozone over water, which can subsequently be transported over coastal areas. Representation of sea breeze, land breeze, the flow over complex mountainous terrain, cold pools and the diurnal evolution of the PBL may all improve with finer resolution models, but they currently remain a challenge.

Sparsity of routine PBL height observations limits the ability to routinely verify model performance of the diurnal evolution of PBL under a variety of conditions.

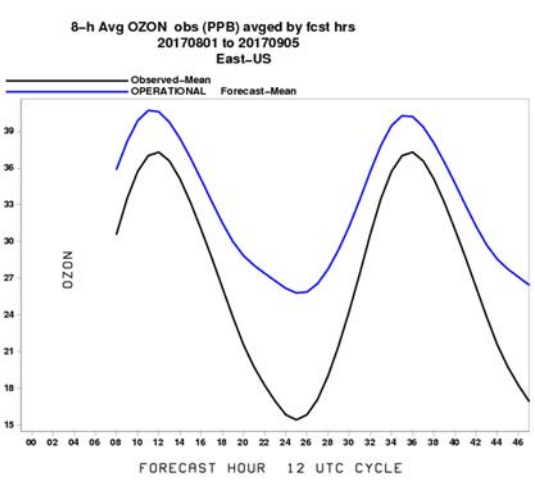


a)

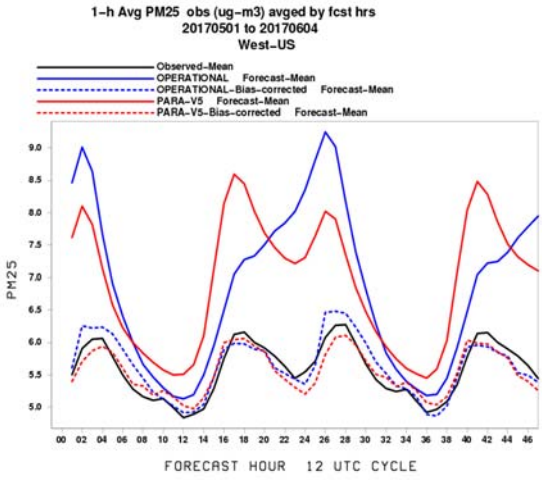


b)

FIGURE 1. Air quality predictions are shown averaged by forecast hour and compared with surface observations from AIRNow network (black). a) Eight-hourly average ozone for late summer in the Eastern U. S. with predictions shown in blue. b) hourly PM2.5 for late spring in the Western U. S. with then operational predictions shown in blue and now operational predictions shown in red.

Observational needs exist for evaluation of model predictions and for improved understanding of:

- PBL height and the extent of vertical mixing controlling pollutant concentrations
- Diurnal evolution of PBL exporting pollutants into the free troposphere
- PBL in the coastal environment, land breeze, sea breeze
- Urban PBL at night time
- Cold air pools that can trap pollution near the surface
- Flow over complex terrain
- PBL meteorology and its impacts on the amount of pollutant emissions (e.g. wildfires, dust), chemical processing and dispersion of pollutants as well as their wet and dry deposition
- Atmospheric moisture profiles in PBL
- Atmospheric composition profiles in PBL including ozone, and precursor species like NOx and VOCs, and particulate matter with characterization of its size and composition

# Breathing in the Boundary Layer

Sherri W. Hunt, Vito Ilacqua, and Jon Pleim
US EPA, Office of Research and Development

Atmospheric scientists and meteorologists consider the complexity of the planetary boundary layer with multiple mixing states and changes that occur throughout the day. Many health researchers will consider the thin layer of the atmosphere in which we live and breathe in a less complex manner. While there is an understanding that pollutant concentrations change over the course of a day in response to emissions, chemistry, and meteorology, the complex mixing processes and factors impacting the change in the boundary layer height and composition are often not considered.

Health estimates of the impacts and risks of air pollution are based on a combination of exposure estimates and health measures. A lack of understanding of the boundary layer may lead to in accuracies in the degree of pollutant exposure that is calculated for an analysis. For health researchers lack of understanding of the planetary boundary layer may lead to errors in epidemiology studies and risk assessments. Uncertainty and error in the health metrics is beyond the scope of this discussion.

Air pollutant epidemiology studies may depend on changes in pollutant concentration over time or space with a range of temporal and spatial scales of interest. These will vary depending on the health effect considered and the method for estimating pollutant exposure for study subjects. The simplest exposure models use the pollutant concentration measured at the nearest air quality monitor as the level for exposure. In this case, uncertainty in the boundary layer may impact an exposure estimate if the spatial variation leads to different characteristics at the monitor and the subject's location. Exposure is often estimated with a land-use regression model which includes measurement data from nearby monitors and information regarding key sources such as busy roadways or point sources. Spatial scale may also impact the accuracy of exposure modeled with this method.

The degree of spatial resolution needed for an exposure estimate is inversely related to the time frame of interest for a health impact. Random spatial errors in estimating the boundary layer height lead to errors that generally decrease the strength of observed effect, especially for short-term studies. For long-term impacts, for instance the development of cardiovascular disease, the length of time decreases the importance of small local changes in exposure. Even at these longer time scales, however, the error in estimating the mixing height could have a significant impact if it has a significant temporal correlation with the emissions pattern, or if it’s constant over space (e.g. topography effects). In such cases, it may lead to either over- or underestimating the association between exposure and health effect. For risk assessment studies, assuming a known dose-response relationship, the error in risk estimates also depends on the error in assessing the spatial or temporal variability of the boundary layer, as risk assessments tend to focus on higher percentiles of the risk distribution. The comparability of epidemiological and risk analyses may also be affected by a variable BL error in different geographic locations. Systematic errors in BL estimation that do not meaningfully depend on space and time are generally less problematic for epidemiology and risk analysis.

From the perspective of air quality models, ground level pollutant concentrations are sensitive to the boundary layer height and diurnal evolution, the boundary layer mixing at night

when stable boundary layer depth is very shallow and turbulence is weak, and the timing of evening transition when rush hour mobile emissions dominate. Additional key characteristics are the interactions between the boundary layer model and resolved dynamics which impact wind profiles and transport. Historically, meteorology and air quality models tend to underpredict mixing during evening transition and overnight, which leads to overpredictions of surface emitted species (e.g. NOx, CO, EC, primary organic carbon) and underprediction of secondary species such as $O_3$.

Moving forward the most useful type of boundary layer model depends on the atmospheric conditions (e.g. stable or convective) and the type of health study. Boundary layer models should include mass flux schemes which are consistent for both air quality and meteorology models. Accuracy would be improved for models that combine mass flux schemes for stable and convective conditions and bridge the grey-zone where the energy-containing turbulence scale and spatial filter scale are comparable. Finally, more research is needed into how to model very stable boundary layers with intermittent turbulence, top-down turbulence driven by radiative cooling from cloud decks, and combining boundary layer models with shallow convective cloud models.

# Diode lasers for methane and hydrocarbon sensing in the atmosphere

Leo Hollberg
Department of Physics, and HEPL
Stanford University

Many types of optical sensors for atmospheric gases have been developed and applied as monitoring systems and in other applications.[i] Recently, advances in semiconductor diode lasers have resulted in new lasers that perform well at IR wavelengths and that overlap molecular absorption bands of key atmospheric constituents and trace gases. In a small project at Stanford we have set up a compact IR laser-based spectrometer for measuring methane concentrations in air and evaluating its performance characteristics and capabilities. The spectrometer uses an advanced Distributed FeedBack Interband- Cascade-Laser (DFB-ICL) based on InGaAsSb that operates single frequency (wavelength), is tunable over a small range near 3.27 μm, and operates at room temperature.[ii] That wavelength overlaps some favorable C-H stretch absorption lines in methane, ethane, water, etc. Our focus is primarily on methane detection and monitoring, but the technology is more generally applicable and could be used for any gas-phase organic molecules.

The objective of our project is to develop, demonstrate and evaluate a simple compact infrared laser system that measures with precision and reproducibility atmospheric methane concentrations, including natural variations in methane concentrations (over time and location), and readily detect sources, sinks, and natural gas leaks. To make a significant impact we think that the sensors eventually need to be low cost, reliable, robust and mass producible for widespread distribution. The spectrometer is evaluated in our laboratory environment, but it is designed to be simple and compact, and to require low power consumption for battery-powered capability and wide use in field settings. The grand vision would be the realization of low-cost laser sensors of methane and other atmospheric gases that could be mass produced and widely deployed in real-time monitoring networks.

The simple spectrometer performs surprisingly well and provides sufficient precision that it is feasible to measure methane concentrations in air rapidly (≈ 1s) with an inaccuracy of 1% of the normal concentration levels. That level of performance is our present target goal, with the hopes that such sensors could make a significant impact on climate monitoring, source and sink measurements and leak detection.

The spectroscopic methods that we have been exploring are based on a non-commercial DFB-ICL laser source that was produced in a collaboration between the Naval Research Laboratory and JPL and supplied to our group at Stanford as a laser chip on a small heatspreader.

Images of the tiny semiconductor device and mounting hardware are shown below.

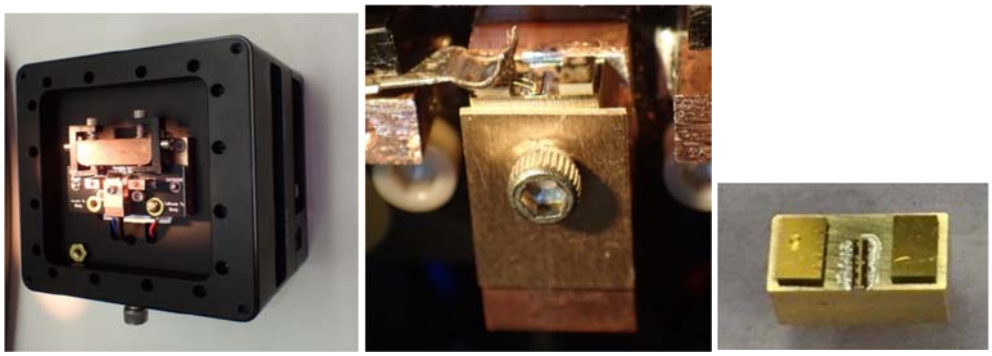

On the right is an image of a InGaAsSb ICL-DFB laser bonded onto a heat-spreader with wirebonds for electrical connection to the actual laser chip in the center. The laser is then installed in a modified commercial diode laser mount, center and left images respectively.

The ICL-DFB laser serves as the source for a very simple absorption spectrometer that uses an IR photo-detector and associated electronics and is able to measure methane concentrations in air over an optical path length of less than two meters. Everything operates at room temperature and in principle could be battery powered. The ICL laser frequency (wavelength) is scanned by changing the laser temperature or the injection current.

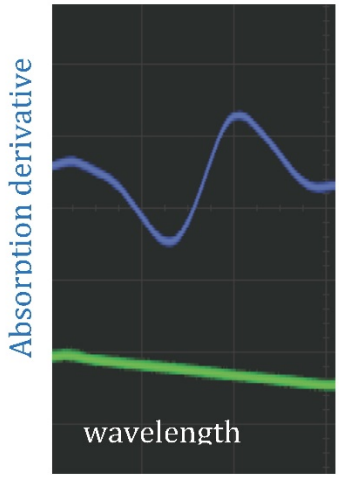


The blue trace shows a typical absorption signal due to methane in the atmosphere and measured over a 1.5 m path length across an optical table in our lab. The laser beam is detected on a room-temperature PbSe photo detector. For atmospheric measurements, we are currently using standard FM-spectroscopy methods that produce an output approximately the first-derivative of the methane absorption signal along the path. The green trace indicates the linear scan of the laser wavelength. The total scan range is ≈ ** GHz.

The system is sufficiently sensitive and low enough noise to measure normal methane concentrations (≈ 1.8 ppm) in air over a short 1.5 m free-space optical path. For those conditions, we observed 1% absorption due to $CH_4$ with a signal to noise ratio of 1400 in 1 Hz detection bandwidth and for a detected optical power of 250 μW.

Initial measurements also show that some characteristics of the diode laser sensors could be improved with relatively minor modifications and upgrades of components that should increase the overall performance and functionality. Performance characteristics (sensitivity, detection bandwidth, dynamic range, accuracy, precision, reproducibility) could be optimized for specific performance goals or applications

Other groups are pursuing similar or related methods and, all combined, these proof-of-principle demonstrations provide convincing evidence that simple spectroscopic systems can be designed and built using advanced ICL-DFB lasers operating at the C-H stretch wavelength region (roughly 3000 $cm^{-1}$, 3.3 μm). The detection sensitivity and

signal-to-noise ratio achieved would support our goal of building a small system that can measure $CH_4$ in air under normal atmospheric conditions with an accuracy of 1% of normal 1.8 ppm concentrations or better. It is technologically feasible to build compact, reliable systems based on this laser technology. The approach is quite general and with proper development of lasers, diode laser sensors could be developed for most any atmospheric gas. Given the importance of better measurements and understanding of carbon, methane, and other atmospheric constituents, these ICL and related QCL laser technologies could be enabling. A remaining big question is whether there is sufficient support from the science, technology and policy fronts to build the political will necessary to motivate the mass production of this type of laser so that costs can be low enough for widespread distribution and use.

## ACKNOWLEDGEMENTS

This work was supported by the Stanford Natural Gas Initiative and benefited from key contributions of a semiconductor IR laser by M. Bagheri of JPL and associated optoelectronic
and mechanical hardware from Thorlabs.

## REFERENCES

Hodgkinson, J., and R. P. Tatam. 2013. Optical gas sensing: a review. *Measurement Science and Technology* 24:012004. DOI:101088/0957-0233/24/1/012004

Forouhar, S., C. Borgentun, C. Frez, R. M. Briggs, M. Bagheri, C. L. Canedy, C. S. Kim, M. Kim, W. W. Bewley, C. D. Merritt, J. Abell, I. Vurgaftman, and J. R. Meyer. 2014. Reliable mid-infrared laterally-coupled distributed-feedback interband cascade lasers. *Applied Physics Letters* 105:051110. DOI: 10.1063/1.4892655.

# Accurate, Precise and Traceable Laser Spectroscopy: Emerging Technology for the Study of Atmospheric Constituents

Adam J. Fleisher, David A. Long, Joseph T. Hodges, Gerd A. Wagner,
and David F. Plusquellic
National Institute of Standards & Technology

## 1. INTRODUCTION

Accurate, precise, and traceable measurement science enables remote sensing over local, regional, continental, and planetary scales. Over the last 50 years, synergistic leaps in laboratory spectroscopy, optical engineering, theoretical physical chemistry, and computer science have enabled satellite, aircraft, and ground-based field campaigns with impressively low uncertainties. To further improve the accuracy of the reference data required by current and future remote sensing campaigns, as well as to explore fundamental molecular, atomic and collisional physics, new high-precision experimental techniques are required with traceability to the International System of Units (SI). Here we present an overview of ongoing NIST developments in laser instrumentation for the rapid acquisition of molecular spectra at the highest levels of accuracy and precision, and introduce extensions of these emerging laboratory technologies to applications in remote sensing and laser ranging.

## 2. EMERGING LABORATORY TECHNOLOGY – RAPID SCANNING AND MULTIPLEXING

Frequency agile, rapid scanning (FARS) spectroscopy mitigates the largest sources of systematic uncertainty in the measurement of accurate spectroscopic parameters (e.g., transition frequencies and intensities, broadening and collisional parameters, temperature coefficients, etc.) by tuning the probe laser at kHz rates [1]. Compared to traditional laser scanning methods (e.g. temperature, current, mechanical grating), radio-frequency sideband tuning is more than 1 000 times faster, and thus “freezes” the systematic biases associated with drifts in sample conditions which general occur over ≥ 1 s. Rapid scanning integrated path, differential absorption light detection and ranging (IPDA LIDAR) of the Earth’s planetary boundary layer (PBL) was used recently to measure CO2 and CH4 dry air concentrations over an open path in proximity to the Rocky Mountain Flatirons in Boulder, Colorado (see Fig. 1) [2].

In addition to rapid scanning, we demonstrated multiplexed spectroscopy using electro-optic (EO) frequency combs and dual-comb spectroscopy (DCS). Multiplexed DCS is often described as Fourier transform spectroscopy without moving parts. Importantly, the optical generation of EO frequency combs provides unprecedented user control and frequency agility for multiplexed sensing, a high signal-to-noise ratio, and compatibility with a variety of enhancement cavities. EO frequency combs therefore enable the rapid spectroscopy of weak molecular transitions over effective path lengths of > 10 km from a compact and robust laboratory instrument. In Fig. 2, we apply cavity-enhanced DCS to the study of atmospheric constituents (included deuterated water) in a sample of synthetic air [3].

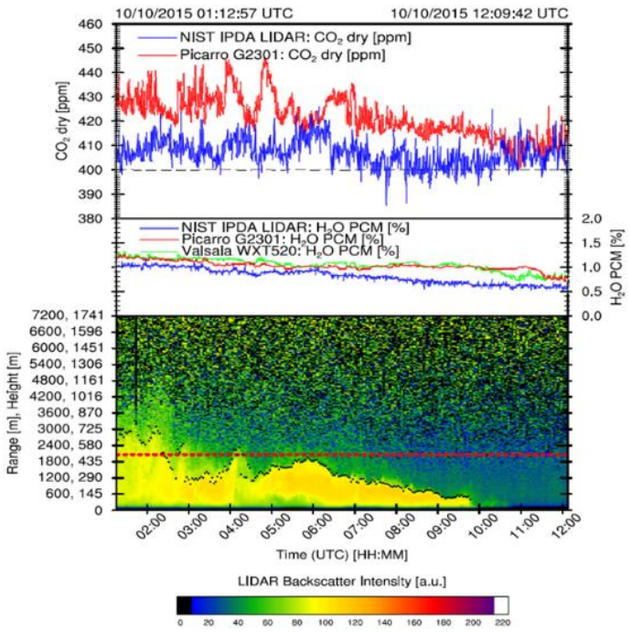


FIGURE 1. Top panel, CO2 dry air concentrations measured by fast scanning IPDA LIDAR (blue) and a point sensor (red). Middle panel, corresponding H2O concentrations. Bottom panel, LIDAR backscatter intensity, where red dots indicate the boundary layer height. [Fig. 13a; Wagner and Plusquellic, *Appl. Opt*. **55,** 6292-6310 (2016).]

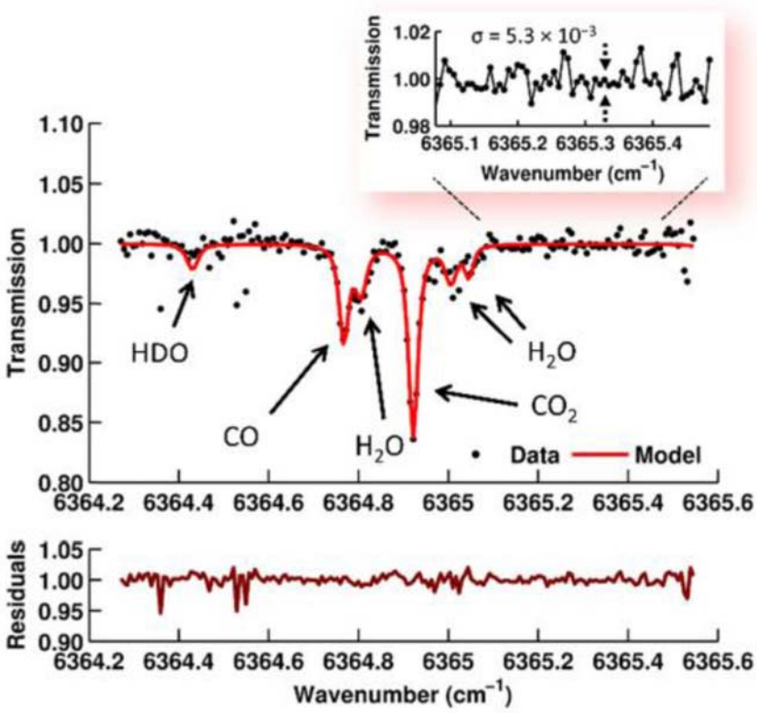


FIGURE 2. Cavity-enhanced dual-comb spectroscopy of synthetic air performed using electro-optic frequency combs. Constituent species including H2O, HDO, CO, and CO2, all acquired simultaneously and in as little as a few μs. [Fig. 4; Fleisher et al., *Opt. Express* **24,** 10424-10434 (2016).]

## 3. ENABLING MEASUREMENT SCIENCE – LASER SENSING OF AMBIENT RADIOCARBON (14C)

Radiocarbon (14C) is an important atmospheric tracer for CO2 source apportionment [4]. In combination with atmospheric transport models, 14C is widely used to identify carbon sources and sinks. However, 14C analysis at the highest levels of precision is slowed by the necessary shipment of samples to off-site accelerator mass spectrometry (AMS) facilities. Recently we demonstrated the optical measurement of 14C in CO2 samples derived from the combustion of bioethanol [5]. With an uncertainty of 130 fmol/mol (130 parts-per-quadrillion, or ppq) in an acquisition time of 47 min, this emerging technology, based on the principles of linear absorption spectroscopy, will enable distributed, traceable, and *in situ* sensing of 14C, and thus a new age of 14C metrology.

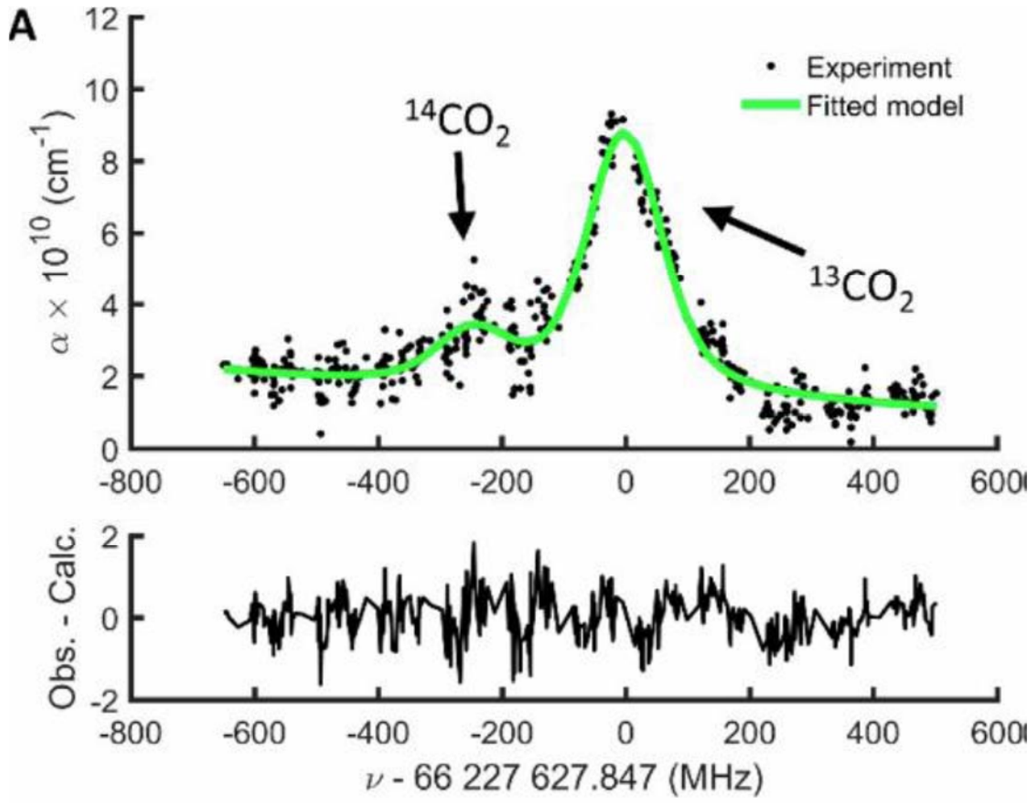


FIGURE 3. Cavity ring-down spectroscopy of CO2 from the combustion of bioethanol. The peak at approximately −250 MHz is the signature 14C absorption. The peak area is proportional to the mole fraction of 14C. [Fig. 2; Fleisher et al., *J. Phys. Chem. Lett.* **8,** 4550-4556 (2017).]

## 4. OUTLOOK

New methods in multiplexed spectroscopy have applications in remote sensing, including open-path sensing and ranging. Using EO frequency combs for IDPA LIDAR enables coherent averaging of backscattering in the time domain via ultrasensitive photon counting techniques (see Fig. 4) [6]. For IDPA LIDAR, the relatively narrow optical bandwidth of EO frequency combs is an advantage, as all the backscattered photons incident on the photon counting and multiplying detector carry information about integrated open-path absorption. In addition to DCS using EO frequency combs, dispersive spectrometers in combination with mid-infrared

mode-locked laser frequency combs also allow for rapid multiplexed spectroscopy over open atmospheric paths [7] and for the time-resolved spectroscopy of transient free radicals [8].

FIGURE 4. First demonstration of multiplexed IPDA LIDAR using electro-optic frequency combs. Averaged reference (blue) and coadded photon counting (red) interferograms are in excellent agreement following real-time phase corrections. The coadded photon counting interferogram contains absorption information which reveals the CO2 dry air concentrations. [Plusquellic et al., *CLEO* (2017), paper AM1A.5.]

Distributed measurements of rare isotopologues, particularly the 14C isotopologues of CO2, CH4, and carbonaceous aerosols, would enable the partitioning of carbon emissions into specific sources and sinks. Currently fossil fuel CO2 emissions (CO2ff) are routinely quantified via a ground-up approach, where economic data with uncertainties of approximately 5-10% are used to estimate CO2ff [4]. A distributed network of *in situ* optical measurement of 14C tracers could constrain atmospheric transport models, including key details on the PBL. As a worked example, a previous National Academies of Science report details how 10,000 measurements of 14C per year could yield CO2ff emissions uncertainties of 10-25% [9]. In lieu of a dedicated AMS facility, distributed optical sensors could potentially accomplish this ambitious measurement goal.

## REFERENCES

[1] G.-W. Truong, K. O. Douglass, S. E. Maxwell, R. D. van Zee, D. F. Plusquellic, J. T. Hodges, D. A. Long, "Frequency-agile, rapid scanning spectroscopy," *Nat. Photonics* **7,** 532-534 (2013).
[2] G. A. Wagner, D. F. Plusquellic, "Ground-based, integrated path differential absorption LIDAR measurement of CO2, CH4, and H2O near 1.6 μm," *Appl. Opt.* **55,** 6292-6310 (2016).
[3] A. J. Fleisher, D. A. Long, Z. D. Reed, J. T. Hodges, D. F. Plusquellic, "Coherent cavity-enhanced dual-comb spectroscopy," *Opt. Express* **24,** 10424-10434 (2016).
[4] *Radiocarbon and Climate Change: Mechanisms, Applications and Laboratory Techniques*, E. A. G. Schuur, E. R. M. Druffel, eds. (Springer, 2016).
[5] A. J. Fleisher, D. A. Long, Q. Liu, L. Gameson, J. T. Hodges, "Optical measurement of radiocarbon below unity fraction modern by linear absorption spectroscopy," *J. Phys. Chem. Lett.* **8,** 4550-4556 (2017).
[6] D. F. Plusquellic, G. A. Wagner, A. J. Fleisher, D. A. Long, J. T. Hodges, "Multiheterodyne spectroscopy using multi-frequency combs," in *Conference on Lasers and Electro-Optics*, OSA Technical Digest (online) (Optical Society of America, 2017), paper AM1A.5.
[7] L. Nugent-Glandorf, F. R. Giorgetta, S. A. Diddams, "Open-air, broad-bandwidth trace gas sensing with a mid-infrared optical frequency comb," *Appl. Phys. B* **119,** 327-338 (2015).
[8] A. J. Fleisher, B. J. Bjork, T. Q. Biu, K. C. Cossel, M. Okumura, J. Ye, "Mid-infrared time-resolved frequency comb spectroscopy of transient free radicals," *J. Phys. Chem. Lett.* **5,** 2241-2246 (2014).
[9] *Verifying Greenhouse Gas Emissions: Methods to Support International Climate Agreements* (National Academies Press, 2010).

# Long-path atmospheric measurements using dual frequency comb spectroscopy

Kevin Cossel, Eleanor Waxman, Fabrizio Giorgetta, Eli Hoenig, Sara Swenson, Gar-Wing Truong, Scott Diddams, Gabe Ycas, Ian Coddington, Nathan R. Newbury
National Institute of Standards and Technology

**SUMMARY**

Dual frequency comb spectroscopy is being pursued for a number of atmospheric applications since it provides broad spectral coverage with high spectral resolution across long open-air paths. Such measurements fill in an observational gap between point measurements and total vertical column measurements. We have constructed a portable dual-comb spectrometer that can be operated independently of any laboratory references, yet still measures atmospheric spectra with high accuracy in the near infrared. This system measures the column-averaged $CO_2$, $H_2O$, HDO and $CH_4$ mixing ratios across paths ranging from several-hundred meters to >5 km. We have used this system for city-scale greenhouse gas measurements by measuring across two paths simultaneous for two months. We have also developed the ability to horizontally and vertically scan the measurement path using an unmanned aerial system (UAS), which enables rapid detection of emissions sources. Further improvements to the near infrared dual-comb spectrometer as well as efforts to extend the technology to the mid-infrared and visible will enable the detection of additional species.

## 1. INTRODUCTION

Dual frequency comb spectroscopy (DCS)[1,2] is a rapidly evolving new tool for broadband spectroscopy that exploits the advantages of frequency combs for precision measurements. A frequency comb is a laser source whose spectrum is composed of hundreds of thousands of perfectly spaced, discrete wavelength elements or comb teeth, which act as a massively parallel set of single-frequency lasers with highly stable, well-known frequencies. As sketched in Figure 1a, DCS utilizes two frequency combs with slightly different repetition rates (here $f_{r,1}$ and $f_{r,2)}$ to rapidly measure an absorption spectrum with comb-tooth resolution. The two combs are interfered on a photodetector, which leads to a measureable radiofrequency (rf) comb with a one-to-one correspondence with the optical comb teeth. If one, or both, of the frequency combs pass through a gas sample, then the sample's absorption spectrum is also mapped to the measured rf spectrum. This results in a spectrum measured across a large bandwidth (tens of THz or hundreds of $cm^{-1}$) with a point spacing typically on the order of 200 MHz (0.0067 $cm^{-1}$), with virtually no instrument lineshape, and with near perfect frequency calibration spectrum[3,4]. In this way, dual-comb spectroscopy combines the advantages of tunable laser spectroscopy, e.g. high resolution and a spatially-coherent beam, with the advantages of Fourier Transform Spectroscopy, e.g. multi-species detection.

## 2. OPEN-PATH DCS

One application of dual-comb spectroscopy is km-scale, open-path atmospheric measurements. Here, the diffraction limited output of the frequency comb laser source allows for much longer path lengths than is possible with conventional FTS using a thermal source.

Such kilometer-scale open-air paths are well matched to atmospheric transport models and are attractive for measuring both point and distributed sources. In addition, DCS measures the full spectrum simultaneously (i.e. no scanning is necessary) and typically in around 1 millisecond. This leads to a high immunity to turbulence-induced intensity noise that can distort the spectrum in broadly swept laser systems. Finally, the high-resolution spectra obtained with dual-comb spectroscopy are well suited to tackling the challenging problem of separating the overlapping lines from the multiple small molecules in the atmosphere and the lack of an instrument line shape makes the system calibration free.

As shown in Figure 1c, we have developed a fieldable near-infrared dual-comb spectrometer[5] based on robust erbium-fiber lasers[6,7] that have been deployed over 1-12-km open-air paths to measure of $CO_2$, $H_2O$, HDO, and $CH_4$ in the 1.6-micron spectral region. Detection of $O_2$, N2O and NH3 should be possible with additional spectral broadening. The measured $CO_2$ precision over a 2-km path is 0.85 ppmv in 32 seconds, improving to 0.17 ppmv in 1024 seconds. For $CH_4$, the precision is 9.1 ppbv in 32 seconds, improving to 1.17 ppbv in 1024 seconds. In a recent intercomparison[8], we found that two independent DCS instruments agree to 0.14% for $CO_2$ and 0.35% for $CH_4$ over two weeks with no bias correction or calibration, which is one to two orders of magnitude better agreement than existing open-path measurement technologies.

## 3. APPLICATIONS

As shown in Figure 2, we have deployed the near-IR DCS system in multiple configurations for regional carbon monitoring as well as for spatial mapping of emissions. In the first example (Fig. 2a), we have used this system to simultaneously measure greenhouse gases across the city of Boulder, CO and across a background path on the edge of the city nearly continuously for two months. By combining the relative $CO_2$ enhancement over the city with measurements from local wind sensors, we can quantify the source strength of the vehicular $CO_2$ in the city. We were also able to measure the diurnal cycles of $CO_2$ and $CH_4$, which were dominated by commuter traffic peaks and on changes in the boundary layer, respectively.

We have also conducted a series of experiments where the dual-comb spectrometer measures the atmospheric absorption out to a retroreflector mounted on an unmanned aerial system[9] (Fig. 2b). This configuration provides the ability to measure horizontal and vertical profiles, which provide information about dispersion and mixing in the boundary layer. By measuring a vertical screen downwind of an emissions source, we are also able to quantify the emissions strength.

As shown by these results, dual comb spectroscopy has promise as an addition to the current suite of atmospheric measurement tools. In the near-infrared, DCS can provide multispecies detection over paths longer than for open-path FTS and with the high accuracy of laser spectrometry. Such long paths enable regional monitoring over length scales more comparable to atmospheric dispersion models. In addition, future continued advances in comb technology should extend open-path dual-comb spectroscopy to other atmospheric windows such as the mid-infrared and visible with access to an even greater variety of species.

## REFERENCES

1. Coddington, I., Newbury, N. & Swann, W. Dual-comb spectroscopy. *Optica* **3,** 414 (2016).
2. Ideguchi, T. Dual-Comb Spectroscopy. *Opt. Photonics News* **28,** 32 (2017).
3. Zolot, A. M. *et al.* Direct-comb molecular spectroscopy with accurate, resolved comb teeth over 43 THz. *Opt.*
*Lett.* **37,** 638–640 (2012).
4. Okubo, S. *et al.* Ultra-broadband dual-comb spectroscopy across 1.0–1.9 μm. *Appl. Phys. Express* **8,** 82402
(2015).
5. Truong, G.-W. *et al.* Accurate frequency referencing for fieldable dual-comb spectroscopy. *Opt. Express* **24,**
30495–30504 (2016).
6. Sinclair, L. C. *et al.* Operation of an optically coherent frequency comb outside the metrology lab. *Opt. Express*
**22,** 6996–7006 (2014).
7. Sinclair, L. C. *et al.* Invited Article: A compact optically coherent fiber frequency comb. *Rev. Sci. Instrum.* **86,**
81301 (2015).
8. Waxman, E. M. *et al.* Intercomparison of open-path trace gas measurements with two dual-frequency-comb
spectrometers. *Atmos Meas Tech* **10,** 3295–3311 (2017).
9. Cossel, K. C. *et al.* Open-path dual-comb spectroscopy to an airborne retroreflector. *Optica* **4,** 724–728 (2017).

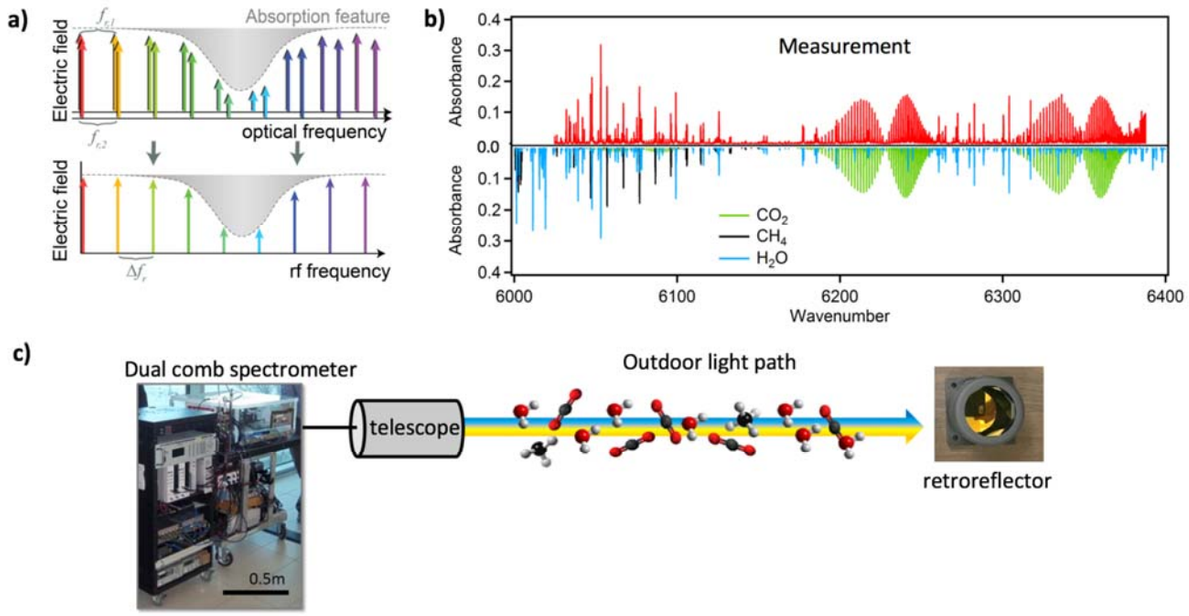


FIGURE 1: Dual comb spectroscopy. a) Concept of dual comb spectroscopy. Two frequency combs with tooth spacing of fr,1 and fr,2 (different by Dfr) are mixed, resulting in a measurable comb in the rf with a one-to-one correspondence to the optical comb. Thus, the rf spectrum can be measured and mapped back to an optical spectrum. b) Measured data from a 2-km open-air path (red) and the fit constituents (inverted). c) Portable dual comb spectrometer for long-path measurements of $CO_2$, $CH_4$, and $H_2O$.

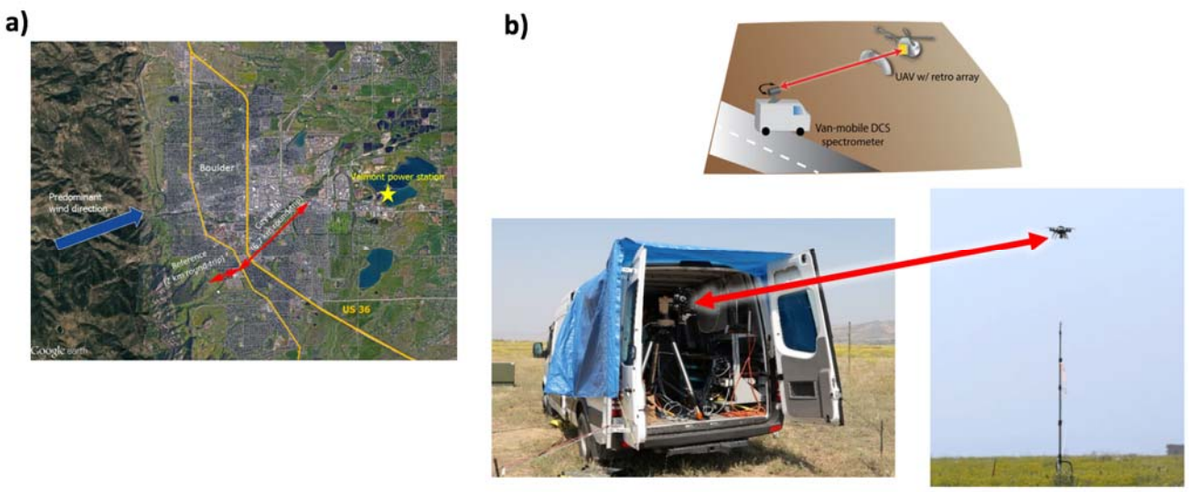


FIGURE 2. Applications of DCS. a) City-scale emissions monitoring. b) Spatial scanning for vertical profile and source quantification.

# Saildrone: A new autonomous surface vehicle for boundary layer observations

Meghan F. Cronin
NOAA Pacific Marine Environmental Laboratory

Saildrones are a new wind- and solar-powered autonomous surface vehicle that offers a wide range of capabilities for observing the ocean and atmosphere boundary layers. With a 3-dimensional ultrasonic wind sensor mounted at the top of the solid wing at 5 m height, wind and potentially wind stress and turbulent buoyancy flux are measured at a level comparable to buoy wind observations. The platform also includes an air-temperature and relative humidity package on the forward boom at 2.4 m height, barometric pressure on the deck, a Sea Surface Temperature (SST) and sea surface salinity sensor on the keel at 0.6 m depth, and a downward looking infrared (IR) pyrometer mounted on the boom to measure skin SST. Data from these sensors thus can be used to estimate turbulent air-sea heat, moisture and momentum fluxes from bulk algorithms such as Fairall et al. (2003). In order to estimate the full net surface heat flux, Saildrone also carry radiometers to measure downwelling longwave and solar radiation. Because solar radiation is sensitive to platform motion that changes its effective zenith angle, an SPN1 radiometer is used that measures both the diffuse and total insolation, from which the direct component can be computed and corrected for zenith angle changes associated with the platform motion. Two Saildrone are currently at the Salinity Processes in the Upper Ocean Regional Study-2 (SPURS-2) as part of a NOAA-funded Tropical Pacific Observing System (TPOS) mission. These Saildrone also carry an ADCP to measure upper ocean current profile between about 4-80 m, a suite of biogeochemical sensors to monitor the air-sea $CO_2$ flux, pH, surface water dissolved $O_2$, Chla, CDOM concentration, and red backscatter; and a set of cameras that view the sky and sea state.

These, and other sensor packages, have been integrated into the Saildrone system through a Cooperative Research And Development Agreement (CRADA) between Saildrone Inc. and PMEL. While all raw data are stored onboard and can be processed at the end of the mission, most sensor packages also involve onboard processing and telemeter data to shore in realtime. With high resolution and precise navigation data, measurements that are sensitive to platform motion, such as wind, currents and solar radiation can be transformed from the platform coordinate system to Earth coordinates. Tests to verify these onboard transformations and corrections are underway and appear to be quite good. Saildrone thus appears to be an ideal platform for measuring air-sea interaction.

Combining racing sail-powered vehicle technology with the needs of oceanographic research, Saildrone can be launched and recovered from a dock, and travel thousands of nautical miles to the study site. The present drones can transit at ~1.5 knots with 10 knot winds, and with stronger winds, the drones can reach up to 7 knots. Future generations may also include a small motor to power through periods of light winds or very strong currents. Saildrone, thus, have some of the capabilities of a research vessel, though with longer endurance. The longest voyage thusfar has been 12 months, with over 16,000 km covered. Saildrone can be used in a range of sampling modes: holding station as a pseudo-mooring, circling a location to provide horizontal gradients at a site (and potentially vertical velocity from the divergence of horizontal currents), making repeat sections, “mowing the lawn” surveys, or doing adaptive sampling such as following a front or eddy as it evolves. The TPOS-2020 project is considering their potential use within the tropical Pacific. Because Saildrone move, it is unlikely that the fishing fleet will tie up to them to use as “Fish Aggregating Devices” (FAD) as they do with moored buoys. This technique has resulted in data returns between 30-50% along the easternmost line of tropical

buoys at 95°W. There is thus discussion of replacing this line of buoys with Saildrone and Argo floats. Saildrone could also provide zonal and or meridional sections at “super-sites” within the array, such as at 0°, 140°W, where it is hoped that an array of platforms could be used to monitor the Ekman divergence and upwelling that results in the equatorial cold tongue. There are also discussions of using Saildrone to monitor the eastern edge of the warm pool as it migrates eastward during El Nino. Saildrone potentially could provide a direct measurement of wind stress. A global array of Saildrone could then be used as in situ reference for scatterometer satellite measurements of wind stress. Finally, in the coming decade it is likely that numerical weather prediction models will begin to use coupled data assimilation techniques in which the ocean and atmosphere measurements are assimilated simultaneously. For these systems, simultaneous, co-located ocean and atmosphere surface measurements, such as from Saildrone, are ideal. One could imagine a global array of Saildrone, similar to the Argo array of floats, could provide coincident ocean and atmosphere observations for coupled data assimilation at a time resolution that cannot be matched by satellite data.

It would be expected that if Saildrone were mass produced, the price point would reduced. When comparing the price point of Saildrone to other platforms, it is important to consider that Saildrone are launched from shore and thus do not require shiptime, often a hidden cost in other observational schemes. Also, the business model of Saildrone Inc. is different than most. The researcher leases the Saildrone and provides the mission plan and pilot instructions, while Saildrone Inc. is responsible for maintaining the Saildrone system, piloting it, and processing the data. Rather than purchasing the Saildrone system, the researcher essentially purchases data. Researchers will no longer need to maintain a group of technicians, programmers, and engineers. This, along with the expanded capability provided by Saildrone, may radically change the future of boundary layer observing.

# Use of Unmanned Aircraft and Tethered Balloons to Advance Understanding of Arctic Boundary Layers: Examples from the Field

Gijs de Boer
Cooperative Institute for Research in Environmental Sciences (CIRES)

Detailed understanding of the Arctic boundary layer requires a variety of new perspectives. For example, the atmospheric conditions found over thin sea ice are likely very different than those observed during previous historical campaigns (e.g. SHEBA, Uttal et al. 2002). Many open questions exist about the interplay between the mixed water/ice surface and its influence on turbulent and radiative fluxes, and on aerosol properties in the lower atmosphere ultimately impacting cloud properties. Unfortunately, traditional observing systems, including towers and other surface-based equipment cannot easily be positioned in environments with weak or broken ice. Similarly, the multifaceted nature of the Arctic surface is hypothesized to result in substantial horizontal variability in atmospheric boundary layer states. In order to capture this sort of variability, much of which occurs at grid scales smaller than those covered by the grid scale used in numerical models, we are reliant upon networks or mobile sensor systems. Finally, because of the frequent occurrence of stable conditions in the lower Arctic atmosphere, surface measurements alone cannot provide a clear picture of what is happening aloft and what is driving the formation of surface energy budget modulating entities such as clouds. For all of these reasons modernization of our observing capabilities is required in this critical but remote environment.

One of the platforms being used to provide information in the ways discussed above are unmanned aerial systems (UAS). Arctic UAS operations have been conducted by a variety of agencies and institutes, and have included flights by platforms ranging from the very large (e.g. the NASA Global Hawk) to the very small (e.g. the University of Colorado DataHawk). While the cost to operate these platforms varies greatly, initial measurements from trial campaigns have shown significant promise in providing information previously unavailable to theoreticians and model developers. Certain agencies, including the US Department of Energy (DOE) and National Oceanic and Atmospheric Administration (NOAA) have provided leadership in the use of UAS in the US Arctic by supporting campaigns and research efforts using these systems. The DOE has further supported activities within previously established restricted airspace (e.g. Oliktok Point, Alaska; de Boer et al., 2016a) by providing complementary ground-based observational facilities and by engaging the FAA to find new opportunities for use of UAS.

In particular, several groups have leaned heavily on the use of small (<55 lbs.) and micro (<4.4 lbs.) scale UAS due to the relative ease of operating these platforms and their lower cost, with some platforms having a total parts cost of only $1k. The latter is particularly important due to the many challenges associated with the operation of UAS in the Arctic atmosphere, including icing, navigation issues, and the impact of extreme cold on hardware, and the associated risk of potential loss of aircraft during operations. These platforms are able to provide flight endurances of up to several hours, covering altitudes between the surface and 4 km or more and can carry a variety of instrumentation relevant to boundary layer research. Specific examples include sensors to sample atmospheric thermodynamic state, turbulence, three component winds, aerosol particle

properties, radiation, and cloud microphysics. Given these characteristics, these small systems can provide the perspectives outlined in the opening paragraph, providing information on vertical and spatial variability, while simultaneously being able to operate over unstable surfaces and in "high-risk" environments.

In addition to unmanned aircraft, tethered balloon systems (TBS) are also being used to provide measurements of the atmospheric boundary layer and associated cloud and aerosol conditions. TBS offer some advantages over UAS. Specifically, they have the ability to sample continously over extended time periods given their ability to stay aloft for days at a time, weather permitting. Additionally, these systems are less prone to issues related to icing in supercooled clouds often observed in the lower Arctic atmosphere, making them a better candidate for measuring cloud microphysical properties in this environment. While their ability to provide information over broken ice or on spatial variability is limited, these platforms provide excellent information on the vertical structure of the atmosphere, thereby strongly complimenting continuous ground-based measurements. One significant associated with the operation of these platforms is their sensitivity to higher wind conditions, as well as the elevated cost of equipment and operations relative to small UAS.

Because of the advantages outlined above, the University of Colorado and US Department of Energy have worked together over the past several years to deploy small UAS and TBS on the North Slope of Alaska, at the Oliktok Point Observatory. This includes several deployments with the DataHawk UAS (Lawrence and Balsley, 2013), a deployment of the Pilatus UAS (de Boer et al., 2016b) and numerous TBS flight activities. These operations have resulted in lower atmospheric measurements obtained using a variety of sensors, including thermodynamic sensors, a 3D sonic anemometer, a miniaturized optical particle spectrometer, broadband radiometers, liquid water content sensors and ice crystal imagers. In this presentation, we will provide a quick overview of these activities and the platforms used to undertake them, including examples of UAS and TBS measurements of Arctic boundary layer state, and how they are being used to evaluate and improve modeling tools.

## REFERENCES

de Boer, G., Ivey, M.D., Schmid, B., McFarlane, S. and Petty, R. 2016a. Unmanned Platforms Monitor the Arctic Atmosphere, *EOS*, **97**, 20-24, doi:10.1029/2016EO046441.

de Boer, G., S. Palo, B. Argrow, G. LoDolce, J. Mack, R.-S. Gao, H. Telg, C. Trussel, J. Fromm, C.N. Long, G. Bland, J. Maslanik, B. Schmid, and T. Hock, 2016b: The Pilatus Unmanned Aircraft System for Lower Atmospheric Research, *Atmos. Meas. Tech.*, 9, 1845-1857, doi:10.5194/amt-9-1845-2016.

Lawrence D.A. and Balsley, B.B. 2013. High-Resolution Atmospheric Sensing of Multiple Atmospheric Variables Using the DataHawk Small Airborne Measurement System. *J. Atmos. Oceanic Technol.*, **30**, 2352–2366, doi: http://dx.doi.org/10.1175/JTECH-D-12-00089.1.

Uttal, T., J.A. Curry, M.G. Mcphee, D.K. Perovich, R.E. Moritz, J.A. Maslanik, P.S. Guest, H.L. Stern, J.A. Moore, R. Turenne, A. Heiberg, M.C. Serreze, D.P. Wylie, P.O.G. Persson, C.A. Paulson, C. Halle, J.H. Morison, P.A. Wheeler, A.Makshtas, H. Welch, M.D. Shupe, J.M. Intrieri, K. Stamnes, R.W. Lindsey, R. Pinkel, W.S. Pegau, T.P. Stanton and T.C. Grenfeld. 2002: Surface Heat Budget of the Arctic Ocean. Bulletin of the American Meteorological Society: Vol. 83, No. 2, pp. 255–275.

# In situ observation of the boundary layer using altitude-controlled balloons

Paul Voss
Smith College
Contributors: Lars Hole (MetNo), Tjarda Roberts (LPC2E/CNRS), David Fitzjarrald (SUNY/Albany)

## INTRODUCTION

The development of miniature sensors, communications, and power systems is enabling a wide range of novel autonomous platforms. While unmanned aircraft systems (UAS) are the forefront of this revolution, other platforms also promise to provide more routine access to the boundary layer. We present our experience developing and operating small altitude-controlled balloons that have some advantages in terms flight duration, aviation safety, and regulatory oversight. The unique capabilities and limitations of these controlled meteorological (CMET) balloons offer insight into the challenges of making in situ measurements in the boundary layer with UAS more generally.

## ALTITUDE-CONTROLLED BALLOONS

Controlled meteorological balloons are similar in size to standard rawinsondes but can remain airborne for multiple days while changing altitude on command via satellite (Fig. 1). Altitude is controlled using reversible lift-gas compression with a high-pressure reservoir and miniature pump and valve. The resulting balloon is metastable, allowing it to traverse a large altitude range (many kilometers) with minimal energy consumption. Power is provided by a 10 Whr battery and a 2-3 Watt thin-film solar panel. Global two-way communication is via Iridium satellite modem (short-burst data service). On board sensors include aspirated temperature (+/- 0.2 C) and fast-response relative humidity (+/-10% in practice), pressure altitude, and GPS position and winds. Total payload mass ranges between 200-300 grams.

To date, these CMET balloons have been treated as *small balloons* under the FAA's FAR 101.7 and as *light balloons used exclusively for meteorological purposes* under ICAO Annex II. These minimally regulated categories allow the balloons to be flown beyond line of site, at night, in low-visibility conditions, and across international borders in some circumstances. The balloons are therefore at the most permissive extreme of the regulatory spectrum and reveal some of the opportunities and limitations of scientific UAS in the future. In practice, we have limited our balloon flights to remote regions including the Amazon, Arctic and Antarctica, with all operations carried out in close coordination with air traffic control and other relevant authorities.

## CAPABILITIES AND LIMITATIONS

Since 2004, CMET balloons have accrued over 50 missions totaling more than 1000 hours of flight time in environments ranging from the tropics to the poles. Reliable operation has been demonstrated in the altitude range from the surface to 4000 m msl for flight durations up to three days. Flights up to 6000 m msl and durations up to 6.5 days have been achieved.

The CMET balloons have gained access to new regions in part because altitude control enables them to steer clear of congested areas, remain below established ceilings, and honor requests from air-traffic control authorities. The balloons are also small and light enough that they can be mailed to collaborators in remote areas of the world, prepared in a small space, and launched with only modest effort. This flexibility has greatly reduced the cost of the flights and resulting data, perhaps by a factor of 10, in comparison with our early field campaigns.

Altitude control coupled with long-duration flight capability provide unique opportunities for:

a) Observations in remote and hazardous regions
b) Navigation and persistence in study regions using wind shear
c) Layer tracking (nocturnal jets, quasi-Lagrangian studies)
d) Automated continuous soundings (flux and process studies)
e) Descent to the surface (ice and ocean-atmospheric interactions)
f) Controlled ascent/descent rates (fine-scale structure, long sensor $\tau$)
g) Cloud penetration, nocturnal observations, diurnal cycles and transitions

Current limitations include:

a) Aviation safety is critically important and generally limits balloon operations to remote areas
b) Balloons cannot withstand sustained precipitation or icing conditions
c) Diffusional loss of lift gas, due to high surface/volume ratio, limits flight duration to several days
d) Current balloons have limited capacity to carry additional sensors (limited to grams, mW)
e) Balloons can travel thousands of kilometers and are often not recovered

## OVERVIEW OF SOME RECENT STUDIES

The figures and captions below provide a few brief examples of recent flights in the Arctic, Amazon, and Antarctica. These studies include the first long series of automated soundings and a comparison with reanalysis model data (Fig. 2), operation of multiple balloons simultaneously over a large geographic area (Fig. 3), a study of boundary layer processes in Amazon in 2016 (Fig. 4), navigation and targeted studies in Antarctica (Fig. 5), and the longest flight to date, across Antarctica, in 2017 (Fig. 6).

## CONCLUSIONS

Small altitude-controlled balloons have become significantly more capable and reliable in recent years. These balloons provide a unique platform for boundary layer studies that can complement manned and unmanned aircraft, remote sensing, and rawinsondes. Ongoing work aims to expand the altitude range, flight duration, conditions under which the balloons can operate while building collaborations that contribute to our knowledge of the atmosphere.

While small meteorological balloons have had unparalleled freedom of navigation, our work over the past decade also illustrates the challenging issues facing the broader scientific UAS community. Even for the smallest balloons and UAS, aviation safety considerations are paramount and substantially restrict when and where these systems can operate. Addressing these concerns through conservative deployments of smaller, lighter, and geographically bounded UAS may provide one viable path forward.

FIGURE 1. Left: A conventional ozonesonde being launched from Ny-Alesund, Norway. Right: A CMET balloon being launched from the same location.

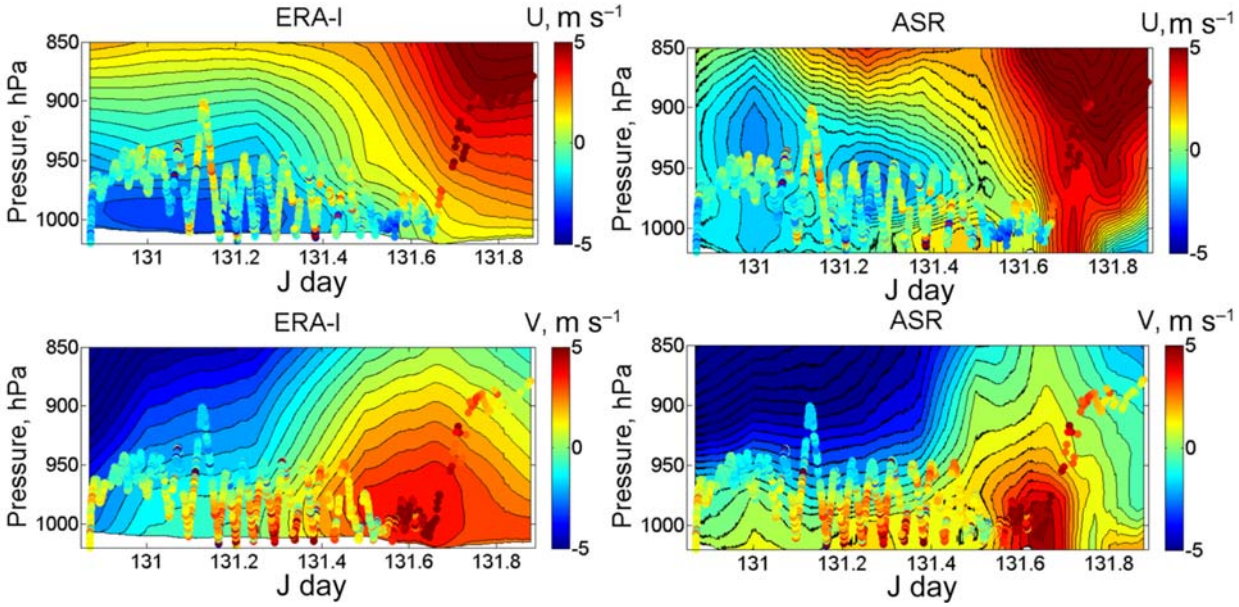


FIGURE 2. An example showing wind measurements made during 18 automated balloon soundings in the marine boundary layer in western Svalbard in 2011. The saw-tooth pattern in the foreground shows the balloon data. The background shows reanalysis data (4-D interpolated latitude, longitude, pressure, time) from ECMWF ERA-Interim and the Arctic System Reanalysis. Figure from Roberts *et al.*, 2016.

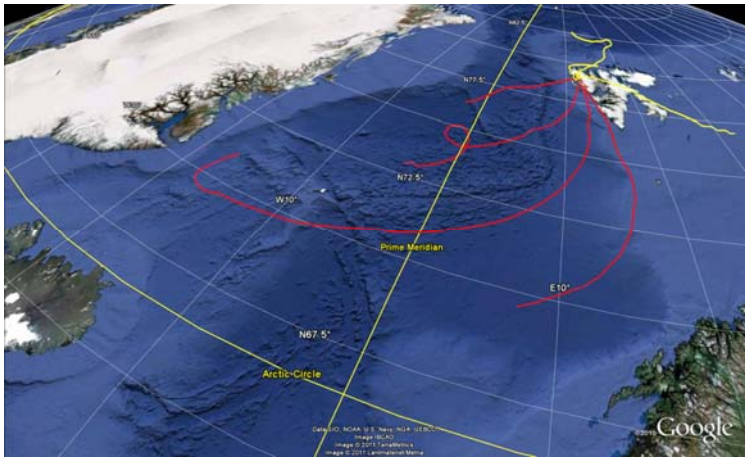


FIGURE 3. Four CMET balloons in the air simultaneously over the Norwegian and Greenland Seas in 2010. These early CMET balloons did not have the ability to perform automated soundings and were therefore flown primarily at constant altitude of approximately 2500 m msl.

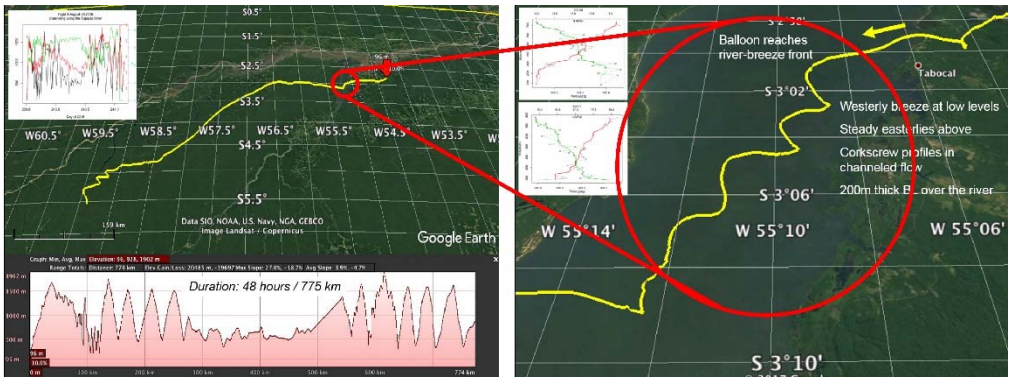


FIGURE 4. Left: A two-day 775 km flight across the Amazon with automated deep soundings through the boundary layer, one of seven long flights in this region during September of 2016. Right: The inset shows the balloon descending into one target region, the river-induced breeze above the Tapajos River, and performing corkscrew-like automated soundings.

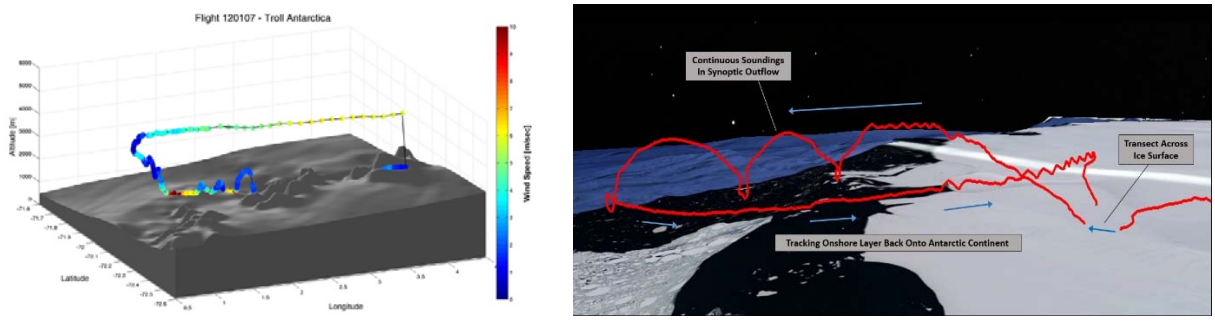


FIGURE 5. Left: Trajectory of a CMET balloon in 2012 following the katabatic winds from the Antarctic plateau before ascending and returning to the plateau for another pass. Right: Automated soundings, landing on the ice, and navigation back on shore using wind shear and layer tracking in Queen Maud Land, Antarctica in 2016.

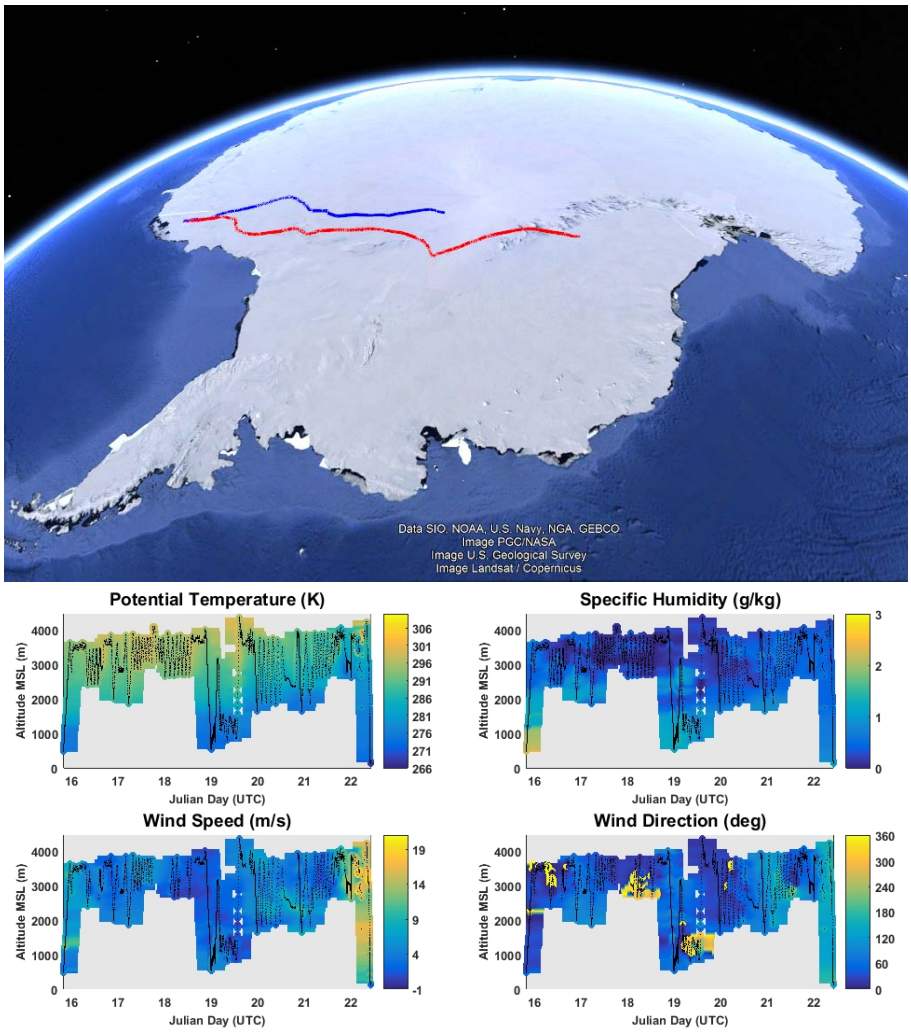


FIGURE 6. Top: Three-day (red) and six-and-a-half-day (blue) balloon trajectories crossing Antarctica in January of 2017. These two balloons were mailed to Antarctica via Novo and launched by collaborators at Finland's Aboa station. Bottom: Approximately 50 profiles, 1-3 km in extent, show the potential temperature, absolute humidity, and winds during the cross-continent flight. These plots, which are interpolated for visibility, are generated automatically and used in real-time for flight planning.

## REFERENCES

Hole L. R., Bello, A. P., Roberts, T. J., Voss, P. B., and Vihma, T.: Measurements by controlled meteorological balloons in coastal areas of Antarctica, Antarct. Sci., CJO2016, doi:10.1017/S0954102016000213, 2016.

Stenmark, A., Hole, L. R., Voss, P., Reuder, J., and Jonassen, M. O.: The influence of nunataks on atmospheric boundary layer convection during summer in Dronning Maud Land, Antarctica, J. Geophys. Res. Atmos., 119, 6537–6548, doi:10.1002/2013JD021287, 2014.

Roberts, T. J., Dütsch, M., Hole, L. R., and Voss, P. B.: Controlled meteorological (CMET) free balloon profiling of the Arctic atmospheric boundary layer around Spitsbergen compared to ERA-Interim and Arctic System Reanalyses, Atmos. Chem. Phys., 16, 12383-12396, https://doi.org/10.5194/acp-16-12383-2016, 2016.

Voss, P. B., Zaveri, R. A., Flocke, F. M., Mao, H., Hartley, T. P., DeAmicis, P., Deonandan, I., Contreras-Jiménez, G., Martínez- Antonio, O., Figueroa Estrada, M., Greenberg, D., Campos, T. L., Weinheimer, A. J., Knapp, D. J., Montzka, D. D., Crounse, J. D., Wennberg, P. O., Apel, E., Madronich, S., and de Foy, B.: Long-range pollution transport during theMILAGRO-2006 campaign: a case study of a major Mexico City outflow event using free-floating altitude-controlled balloons, Atmos. Chem. Phys., 10, 7137–7159, doi:10.5194/acp-10-7137-2010, 2010.

Voss, P. B., Hole, L. R., Helbling, E., and Roberts, T. J.:. Continuous in-situ soundings in the Arctic boundary layer: A new atmospheric measurement technique using controlled meteorological balloons, J. Intell. Robotic Syst., 70, 609, doi:10.1007/s10846-012-9758-6, 2012.

# Airborne and ground-based mobile measurement platforms, and their role in boundary-layer research

Donald H. Lenschow
National Center for Atmospheric Research, Boulder, CO

In situ measurements of the atmospheric boundary layer (ABL) from fixed surface-based platforms, although relatively straightforward, have inherent limitations. They are not able to measure horizontal variations and they depend on the mean wind to advect the atmosphere past the fixed location; thus for turbulence variables it is assumed that advection contributed by turbulent circulations themselves is small and that therefore the advection of a field of turbulence past a fixed point can be taken to be entirely due to the mean flow (also known as the Taylor "frozen turbulence" hypothesis).

To obviate this assumption, over the years a variety of mobile platforms have been utilized for probing the ABL, each with their own advantages and limitations. These include manned powered and unpowered aircraft, unmanned aerial vehicles (UAVs), cars, blimps, controlled towed vehicles (CTVs), a trolley suspended on a cable (Oncley, 2009), and balloons. A problem that is intrinsic to all these mobile platforms is measuring their location, velocity, and angular orientation. Measurement of the wind relative to the Earth requires calculating the difference between the platform velocity and the velocity of the air relative relative to the platform in an Earth-based coordinate system. Thus angular orientation of the platform is required for resolving the 3-dimensional wind vector in an earth-based coordinate system. That requires determining the angular orientation of the platform relative to Earth. Techniques for doing this have a long history, but the underlying principle is using the gyroscopic effect to "remember" an initial or reference angular orientation of the platform and measure departures from that reference. There has been remarkable recent progress to improve the accuracy and reliability of this technology while reducing the size and power consumption of the sensors. In addition, satellite navigation systems, typified by the Global Positioning System (GPS), have led to vast improvements in long-term accuracy of attitude angle measurement as well as platform position and velocity (e. g. Cooper et al, 2016).

In contrast, measurement of the air velocity from airborne mobile platforms still depend mostly on differential pressure measurements. For aircraft true airspeed, this means a pitot tube combined with a static pressure measurement to determine the pressure difference, and for obtaining all three components of the air velocity, a 5-hole pressure probe or 5 holes located on the aircraft nose plus a static pressure measurement to obtain 3 pressure difference measurements that measure the two air flow angles and true airspeed. A significant problem with this approach is the airflow distortion that can modify the air velocity vector as the flow approaches the fuselage. One recent development to obviate this is a Doppler laser-based system, shown in Figure 1, that can measure the air velocity vector ten or more meters away from the aircraft. An earlier single-axis version of this Laser Air Motion Sensing (LAMS) system is described by Spuler et al. 2011. Figure 2 shows a potential future extension of this system to measure the velocity vector at multiple points in space unaffected by airflow distortion.

Combining these new technologies with sophisticated Kalman filtering, it is now possible to measure wind velocity on an aircraft to about 0.1 m $s^{-1}$ for the vertical component, and 0.2 m $s^{-1}$ and 0.4 m $s^{-1}$ for the horizontal components normal to and along the aircraft longitudinal axis, respectively (Cooper, 2017). A remaining challenge is to reduce the size and cost of these systems to make them available on smaller and less expensive mobile platforms.

For measuring just the mean horizontal wind components, it is now possible to combine GPS, which accurately measures the aircraft ground speed and heading angle, with pitot-pressure-based airspeed on light, single-engine aircraft (e.g. Conley et al., 2014). Figure 3 shows an application of this technology, where horizontal wind measurements have been combined with concurrent measurements of methane to estimate the size of a natural gas leak by flying circular flight paths encompassing the leak throughout the boundary layer (Conley et al., 2017).

One disadvantage of manned aircraft is that their minimum safe flight altitude may not allow direct measurements in the stably-stratified boundary layer and the surface layer of the convective boundary layer. One way to address this is the use of UAVs. The development and utilization of UAVs are increasing rapidly. They can fly lower and slower and cost much less to deploy than manned aircraft, but have smaller payload and power capabilities, and more limited deployment options. There are now miniaturized systems and instrumentation available using similar measurement techniques as for larger manned aircraft that can be used to measure air velocity from UAVs, but with less accuracy. UAVs have been deployed from land-based sites, aircraft, and ships. Over the ocean they have been used not only for measuring mean and turbulent atmospheric variables, but also ocean surface wave structure (Reineman, et al. 2016).

Another way to make low-level measurements over water is with a CTV, an instrumented platform with a controllable wing tethered to an aircraft that can be towed at an altitude as low as 10 m. A CTV has been developed that utilized an autopilot and radar altimeter to maintain a reference height and instrumented to measure mean and turbulent fluctuations of the three wind components, temperature, humidity, pressure, $CO_2$ concentration, and sea surface temperature (Khelif et al., 2017). A somewhat similar approach is an instrument platform towed beneath a helicopter or blimp. Siebert et al. (2006) describe such a system that was designed to probe the dynamics and microphysics of boundary-layer clouds. Challenges here for CTVs, UAVs, and light aircraft are further miniaturization and improvements in sensor accuracy for both air velocity and scalar measurements.

A "low altitude" approach to making mobile boundary-layer measurements is using instrumented surface vehicles (e.g. cars), boats, or ships with technology similar to that for airborne vehicles. Surface vehicles have the advantage of the possibility of measuring horizontal variability very close to the surface even at night, with smaller fluctuations in platform displacement due to turbulence, and speeds that can range from zero to several tens of meters per second. The typical slower speed of a ground vehicle compared to airborne platforms means that differential pressure sensing of the air velocity vector becomes less viable; however, sonic anemometry, the prevailing sensor for fixed-point measurements of air velocity, has been successfully deployed on a ground vehicle (e.g. Belušic´, et al., 2014). An obvious disadvantage, of course, is the limited terrain or surface types over which it can be deployed.

Aircraft as a platform for deployment of dropsondes is another application with considerable potential. Figure 4 shows, for example, a measurement of divergence and vertical air velocity profiles from flight level down to the surface (Bony et al., 2017) obtained from 12 dropsondes deployed around 200 km diameter circles .

These various instrumented mobile platforms are becoming ever more robust, miniaturized, controllable, and field deployable. With concomitant improvements in signal processing, data recording, and data analysis techniques, mobile platforms are becoming increasingly attractive for deployment in field campaigns. Future desirable enhancements include further development of a robust miniaturized laser-based air velocity sensor, and trace gas sensors that can be used for turbulent flux measurements, trace gas diffusion studies, and air pollution investigations on UAVs and light aircraft.

## REFERENCES

D. Belušic´, D., D. H Lenschow, and N. J. Tapper, 2016: Performance of a Mobile Car Platform for Mean Wind and Turbulence Measurements. *Atmos. Meas. Tech*., **7**, 1825–1837.

Bony, S. and 23 coauthors: 2017: EUREC$^4$A: A Field Campaign to Elucidate the Couplings Between Clouds, Convection and Circulation. *Surv Geophys.* https:// DOI: 10.1007/s10712-017-9428-0.

Conley S., I. C. Faloona, S. Mehrotra, M. Suard, D. H. Lenschow, C. Sweeney, S. Herndon, S. Schwietzke, G. Pétron, J. Pifer, E. A. Kort, and R. Schnell, 2017: Application of Gauss's Theorem to Quantify Localized Surface Emissions from Airborne Measurements of Wind and Trace Gases. *Atmos. Meas. Tech*., **10**, 3345–3358.

Conley, S. A., I. C. Faloona, D. H. Lenschow, A. Karion, and C. Sweeney, 2014: A Low-Cost System for Measuring Horizontal Winds from Single-Engine Aircraft . *J. Atmos. Oceanic. Technol.*, **31**, 1312–1320.

Cooper, W. A., R. B. Friesen, M. Hayman, J. B. Jensen, D. H. Lenschow, P. A. Romashkin, A. J. Schanot, S. M. Spuler, J. L. Stith, and C. Wolff, 2016: Characterization of Uncertainty in Measurements of Wind From the NSF/NCAR Gulfstream V Research Aircraft. NCAR/TN-528+STR, Earth Observing Laboratory, NCAR, Boulder, CO, USA.

Cooper, W. A., 2017: A Kalman Filter To Improve Measurements of Wind From NSF/NCAR Research Aircraft. NCAR/TN-540+STR, Earth Observing Laboratory, NCAR, Boulder, CO, USA.

Khelif, D., J. Barge, H. Jonsson, Q. Wang, and R. Yamaguchi, 2017: Probing the Surface Layer over the Gulf Stream with the Controlled Towed Vehicle: Unique High-Resolution Turbulence Measurements. Abstract, American Meteorological Society 18th Conference on Aviation, Range, and Aerospace Meteorology, Seattle, WA, 22–26 January.

Oncley, S. P., K. Schwenz, S. P. Burns, and J. Sun, 2009: A Cable-Borne Tram for Atmospheric Measurements Along Transects. *J. Atmos. Oceanic. Technol.*, **26**, 462–473.

Reineman, B. D., L. Lenain, and W. K. Melville, 2016: The Use of Ship-Launched Fixed-Wing UAVs for Measuring the Marine Atmospheric Boundary Layer and Ocean Surface Processes. *J. Atmos. Oceanic. Technol.*, **33**, 2029–2052.

Siebert, H., H. Franke, K. Lehmann, R. Maser, E. Wei Saw, D. Schell, R. A. Shaw, and M. Wendisch, 2006: Probing Finescale Dynamics and Microphysics of Clouds With Helicopter-borne Measurements. *Bull. Amer. Meteor. Soc.,* **87**, 1727–1738.

Spuler, S. M., D. Richter, M. P. Spowart, and K. Rieken, 2011: Optical Fiber-Based Laser Remote Sensor for Airborne Measurement of Wind Velocity and Turbulence. *Appl. Opt*, **50**, 842–851.

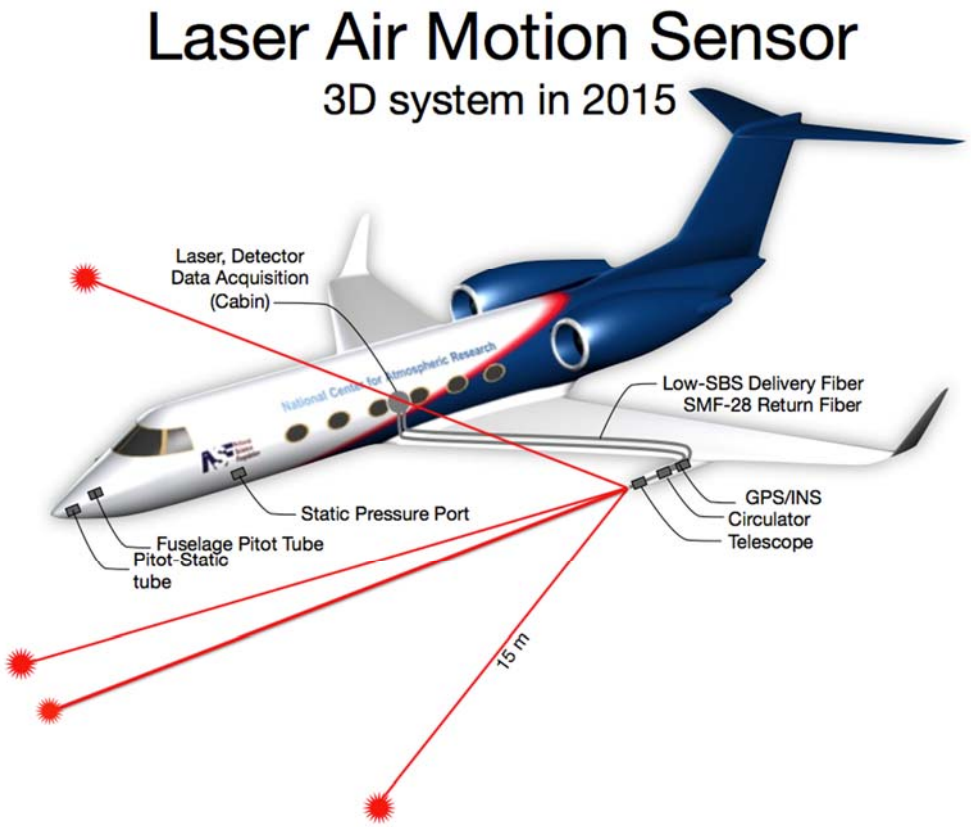


FIGURE 1. A LAMS installation for the NCAR GV. The laser and detector are cabin mounted, with fibers running in the wing connecting them to a small optical bench mounted in a wing-pod that was used to focus the laser at fixed locations about 16 m in front of the nose of the aircraft. The light backscattered from aerosol particles in the focal regions is collected by the lens, and a circulator routes the returned signals, along with a portion of the transmitted signal (generated from a reflection at the end of the transmission fiber) back to the cabin along separate return fibers. The resulting signals, with interference patterns that measure the Doppler shift of the backscattered light, are digitized and recorded by the data acquisition system in the cabin. Output from the four beams can then be processed to obtain the three wind components. Also illustrated in this figure are the approximate locations of the static pressure ports and the fuselage pitot tube used by the research data system to measure static and dynamic pressures. (Adapted from a figure in the article by Spuler et al. [2011] in *Applied Optics*.)

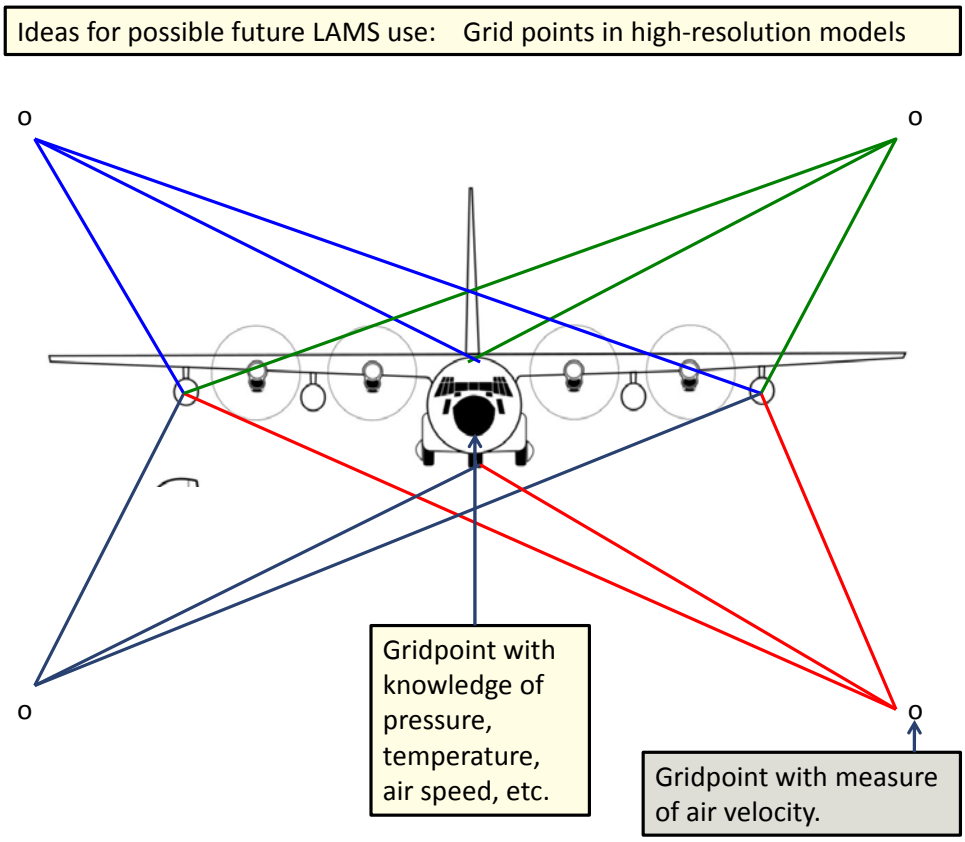


FIGURE 2. With a 12-beam LAMS system emanating from four locations on the aircraft, one can potentially study the three-dimensional structure of turbulence by measuring the wind vector at four locations and make comparisons to predictions from numerical models. Adding a vertical temperature difference measurement may enable a measurement of the Richardson number. (Adapted from a presentation by Jorgen Jensen at the 2nd International Conference on Airborne Research for the Environment (ICARE 2017), Oberpfaffenhofen, Germany.)

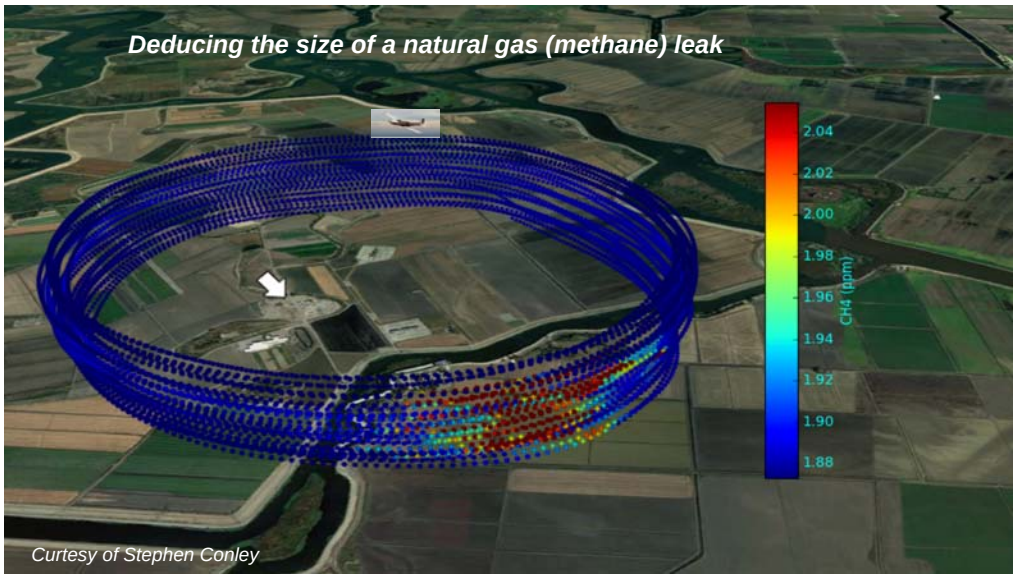


FIGURE 3. Map of the airplane flight pattern sampling a methane plume emanating from an underground storage facility. Wind direction is indicated by the white arrow and the methane mixing ratio is given by the color bar to the right. This flight was conducted on 28 June 2016 and took place between 12:46 and 13:52 LT at altitudes ranging from 91 to 560 m with a loop diameter of approximately 3 km. The measured methane emission rate was 763 ± 127 kg $h^{-1}$ (Adapted from a figure in Conley et al., 2017).

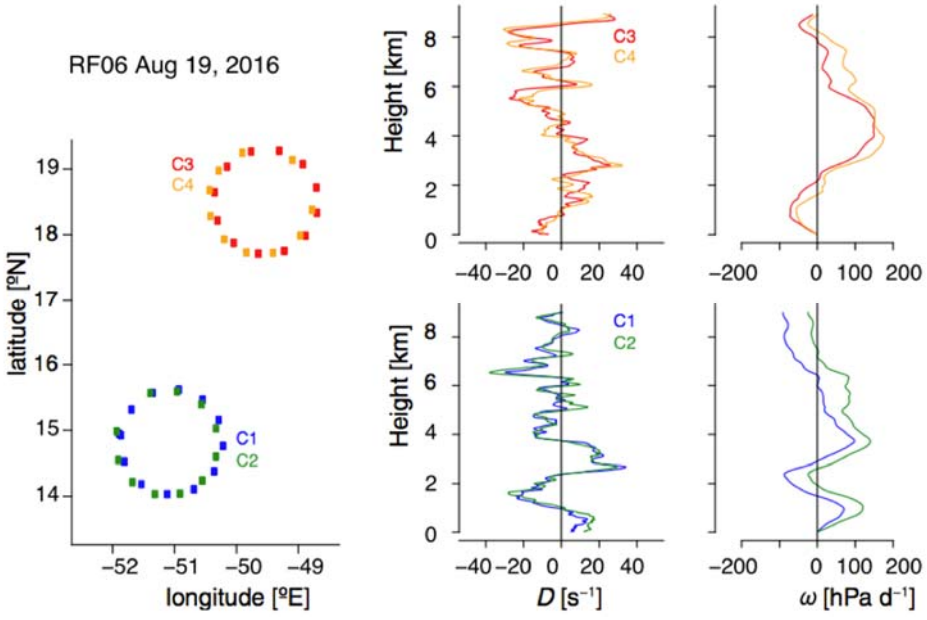


FIGURE 4. (left) Research flights performed during NARVAL2 with the HALO aircraft on 19 August and the vertical profiles of large-scale mass divergence $D$ and large-scale vertical velocity $\omega$ derived from dropsonde measurements for two sets of two circles, each with 12 dropsondes. The first set (blue) shows positive divergence in the boundary layer for suppressed conditions; the second (red) shows negative boundary-layer divergence for a region with a more active low-level cloud layer. The repeatability of the profiles is an indication of the accuracy of the technique (From Bony et al., 2017).

# Leveraging Air Quality Observing Systems in the United States: An Approach to Addressing Operational Gaps and Earth System Science Challenges Related to Atmospheric Composition and Dynamics

Jim Szykman, Lukas Valin, Rohit Mathur, Russell Long, Kevin Cavender
U.S. Environmental Protection Agency

Jim Crawford, Barry Lefer, Bob Swap
NASA

Kelly Chance
Smithsonian Astrophysical Observatory

Several past National Academy reports focused on the challenges and gaps associated with atmospheric observations in the boundary layer with a strong nexus to observational networks for ambient air quality[1,2,3]. An underlying theme within these reports is the need to better integrate networks across agencies to address observational gaps.

Within the U.S. the air monitoring networks maintained by the EPA, NPS, State, Local, and Tribal agencies continue to evolve, and serve as a critical and successful part of the overall air quality management framework; with current infrastructure supporting over 3000 operational monitoring sites across the United States. These ground-based air quality monitoring networks play a central role in characterizing surface air quality and informing policy and regulatory decisions to improve air quality. Within the U.S. the State and Local Air Monitoring Stations (SLAMS) are the principal source of ambient measurements for criteria air pollutants, supplemented by special purpose monitoring networks such as the Photochemical Assessment Monitoring Stations (PAMS), Chemical Speciation Network (CSN), Interagency Monitoring of Protected Visual Environments (IMPROVE), Clean Air Status and Trends Network (CASTNET) and National Atmospheric Deposition Program (NADP). These networks were required or catalyzed by the 1970 Clean Air Act (CAA), subsequent CAA amendments, or National Academy of Sciences (NAS) recommendations. It is important to note that health impacts are the primary driver for changes in the National Ambient Air Quality Standards (NAAQS), which in turn influences the design and location for criteria pollutant monitoring. As such, the monitoring is largely focused on monitoring surface level criteria pollutants in order to identify areas where current air quality is unacceptable, as well as to prevent deterioration in areas where air is relatively free of anthropogenic emission influences. In other words, the current mix of observations within this web of networks is heavily weighted to identify and monitor problems, as opposed to observations which can be used to diagnose the underlying cause of the problem.

In the U.S., new health research has led to a decision to strengthen the NAAQS for ozone to 70 parts per billion (ppb).[4] As a result of the change in the health-based standard, international and non-anthropogenic influences are becoming more significant relative contributors to NAAQS non-attainment. Simultaneously, these extra-regional influences are changing in absolute magnitude due to global development and climate change. The lack of routine and systematic observations to improve our characterization of the 3-dimensional (3D) nature of air pollution throughout the troposphere and across relevant time and space scales continues to limit our ability to better characterize sources, mechanisms, pollutant transport, and the evolving air chemistry to address areas

with persistent non-attainment problems.

The PAMS Network, established in the mid-1990s, was designed to satisfy requirements under Section 182(c)(1) of the Clean Air Act (CAA). The measurement objectives of PAMS are focused on collection of relevant observations which can provide information on the effectiveness of control strategies, emissions tracking, trends, and exposure. Recently, the U.S. EPA finalized changes to the PAMS Network under the revised $O_3$ standard[4]. These forthcoming measurement requirements include, but are not limited to, continuous mixing layer height, a more direct ambient $NO_2$ measurement, hourly VOCs via AutoGC, carbonyls via cartridge sampling (along with a future option to include continuous HCHO), and a re-distribution of sites to provide broader geographic coverage. By June of 2019, the re-designed PAMS network will be merged with the NCore network in Core Based Statistical Area (CBSAs) with a population of 1,000,000 people or more, creating approximately 40+ sites across the U.S. These network changes will provide an improved set of observations for air quality management activities, including improved evaluation of chemical transport models at the regional to national scale and strengthen capability for EPA to track regional trends in precursor concentrations.

Starting in 2010, NASA carried out the Deriving Information on Surface Conditions from COlumn and VERtically Resolved Observations Relevant to Air Quality (DISCOVER-AQ) Earth Venture Mission (2011-2014). With a primary objective to understand how space-based observations can be used to better inform surface air quality, DISCOVER-AQ implemented a strategy to repeatedly and systematically sample boundary layer composition. The primary focus was on key trace gases and aerosols (including optical properties) and planetary boundary layer/mixing heights to better understand how a column-based measurement from space relates to surface composition. To accomplish the mission, NASA developed collaborations with a range of government, academic, and private partners, including the EPA and State and Local Air Quality Agencies. Through an active partnership with the State and Local air quality agencies, the project effectively leveraged the existing national air quality network infrastructure within the study domains; Baltimore, MD (2011), San Joaquin Valley, CA (2013) Houston, TX (2013), and Denver, CO (2014). The local air quality sites, many of them either part of the SLAMS or PAMS networks, served as measurement anchor points for the coordinated 3D sampling strategy (airborne spirals, ground- and aircraft-based remote sensing) and provided context beyond the periods of intensive observations.

DISCOVER-AQ results highlighted both the ability and the importance of routinely monitoring factors affecting the 3D distribution of $NO_2$ (e.g., Figure 1), a precursor of tropospheric ozone, and help shape the PAMS network design through the in-field evaluation of emerging measurement technology [5,6,7]. The suite of mixed layer height measurements, surface in-situ measurements of true $NO_2$ and column $NO_2$ measurements via pandora spectrometers[8] represent a subset of information to be routinely monitored within the PAMS network re-design, with total column $NO_2$ measurements targeted to be included under Enhanced Monitoring Plans at a subset of PAMS sites. In combination, these measurements connect our understanding of surface AQ and space-based measurements, but also provide constraints on the extent of vertical mixing of local emissions. For example, because $NO_2$ is primarily emitted at the surface and has a short lifetime ($\tau \sim$ 2 – 10 hours), the ratio of its surface concentration to its total column loading reflects the depth to which it has been mixed over its lifetime. Before 11AM on 6 August 2014 at Boulder Atmospheric Observatory (Figure 1), the relationship of the $NO_2$ column (top panel, black/red) to surface concentration (gray line) is approximately $1 \times 10^{15}$ molecule $cm^{-2}$ for every 1 ppbv. After 11 AM, the relationship quickly doubles and eventually nearly triples, reflecting the influence of a 3-fold growth in mixing depth or the advection of a deeper polluted layer. Ceilometer backscatter measurements confirm the rapid shift in mixed layer height after 11 AM. By making efforts to more fully understand the factors affecting surface $O_3$ concentrations like that demonstrated in Figure 1, the PAMS network requirements will routinely provide detailed information on composition and dynamics to the broader research community.

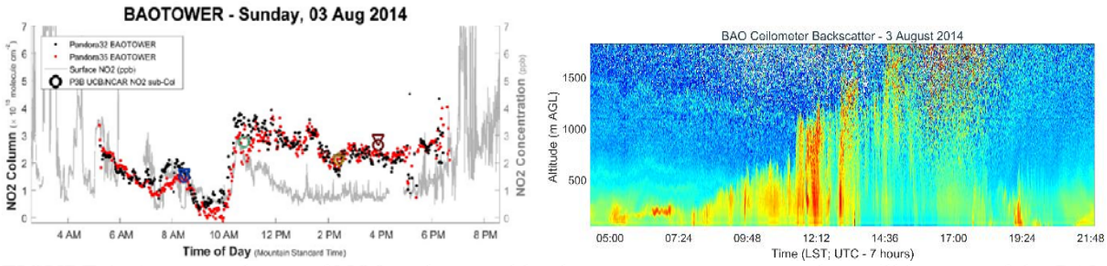


FIGURE 1. An example set of NO2 and aerosol backscatter measurements that will be part of the PAMS network: in situ NO2 measurements (required hourly; left panel gray line), required mixed layer height measurements (e.g., ceilometer backscatter measurements; right panel) and Pandora direct sun NO2 column measurements (e.g., a proposed part of the PAMS required Enhanced Monitoring Plan, left panel red and black). Vertically integrated aircraft in situ NO2 column measurements are also shown (left panel, colored triangle and circles).


FIGURE 2. PAMS Network existing sites (blue and green circles), and required network sites (green circles and squares).

The distribution of PAMS sites (existing, existing required, and new required) is shown in Figure 2. Network revisions will be operational in June 2019. States may choose to continue PAMS operations at existing sites that are no longer required (Figure 1, blue). PAMS requirements are generally intended to be both flexible and thorough. While the technology that states will use to achieve all requirements is not fully defined (e.g., hourly mixed layer heights), there are opportunities to work with states and US EPA to make the native data, and not just time-averaged products available (e.g., 15 second ceilometer backscatter profiles).

Attaining the new $O_3$ standard by 2025 across the United States, excluding California, is expected to cost $1.4 B/yr and yield up to $5.9 B/yr in quantifiable health benefits. In California, it is expected to take additional time to meet the NAAQS, leading to $0.8 B/yr in additional costs but yielding up to $2.1 B/yr in additional quantifiable health benefits.[9] Consistent with recommendation in past NAS reports[1-3] the forthcoming changes to the PAMS network associated with the new ozone standard address boundary layer observations needs within the air quality community, with strong synergies to the weather, climate, and remote-sensing communities. The suite of new measurements, including the addition of ground-based Pandora spectrometers as part of NASA's domestic expansion of the nascent yet rapidly emerging Pandonia Global Network, leverages existing and expanding infrastructure already required and funded by the EPA via the CAA. As these observations are implemented active engagement across the relevant communities will be critical to maximize the use of the data sets beyond the air quality community. EPA has engaged through an ad-hoc working group on PLBH/MLH measurements (http://lidar.umbc.edu/ad-hoc-mixing-layer-height-working-group/) to explore leveraging the MLH measurements with other networks such as NASA's

Micropulse Lidar Network. In addition, EPA has engaged with NASA and the European Space Agency for a subset of these sites to address ground validation needs of satellite instruments such as TROPOspheric Monitoring Instrument (TROPOMI) and Tropospheric Emissions: Monitoring of Pollution (TEMPO). A sustained engagement across these different communities will be required to maximize the use of these new measurements for operations and research.

**REFERENCES**

[1] NRC (2004) Air Quality Management in the United States
[2] NRC (2009a) Global Sources of Local Pollution: An Assessment of Long-Range Transport of Key Air Pollutants to and from the United States
[3] NRC (2009b) Observing Weather and Climate from the Ground Up: A Nationwide Network of Networks
[4] EPA (2015) National Ambient Air Quality Standards for Ozone: Final Rule, *Federal Register*, 80:65291-65224.
[5] Long, R., et al., Evaluation and Comparison of Methods for Measuring Ozone and NO2 Concentrations in Ambient Air during DISCOVER-AQ. EM Magazine. Air and Waste Management Association, Pittsburgh, PA, , August, (2016).
[6] Szykman, J., et al., The Use of LIDAR Technology for Measuring Mixing Heights under the Photochemical Assessment Monitoring Program; Leveraging Research under the Joint DISCOVER-AQ/FRAPPÉ Missions. EM Magazine. Air and Waste Management Association, Pittsburgh, PA, , August, (2016)
[7] Crawford, J., J. Al-Saadi, G. Pierce, R. Long, Jim Szykman, J. Leitch, C. Nowlan, J. Herman, AND A. Weinheimer. Multi-perspective observations of NO2 over the Denver area during DISCOVER-AQ: Insights for future monitoring. EM Magazine. Air and Waste Management Association, Pittsburgh, PA , August, (2016).
[8] Herman, J., et al., 2009. NO2 column amounts from ground-based Pandora and MFDOAS spectrometers using the direct-Sun DOAS technique: Intercomparisons and application to OMI validation. Journal of Geophysical Research: Atmospheres, 114(D13).
[9] EPA (2015), Regulatory Impact Analysis of the Final Revisions to the National Ambient Air Quality Standards for Ground-Level Ozone, EPA-452/R-15-007.

# Leveraging Existing and Future In-Situ Observational Networks

John Horel
Department of Atmospheric Sciences, University of Utah

The 2009 National Academy Report, *Observing Weather and Climate from the Ground Up*, recommended that stakeholders in all sectors (government, commercial, and academia) should "collectively develop and implement a plan for achieving and sustaining a mesoscale observing system to meet multiple national needs". One outgrowth of that report was the establishment of the National Mesonet Program by the National Weather Service, which supports the integration of non-federal sub-, near-, and above-surface observations collected by 40 commercial and academic institutions (https://nationalmesonet.us/). The American Meteorological Society developed the Nationwide Network of Networks Committee that highlighted some of the steps to facilitate weather and climate data exchange from a diverse community of data providers to users (Stalker et al., 2013, *Bull. Amer. Meteor. Soc.*). That committee also sponsored the *2016 Forum on Observing the Environment from the Ground Up* to discuss innovative observing efforts currently underway across the country, prospects for taking advantage of new technologies, improving coordination among the diverse efforts throughout the environmental observing enterprise, and meeting the ever-growing needs of the users of environmental information.

Effectively harnessing existing and future in-situ environmental observing infrastructure remains a critical need to understand and model the global atmospheric boundary layer. Network owners install in-situ systems to meet specific needs (e.g., public safety, air and surface transportation, land resource management, air quality, commercial operations). No existing network or temporary deployment of in-situ equipment for field campaigns is capable of providing adequate information to understand the impact of the complex boundary layer processes above land, water, and ice surfaces. The phrase "the whole is greater than the sum of its parts" captures the potential benefit to leverage the diverse nature of surface-based in-situ networks with "top-down" and "bottom-up" remote sensors.

Attempts to catalog the extent and gaps within the in-situ observing infrastructure on the national scale remain inadequate, primarily because those catalogs rapidly become obsolete as they require considerable effort on the part of network owners to supply information that is not easily managed by them. Leveraging the diverse types and quality of environmental sensors requires greater attention to the metadata to describe where, why, how, and what is being measured. One step to facilitate improved availability of metadata would be to reduce reliance on manual metadata entry by the network owners. Equipment manufacturers could incorporate automated procedures to transmit critical metadata at the time of installation and whenever updates are made as soon as they occur (e.g., current location, sensor characteristics, sensor siting, replacement or recalibration).

Hundreds of government, commercial, and academic entities deploy and manage networks of in-situ sensors that provide millions of observations each day in the U.S. and internationally. Estimating the validity of these observations as they are received is poorly handled at this time for research and data assimilation applications. Sensors are deployed for diverse reasons that intentionally use diverse deployment and reporting strategies that vary from one user community to another (aviation, surface transportation, air quality, climate reference, etc.). Assuming a single standard is applicable to all in-situ sensor data is not practical, nor likely to insure data validity. Current practice for operational data assimilation tends to rely heavily on subjective network allow/deny lists. Data science/informatics research is required to extend beyond traditional quality control metrics (range, rate, buddy, climatological checks, etc.) to identify critical changes in

environmental states that takes into consideration how the information is collected and intended to be used. Separating invalid data from unique information that may help fill a data gap is a critical preprocessing step for data assimilation.

Internet of Things sensors (low-cost home units, wearables, vehicle sensors, etc.) require research and development to assess the extent to which they can be used in data assimilation systems probabilistically rather than deterministically. While millions of pressure observations could be obtained from cell phones in metropolitan areas or current weather along major highway routes, the extent to which adding this information improves operational and research modelling efforts remains unclear and requires more research.

The 2009 *Observing Weather and Climate from the Ground Up* report, American Meteorological Society efforts related to the Nationwide Network of Networks, and the National Mesonet Program highlight that managing data rights is necessary for networks of in-situ and surface-based remote sensors. Agencies such as NOAA often enter into license agreements with network owners to access environmental information with limited rights for the agencies to redistribute that data. Assessing the relative value and impacts of different observational data streams is a critical need to insure that the valuable data streams are available for diverse modeling and research needs. For example, using observations from wind energy companies with sensors mounted on tall towers on- and off-shore would potentially be of great benefit for improved modeling and understanding of the boundary layer. The extent to which the interests of those companies and those of the research and operational communities can be met through data licensing agreements needs to be assessed.

# Airborne Doppler Wind Lidar Investigations of Atmospheric Boundary Layers

G. D. Emmitt
Simpson Weather Associates

## INTRODUCTION

Over the last 15 years, airborne Doppler Wind Lidars have transitioned from early missions that were hardware centric (demonstrating airborne worthiness and utility) to missions focused upon specific science questions, especially the dynamics of the boundary layer. The airborne lidars discussed here use returns from aerosols/clouds and provide high precision (<.1m/s) and low bias (< .25m/s) wind profiles with ~ 50m vertical resolution at 1 -3 km horizontal intervals. Since the focus of this panel is on the observing systems, a brief survey is made of how three different airborne DWLs have been used to study the marine and terrestrial boundary layers.

## THE INSTRUMENTS

There are three USA airborne DWLs that have been and are currently available for atmospheric research on a scheduled basis:

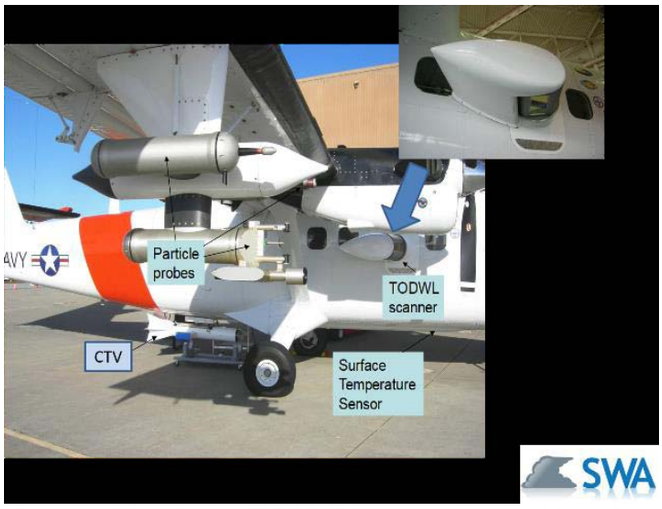


FIGURE 1. Twin Otter Doppler Wind Lidar (**TODWL)** operated by the Naval Post Graduate School in Monterey, CA. The Controlled Towed Vehicle (CTV) is towed at various distances below the Twin Otter. A nominal distance is 1000meters. This Twin Otter also hosts a flux sensor package.


FIGURE 2. **P3DWL** (Multi-agency) operating since 2008 on an NRL P3 and currently operating on NOAAs P3s.The side mounted scanner enables scans above and below flight level. It also enables sampling at both nadir and straight ahead perspectives.


FIGURE 3. Doppler Aerosol WiNd (**DAWN)** developed by NASA LaRC was flown on NASA's DC-8 along with dropsondes and another wind lidar. The German aircraft carried two wind lidars as well and flew in formation with the DC8.

These three USA airborne DWLs have been funded by NASA, NOAA, and DoD to conduct basic research and have participated in the following research activities and field campaigns:

1999-2007: Developing an understanding of airborne and future space-based DWL returns from the earth's surface and the adjacent atmosphere.…. (NPOESS)

2008 TPARC: Tropical cyclone investigations in the western Pacific with an emphasis on the air-sea interactions….(ONR)

2012 UPP: Unified Parameterization Project (EDMF)… (ONR)

2012 MATERHORN: Investigating boundary layer circulations over complex terrain… (ONR)

2014-2015 PolarWinds: Field campaign with a focus on numerical model validation and LLJs, Katabatic flows and atmospheric circulations across ice-land-water transitions…. (NASA)

2017 CPEX: Investigation of convective processes using the promising combination of DWL, APR2, dropsondes and T/RH sounders…. (NASA)

2015-2017 HFIP: Validation of the potential for airborne DWL observations to enhance

operational forecasting of tropical cyclones… (NOAA)

2014 – 2017 FSR: Multiyear study of the role of atmospheric boundary layer structures (LLJs, thermals, inversions) in altering the lifecycle of wing tip vortices threatening air drops… (DoD)

## AIRBORNE DWL APPLICATIONS

The following are a few selected applications of airborne DWLs over the last 10 years.

**Numerical Weather Model Validation**

The TODWL was flown during the MATERHORN mountain meteorology experiment lead by Joe Fernando (ND). Approximately 3000 wind profiles were obtained over and around Granite Mountain in Utah (Figure 4a). The wind soundings were used in comparisons with the Weather Research Forecast (WRF) model run by SWA, University of Utah (Pu) and NCAR (Figure 4b).

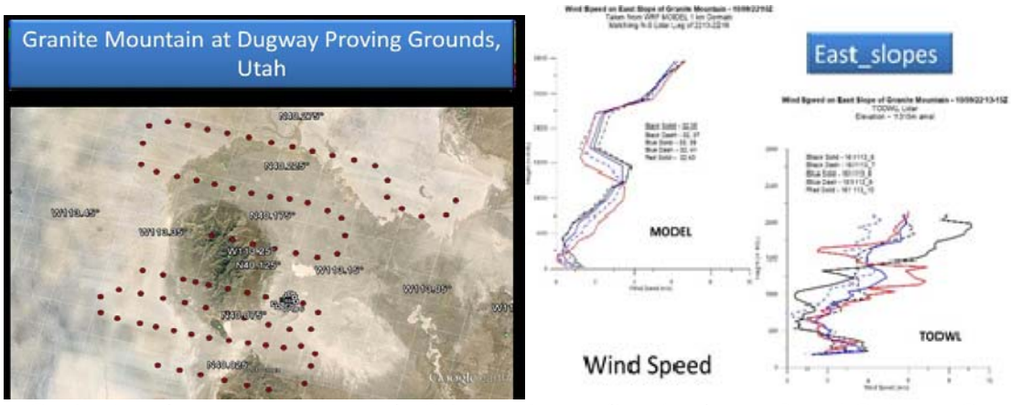


FIGURE 4. Left: Example pattern of TODWL wind profiles (surface to 3km AGL) over Granite Mountain, Utah. Right: Example comparison between TODWL soundings and NCAR WRF soundings

Airborne DWL profiles were also used in studies involving the following models:

- HurricaneWRF (w/R. Atlas and others at Univ, of Miami and AOML)
- PolarWRF (w/John Cassano (CU) and David Bromwich (OSU))
- Miami Coupled Model (UMCM) (w/Shuyi Chen Univ of Wash))

**Marine Boundary Layer Flux Parameterization**

The TODWL was used during a multiyear ONR funded program lead by Joao Teixiera. SWA along with Ralph Foster focused on cases where the TODWL and the Controlled Towed Vehicle(CTV) revealed marine (and terrestrial) boundary layer rolls with Turbulence Transport Channels carrying TKE from the surface to the top of the mixed layer (Figure 5).

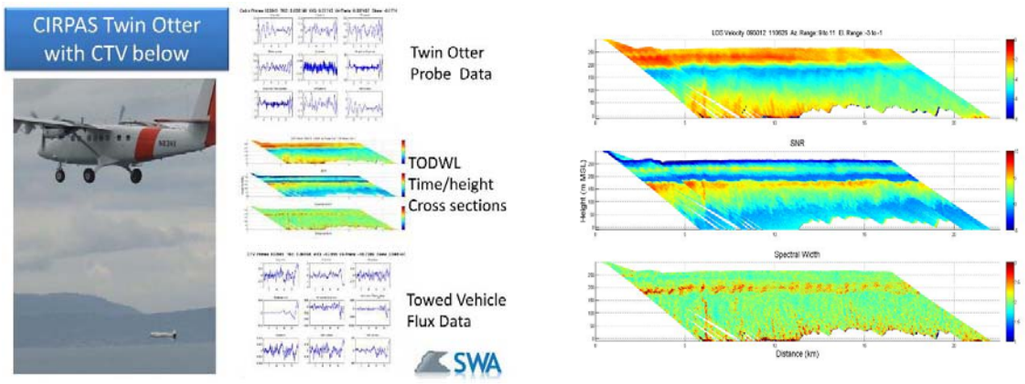


FIGURE 5. The left figure illustrates how the TODWL and CTV were used to prospect the marine boundary off the California coast. The right figure illustrates the three basic data products generated by the TODWL used in a shallow angle (~3 degrees down) look ahead mode. The top panel is the line of sight wind speed detecting wind variability consistent with rolls. The middle panel is Signal to Noise ratio which indicates how the aerosols are distributed. The bottom panel shows the lidar signal spectral width which is directly related to the turbulence on scales of a few 10's of meters.

**Summary of segment statistics**

| Flight Segment | TODWL Altitude | CTV Altitude | Heading | TKE | Sensible Heat (W) | Latent Heat (W) | Skewness |
|---|---|---|---|---|---|---|---|
| 1007 | 284 | 60 | 94 | .19 | 8.55 | 3.43 | -.40 |
| | | | | 1.92 | -1.28 | 15.15 | .90 |
| 1028 | 292 | 25 | 98 | .04 | .22 | .09 | -.18 |
| | | | | .80 | -12.6 | -18.7 | .05 |
| 1106 | 286 | 75 | 294 | .05 | 3.02 | 1.21 | -.51 |
| | | | | 1.1 | -3.36 | -1.19 | -.17 |
| 1111 | 290 | 75 | 293 | .24 | 1.98 | .80 | -.37 |
| | | | | .29 | -.74 | .55 | .22 |
| 1121 | 288 | climbing | 98 | .14 | -1.11 | -.44 | .90 |
| | | | | | | | |

TABLE 1. Example of fluxes computed from the Twin Otter and CTV sensor packages. The TODWL provides visualization and quantification of the organized components of the BL processes.

**Arctic circulations near land-sea-ice transitions**

In 2014 and 2015, The NASA DAWN was used in more than 100 hours of research flights (Figure 6) to investigate boundary layer circulations near land-sea-ice transition zones. PolarWinds I and II, lead by SWA, included numerical model studies by John Cassano and David Bromwich. A paper on the Barrier Jet (ref) has been published.

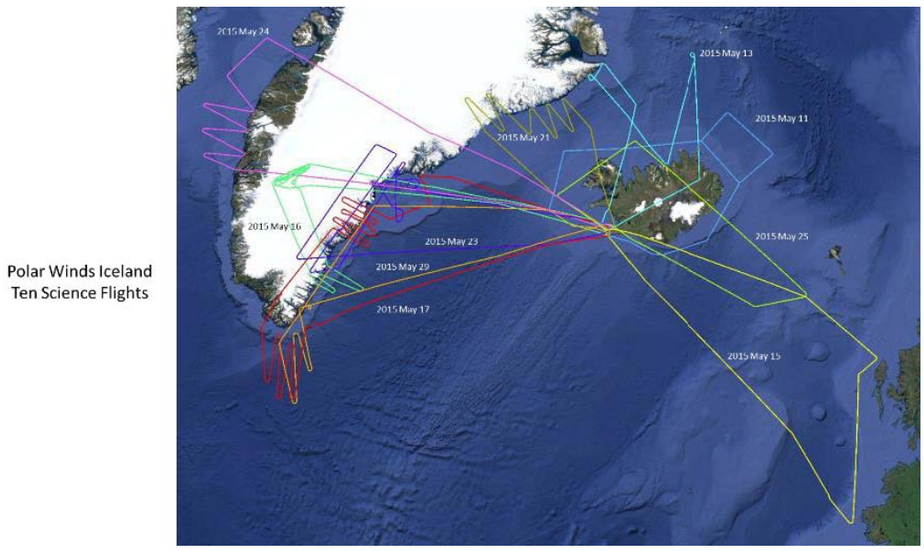


FIGURE 6. Flight paths of the NASA DC8 during the 2015 PolarWinds mission out of Iceland.

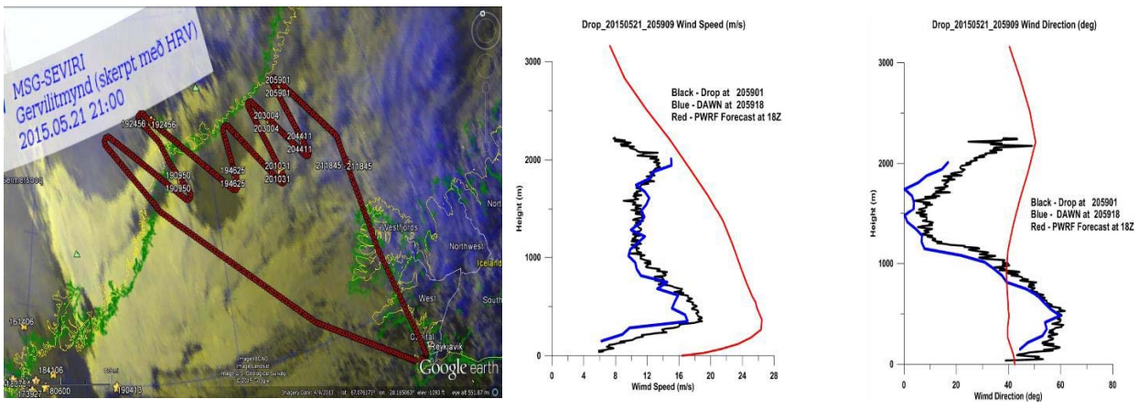


FIGURE 7. Barrier Jet case study off the east coast of Greenland. Wind profiles from DAWN, dropsondes and the PolarWRF are compared in the figures on the right.

**Tropical Dynamics**

In 2008, the TPARC/TC08 experiment was conducted in the western Pacific. The P3DWL (currently on NOAA's P3) was flown (150 hours) on tropical cyclone missions with a special focus on observations of the lowest 3km of the TC circulation. The locations of P3DWL soundings for one mission are shown in Figure 8. In another case (TC Nuri), the P3DWL data were assimilated into the WRF model and showed significant improvement in TC track and intensity forecasts (Figure 9).

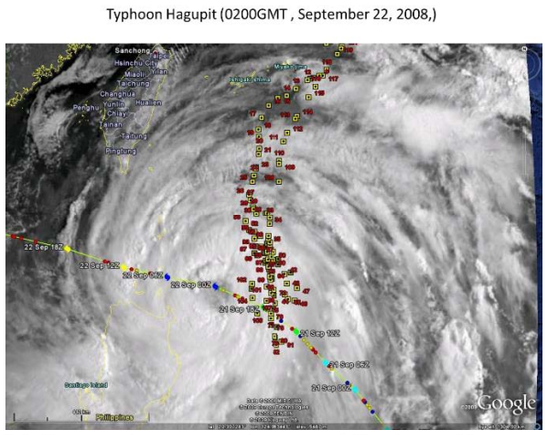


FIGURE 8. Locations of P3DWL soundings near the eye of Typhoon Hagupit during TPARC. On the right is a figure from Pu, Zhang, and Emmitt (2010).

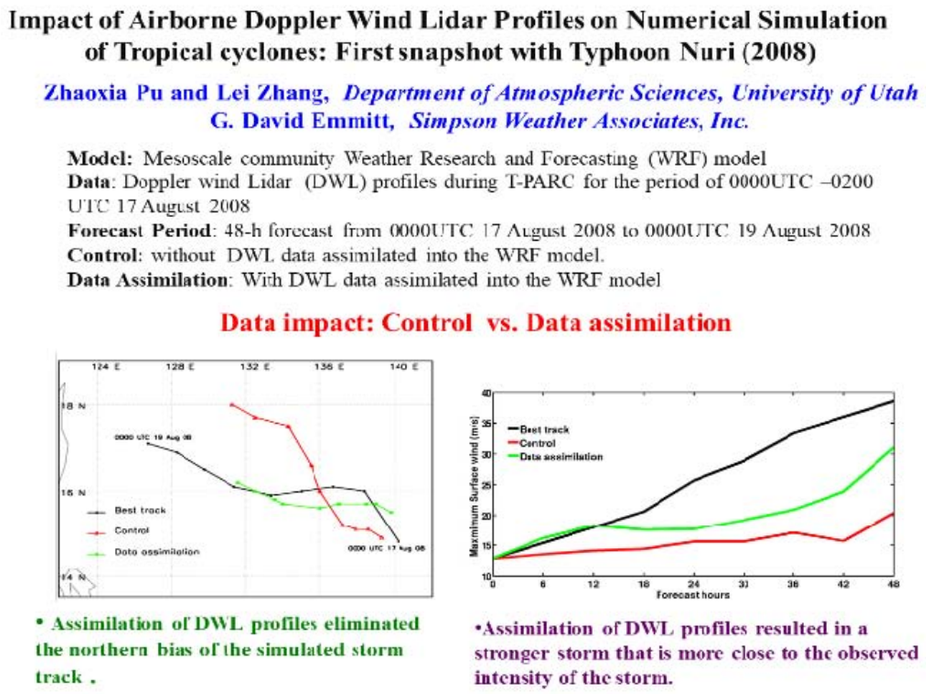


FIGURE 9. Impact of P3DWL wind profile data assimilation on WRF simulation of TC Nuri.

This past summer, NASA supported the Convective Processes Experiment (CPEX) which highlighted the contribution that an airborne DWL (DAWN) can offer in various stages of convection ranging from “clear” to tropical cyclones (Cindy). A major element of the CPEX project is model validation (Shuyi Chen, Zhaxioa Pu and others). Process studies are also being conducted by Emmitt, Zipzer, Garstang and others. Figure 10 is a summary slide provided to NASA headquarters. Figure 11 illustrates the very promising combination of airborne DWL and precipitation radar (APR2).

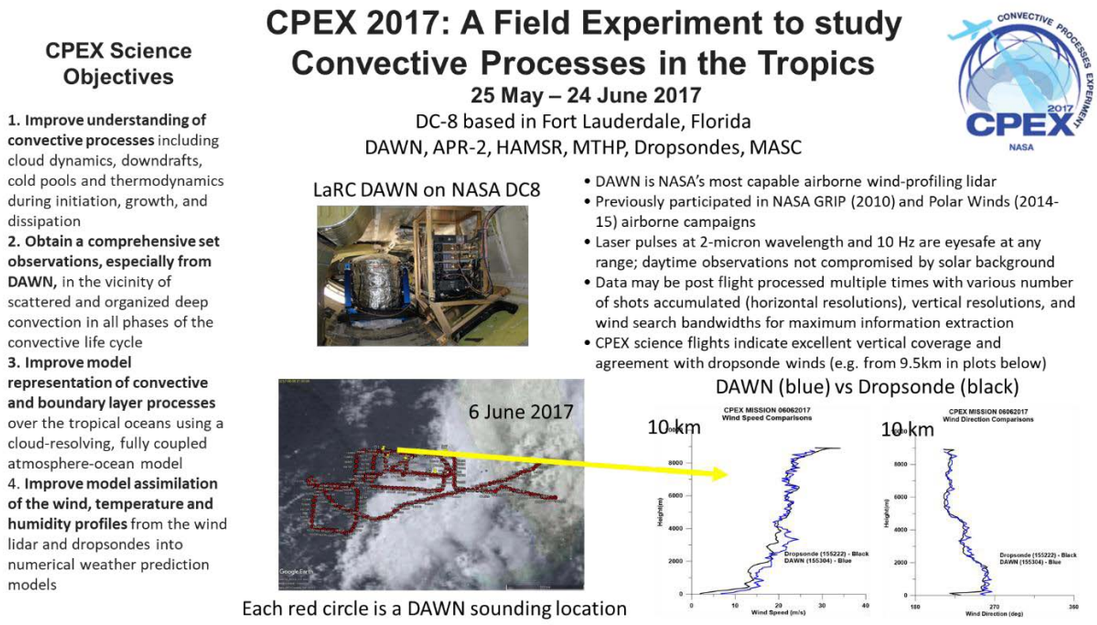


FIGURE 10: A slide prepared for NASA headquarters briefing.

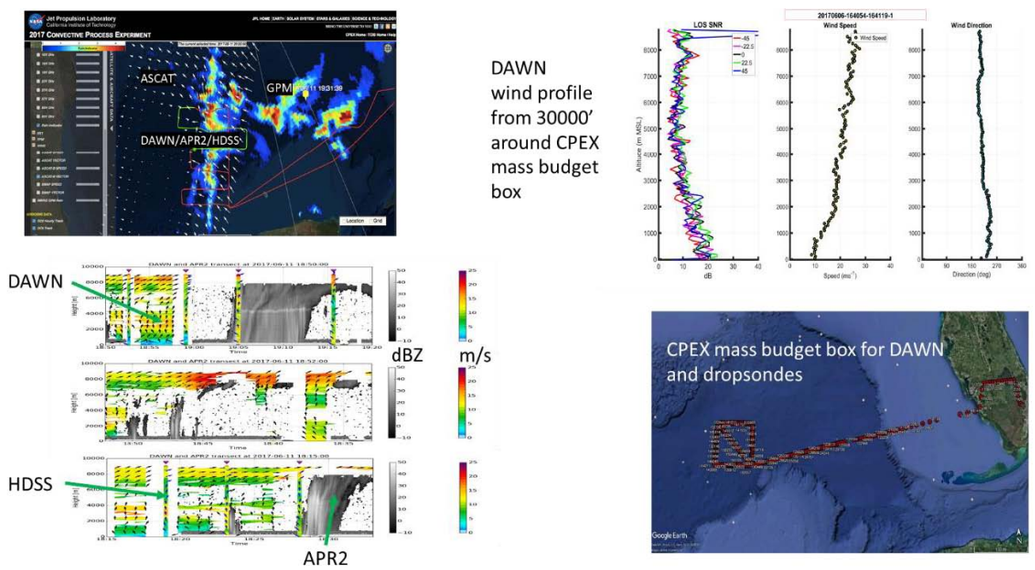


FIGURE 11. On the left is an example (prepared by Shuyi Chen) of the use of DAWN and the APR2 in deep convection observed during CPEX2017. On the right are an example of DAWN wind profiles of aerosol structures, wind speed and wind direction. The lower right panel is an example of a CPEX Box used to measure the convergence/vorticity profile with height (50m resolution) over a 100 x 100km area.

**FUTURE OF DWL: AIRBORNE AND SPACE**

The airborne DWLs mentioned above are “one-of-a-kind”, expensive and very capable in terms of making wind observations under low aerosol conditions or in cloudy situations. For boundary layer work conducted at altitudes below 3km AGL, these systems are more than adequate. The costs and operational complexity of these systems is an impediment to expanding the availability of airborne DWLs. However, the future use of airborne DWLs for atmospheric research is very promising. Wind energy and DoD needs have pushed the market to develop capable yet affordable DWLs. While most of the applications for these systems are ground based or ground mobile, developing airborne versions is underway.

Much of the agency level investment into airborne DWLs has been driven by the goal of global wind observations from space for NWP. More than 10 proposals to put a DWL into space have come and gone over the past 30 years. However, there is still a belief that it will happen. NASA, NOAA and the DoD have long recognized the transformational value of global wind profiles, especially over the oceans and within the tropics. Maturation of the key lidar technologies has accelerated investments, primarily those by NASA.

# Remote Sensing of Turbulence in Cloudy Boundary Layers

Bruce Albrecht
Department of Atmospheric Science
RSMAS University of Miami

## INTRODUCTION

The representation of cloudy boundary layers in regional to global atmospheric models remains a challenge. Stratocumulus clouds, which cover extensive areas of the Earth's surface, are critical elements of the climate system (e.g. Wood, 2012) and have been the focus of many studies. The development and application of Doppler cloud radars have provided a means to characterize the turbulence structure in both marine (Frisch et al. 1995; Ghate et al. 2014; Lothon et al. 2005) and continental stratocumulus clouds (Kollias and Albrecht 2000; Ghate et al. 2010); Fang et al. 2014 a,b). When used in a vertically facing mode, these radar Doppler cloud radars can provide vertical air velocity with a temporal and spatial resolution that can be used to provide profiles of vertical velocity statistics and sub-resolution velocity variance that can be scaled relative to cloud-top height. The spectrum width estimates from Doppler radar observations provide a route to TKE dissipation rates (e.g., Fang et al. 2014a,b) that enable a quantitative examination of key terms in the TKE budget at cloud top and provide new perspectives on cloud top entrainment processes (Albrecht et al, 2016).

Extensive radar observations from the DOE Atmospheric Radiation Measurements (ARM) (Kollias et al, 2000) have provided the basis for several studies of the turbulence in cloudy boundary layers. An example of Doppler cloud radar observations made at the Atmospheric Radiation Measurement (ARM)'s Southern Great Plains (SGP) site during uniform non-precipitating stratocumulus cloud conditions for a continuous 14-hour period is shown in Fig. 1 This figure shows the small-scale temporal variability of reflectivity and the first and second moments of the Doppler spectra. These moments can be used to characterize the turbulence characteristics in the boundary layer.

One advantage of the radar observations from the ARM sites is that observations from other observing systems operating at the site can be used to define additional parameters important for boundary layer studies. For example, ceilometer observations provide cloud-base heights and a microwave radiometer provides liquid water path estimates at the ARM site as illustrated in Fig. 1. The time evolution of the radiative and surface forcing that maintains these clouds can also be estimated from these additional measurements to give a time-dependent convective velocity scale w*.

## TURBULENCE AND LARGE EDDY STRUCTURES

Profiles of the vertical velocity statistics can be obtained from time-height characterizations of the vertical velocity (Fig. 2). The variance and skewness can be calculated

from the vertical velocity time series. The spectrum width (SW) from the radar observations is a measure of the vertical velocity variance within the radar-beam sampling volume, which depends on the radar beam width and the sampling dwell time. The SW can be used to define dissipation rates that can be combined with the variance to provide an integral length scale (see Fig. 2). The long-term observations from the SGP site in the example shown allow a definition of the temporal variability of the vertical velocity variance and the spectrum width (Fig. 3). Although the cloud depth remains about the same for the 14-hous of observations in this case, the cloud top height increases with time. Both the variance and the spectrum width observed in this case evolve with time going from day-time to night-time conditions. The change in skewness between the day and night periods is dramatic and consistent with the differences in the forcing between day and night. The composite structure of coherent eddies in the boundary layer developed from these observations is shown in Fig. 4 and are compared for the daytime and nighttime conditions. These types of characterizations provide a means to study the structure and variability of large eddy structures within the cloudy boundary layer that can be compared with LES characterizations.

## ENTRAINMENT

Cloud-top entrainment in stratocumulus clouds has been the focus of extensive observational and modeling studies (Wood, 2012). Doppler cloud radar observations provide a means to examine cloud-top entrainment processes and parameterizations. The radar estimates of the vertical velocity variance and energy dissipation rate (EDR) can be used in the parameterized turbulent kinetic energy (TKE) budget of the entrainment zone. For the ARM SGP case discussed previously, the vertical velocity variance term correlates strongly with the dissipation rate term in the entrainment zone. This correlation further increases when the night-time decoupling of the boundary layer is considered (Fig. 5). The correlation between the dissipation rate and the variance term has always been assumed in commonly used entrainment parameterizations, but the Albrecht et al, (2016) Doppler radar study provides the first observational confirmation of this relationship. This study indicates a strong potential for making entrainment rate estimates directly from radar vertical velocity variance and the EDR estimates. Further, the results support the concept that eddy dissipation rates from radar observations can be used to estimate entrainment rates directly, and that in some types of models entrainment rates could be estimated from parameterized or explicitly resolved dissipation rates. Using the eddy dissipation rate to determine entrainment rates has two major advantages over vertical velocity parameterizations. First, unlike estimates from the vertical velocity variance, no height scale or mixing length scales are needed. Second, statistically stable representations of the entrainment velocity can be made to allow for retrievals at higher temporal resolution than possible from the vertical velocity variance estimates as shown in Fig. 6.

## OPPORTUNITIES AND CHALLENGES

There are several opportunities for advancing the use of cloud radars for cloudy boundary layer studies that have been enabled by the observing systems and analysis techniques that have been developed during the past decade. One of the most promising areas for future work is on

the use cloud radars for the characterization of cloud-top entrainment rates and processes. The extensive data sets that have been collected at the DOE ARM sites allows for the possibility of estimating cloud turbulence and entrainment rates for a large number of stratocumulus cloud cases under varying synoptic conditions and forcing. Although cloud turbulence estimates have been made from aircraft (Lothon et al, 2005), the full potential for using this technique for studies of cloudy boundary layers has not been realized. The HIAPER Cloud Radar (HCR) that has been developed for use on the NSF/NCAR G-V is a prime candidate for future studies. The radar reflectivity from the cloud radar observations allows for the possibility of estimating liquid water variability that could be used to estimate cloud liquid water fluxes. The use of Doppler lidars allows for the definition of turbulence in the clear air below the cloud (e.g. Hogan et al, 2009; Ghate et al 2014) that can be combined with the radar observations to define vertical velocity characteristic through the entire boundary layer.

A remaining challenge is that shallow marine stratocumulus clouds contain drizzle that complicates the simple use of the first and second moments of the vertical velocity spectra. Techniques that have been developed to separate the contributions of these two processes from the Doppler spectrum (Luke and Kollias, 2013) provide a means for examining the turbulence in drizzling stratocumulus clouds.

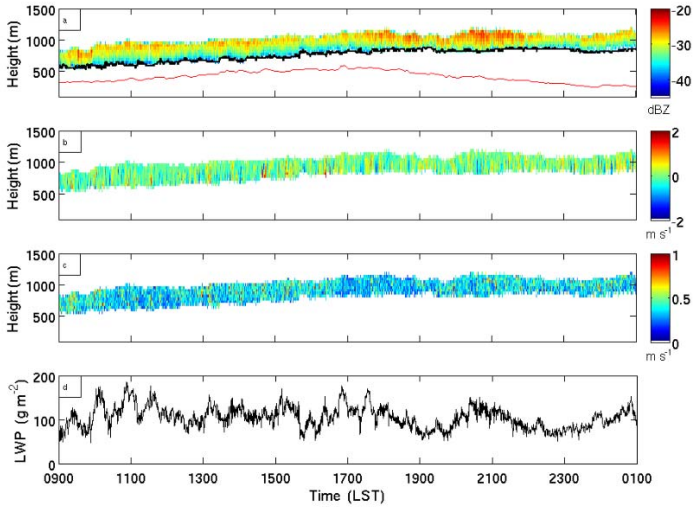


FIGURE 1 Time-height display of (a) reflectivity factor, (b) mean Doppler velocity, and (c) Doppler spectrum width from recorded by the millimeter-wave cloud radar at the ARM site, and (d) liquid water path from the microwave radiometer. The ceilometer-recorded cloud base height (black) and the lifting condensation level calculated from surface observations (red) are also shown in the top panel (Fig. 1; Albrecht et al, 2016)

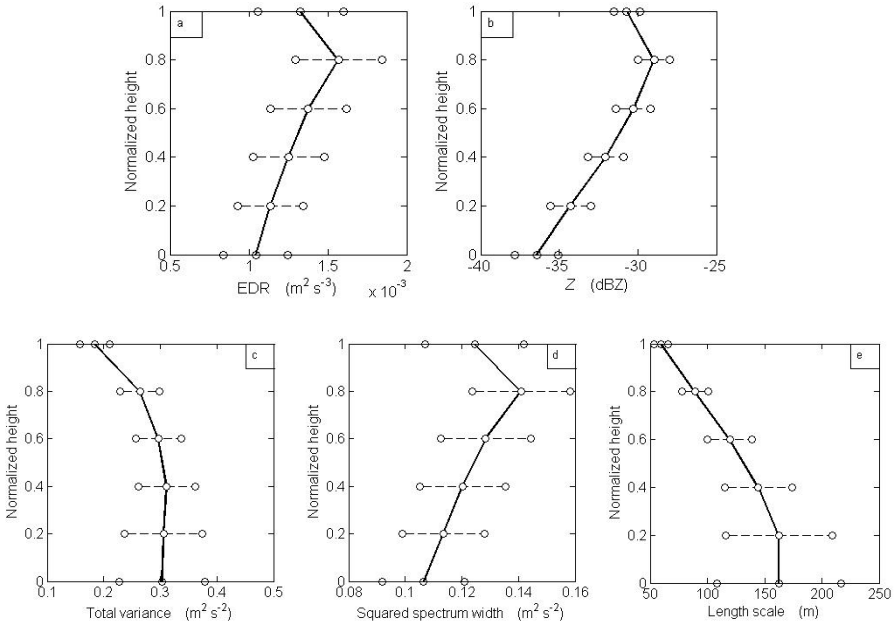


FIGURE 2. Profiles of median EDR (a), *Z* (b), total variance (c) , squared spectrum width (d), and vertical integral length scale (e) over 16 hours. Circles are one standard deviation from associated median values (Fig. 4; Fang et al. 2014b)

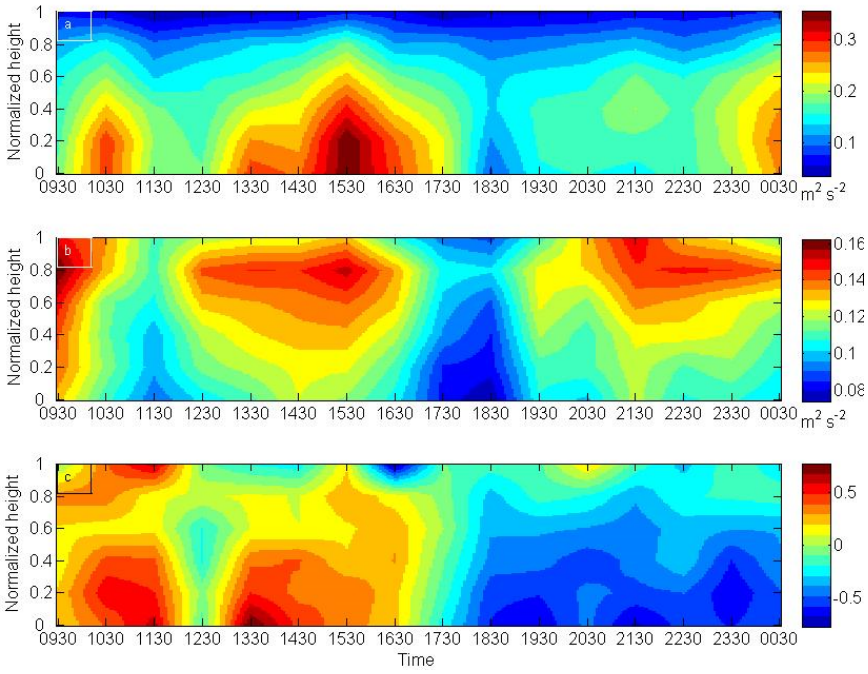


FIGURE 3. Time-height display of radial velocity variance (a), squared spectrum width (b) and skewness (c). The labels on the *x* axis are not at the top of the hours since each displayed value is an hourly median (Fig. 7; Fang et al, 2014a).

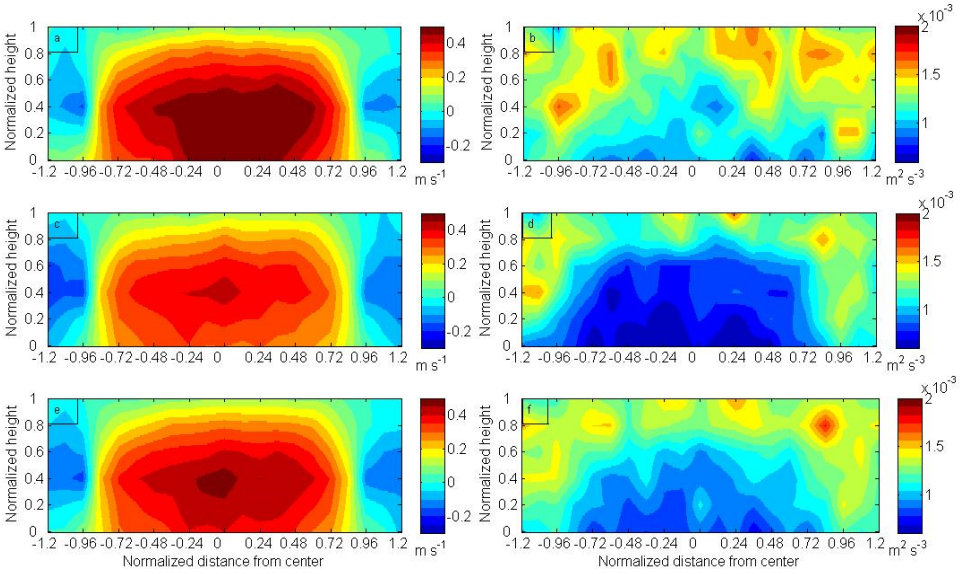


FIGURE 4. Coherent structures of the vertical velocity (left panels) and the EDR (right panels) in updraft region during the day (a, b), night (c, d), and for entire 16-hr (e, f) (Fig. 7; Fang et al, 2014b).

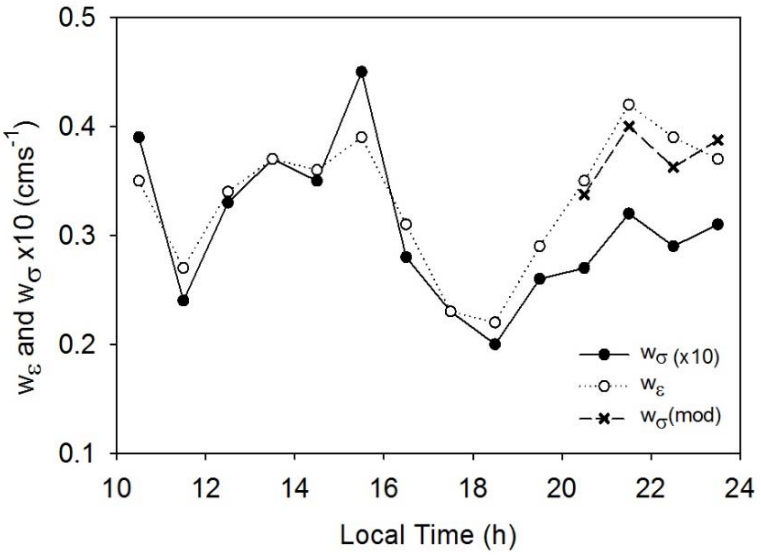


Figure 5: Entrainment velocity from eddy dissipation rate and from the vertical velocity variance terms in the TKE budget and as given by Eqs. (9) and (10), with modified velocity variance terms obtained for the 2030 to 2330 LST (CST) hourly values (-×-) for a reduced BL depth due to decoupling (Fig. 2; Albrecht et al., 2016).

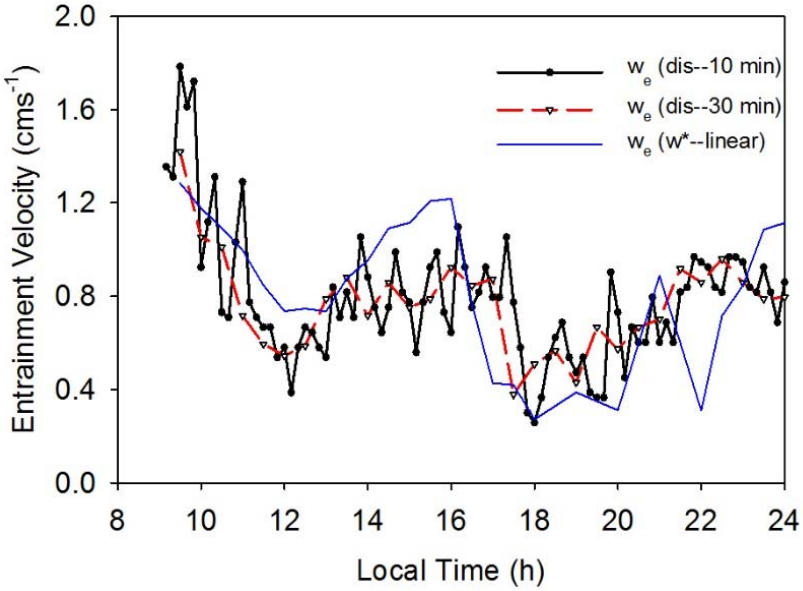


Figure 6: Entrainment rates estimated from radar-derived dissipation rates for 10-min (black) and 30-min (red) averages and from the convective velocity scale (30-min linear average), with parameterization coefficients giving an average entrainment velocity for the 13-h time period of 0.76 cm $s^{-1}$. (Fig 6; Albrecht et al, 2016)

## REFERENCES

Albrecht, B. M. Fang, and V. Ghate. 2016: Exploring stratocumulus cloud-top entrainment processes and parameterizations by using Doppler cloud radar observations, *J. Atmos. Sci.* **73**, 729-742.

Fang, M., B. A. Albrecht, V. P. Ghate, and P. Kollias. 2014a. Turbulence in continental stratocumulus, Part I: External forcings and turbulence structures. *Boundary-Layer Meteorol.*, **149**; DOI 10.1007/s10546-013-9873-34.

Fang, M., B.A. Albrecht, V.P. Ghate, and P. Kollias. 2014b. Turbulence in continental stratocumulus, Part II: Eddy dissipation rates and large-eddy coherent structures. *Boundary-Layer Meteorol.*, **149**; DOI 10.1007/s10546-013-9872-4.

Frisch AS, Lenschow DH, Fairall CW, Schubert WH, Gibson JS. 1995: Doppler radar measurements of turbulence in marine stratiform cloud during ASTEX, J Atmos Sci 52: 2800–2808

Ghate, V.P., B.A. Albrecht, and P. Kollias, 2010: Vertical velocity structure of non-precipitating continental boundary layer stratocumulus clouds. *J. Geophys. Res.*, **115**, D13204, doi:10.1029/2009JD013091.

Ghate, V.P., B. A. Albrecht, M. A. Miller, A. Brewer, and C.W. Fairall. 2014: Turbulence and radiation in stratocumulus-topped marine boundary layers: A case study from VOCALS-REx. *J. Appl. Meteorol. and Climatol.*, **53**, 117-135.

Hogan RJ, Grant ALM, Illingworth AJ, Pearson GN, O'Connor EJ. 2009: Vertical velocity variance and skewness in clear and cloud-topped boundary layers as revealed by Doppler lidar. Q J R Met. Soc 135: 635–643.

Kollias P, Albrecht BA, 2000: The turbulence structure in a continental stratocumulus cloud from millimeter-wavelength radar observations. J Atmos Sci 57: 2417–2434.

Kollias, P., E.E. Clothiaux, M.A. Miller, E. Luke, K.L. Johnson, K.P. Moran, K.P. Widener, and B.A. Albrecht, 2007: The Atmospheric Measurement Program cloud profiling radars: Second generation sampling strategies, processing, and cloud data products. *J. Atmos. Ocean. Tech.*, **24**, 1199-1214.

Kollias, P., E.E. Clothiaux, M.A. Miller, B.A. Albrecht, G.L. Stephens, and T.P. Ackerman, 2007: Millimeter-Wavelength Radars-New Frontier in Atmospheric Cloud Research. *Bull. Amer. Met Soc.*, **88**, 1608-1624.

Lothon, M., D.H. Lenschow, D. Leon, and G. Vali, 2005: Turbulence measurements in marine stratocumulus with airborne Doppler radar. *Quart. J. Roy. Meteor. Soc.*, **131**, 2063–2080.

Luke, E. and P. Kollias, 2013: Separating Cloud and Drizzle Radar Moments during Precipitation Onset Using Doppler Spectra. J. Atmos. Ocean. Tech.,30, 1656-1671.

Wood, R., 2012: Stratocumulus clouds. *Mon. Wea. Rev.*, **140**, 2373–2423.

# Observations of the Atmospheric Boundary Layer Using Ground-Based Active Electromagnetic Remote Sensing

Phillip B. Chilson
University of Oklahoma

## INTRODUCTION

The dawn of using active remote sensing techniques based on electromagnetic wave propagation to study the optically clear lower atmosphere can be traced back to the development of radar during the second World War. The anomalous `angel echoes' and `dot echoes' observed by military radar at the time were attributed to atmospheric clear air turbulence. It was discovered that turbulent eddies in the atmosphere could produce enhanced radio-wave backscatter if the scale size of the eddies were half the wavelength of the probing radar. This condition is referred to as clear-air scatter or Bragg scatter. Such early observations laid the foundations for using active electromagnetic remote sensing methods for clear-air atmospheric studies.

A wide range of bround-based active electromagnetic remote sensing technologies are available to atmospheric scientists. For example, lidar based ceilometers were developed to detect the base of clouds, but they are also used to study the evolution and structure of the atmospheric boundary layer (Schween et al. 2014). Additional active remote sensing techniques such as water vapor differential absorption lidar (DIAL) (Weckwerth et al., 2016) and raman lidar (Froidevauz, et al., 2013) are being used with great success in atmospheric boundary layer research. Moreover, there are many varieties of passive electromagnetic remote sensing devices. An overview of active and passive techniques can be found in Lundquist et al., (2017). Here we only briefly touch upon a few aspects of how radapr and lidar have been incorporated into atmospheric research and consider outlooks for the future.

## ATMOSPHERIC RADAR

Here we consider two types of atmospheric radar (radar wind profilers and weather radar) and how they can be used individually or collaboratively for boundary layer observations

*Radar Wind Profilers*: The term radar wind profiler (RWP) is used to describe a class of Doppler radar, which has been designed to detect scatter from clear-air turbulence (Bragg scatter), primarily for the purpose of estimating wind speed and direction aloft. Often this is achieved using a scanning, pulsed Doppler radar system. Much of the early development focused on MST (Mesosphere Stratosphere Troposphere) class RWPs operating at VHF (Hocking et al., 2016). In the late 80's, NOAA demonstrated that UHF RWPs could be deployed for ST (Stratosphere Troposphere) as well as for boundary layer research.

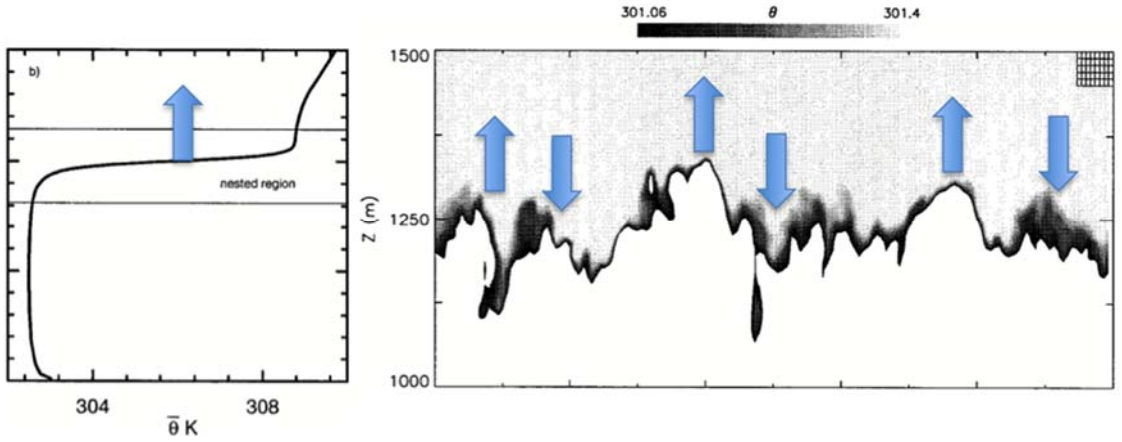


FIGURE 1. Schematic of entrainment-induced growth in a single vertical profile of potential temperature (left), and over a 2-dimensional field of potential temperature with horizontal distance as the x-axis (right). Image from Jacobsen (2014), which was adapted from Sullivan et al. (1998).

A Boundary layer RWP or boundary layer radar (BLR) typically operates at UHF (400 MHz or 1 GHz) and uses the Doppler Beam Swinging (DBS) technique to estimate the three-dimensional wind vector as a function of height directly above the radar system. The beam will be steered using a phased-array antenna, a mechanically scanning antenna, or an arrangement of static fixed position antennas. The beam orientations will be vertical or near-vertical. The backscattered signal results generally from Bragg scatter, Rayleigh scatter from insects or hydrometeors, or sharp gradient in the refractive index (Fresnel scatter).

BLRs are particularly adept at detecting the interface between the boundary layer and the free atmosphere. Sharp gradients of meteorological variables occur at the interface along with regions of localized turbulence. As such, this region is typically associated with enhanced radar backscatter. The rate of entrainment and even simply the height at which it occurs is of great importance. A depiction of the process is presented in Figure 1.

Patterns in radar data similar to those shown in Figure 1 are seen in the radar image of backscattered power collected using an S-Band FMCW (frequency modulated, continuous wave) radar (Figure 2). The radar beam was oriented vertically and recorded backscattered signals with a resolution of 2 m. The image is of significance in the context of the present discussion for two reasons: 1) it presents the intricate and elaborate structure contained within the atmospheric boundary layer, which correspond to the presence of clear-air turbulence and 2) it demonstrates that Bragg scatter can be detected at S-Band. We refer back to point 2 later in the discussion.

Such vertical resolution is not generally possible with pulsed Doppler RWP; however, techniques like range imaging (RIM) are being used to improve the range resolution of RWP (Palmer et al, 1999). Figure 3 shows results from an experiment conducted in Colorado during which a UHF BLR was operated in a RIM mode alongside an S-Band FMCW radar. As can be seen in the images, RIM processing of the data produced results with considerable more clarity than with the standard processing and the RIM images exhibit similar features to those obtained from the FMWC radar. It should be mentioned that the RIM processing utilized an adaptive signal processing technique, which is capable of suppressing some interference.

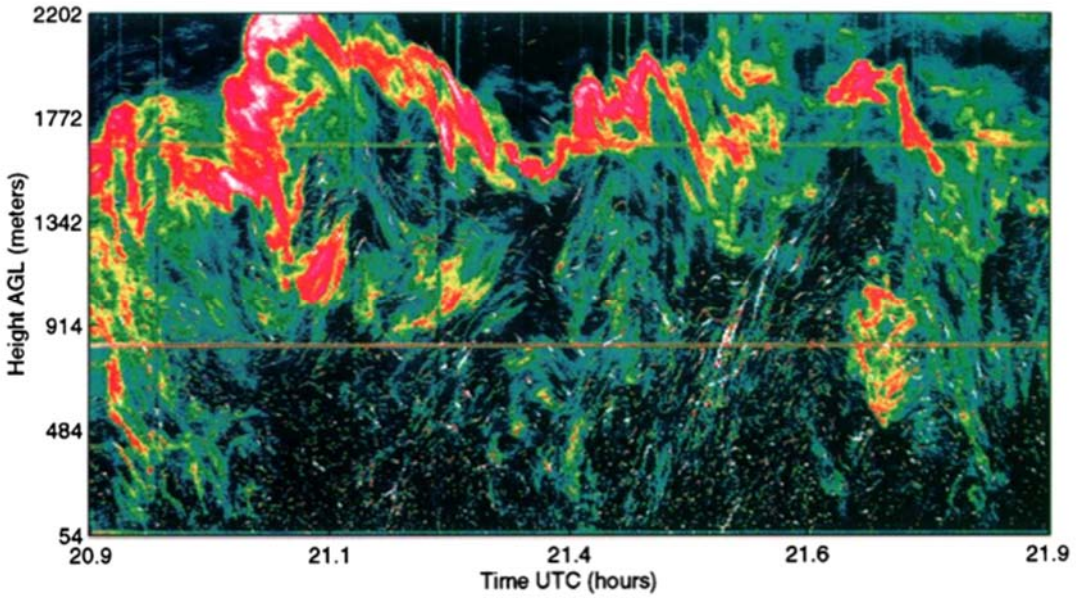


FIGURE 2. Time-height intensity plot showing backscattered power measured using an S-Band FMCW radar. Image is from Eaton et al.,(1995).

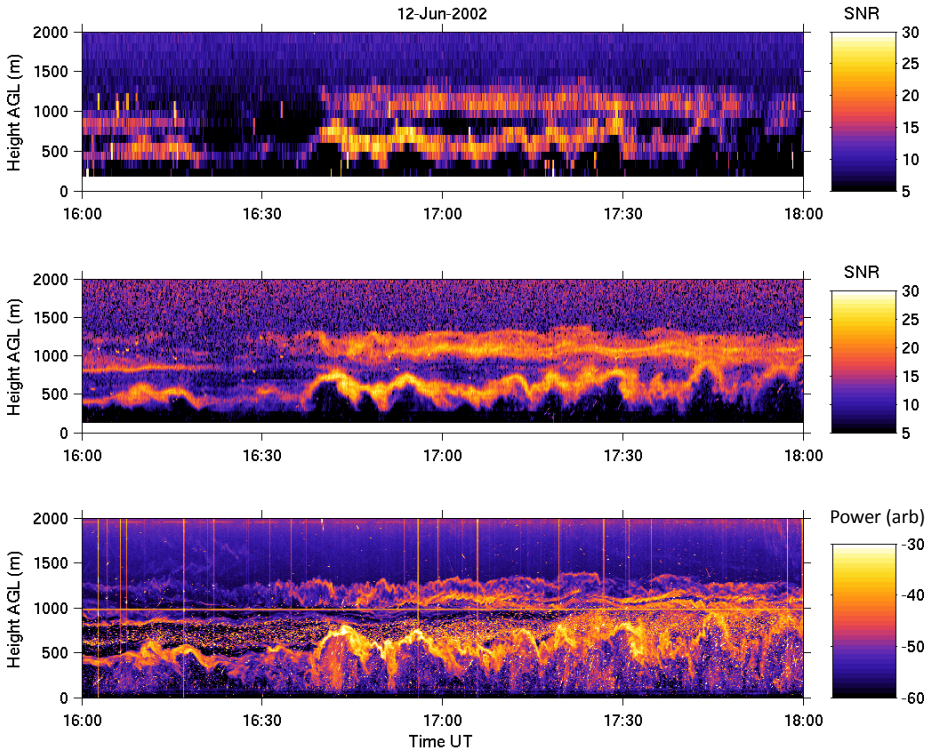


FIGURE 3. Radar observations from collocated radars in Colorado. The two upper images correspond to data collected using a UHF wind profiler operating in RIM mode. In the uppermost image, the data have been evaluated using standard radar processing. In the plot below, RIM processing has been used. For comparison, the lowermost image shows the backscattered signal recorded using an S-Band FMCW radar with a range resolution of 2 m.

*Weather Radar:* Weather radars are a powerful asset in gaining a sense of meteorological situational awareness. Their breadth of coverage is a principal advantage, as they offer a view of what is occurring over hundreds of kilometers, or even thousands of kilometers when working as a network. Unlike RWP, they rely on radio-wave scatter from hydrometeors. Moreover, they utilize a scanning strategy in which the radar beam is directed primarily at low elevation angles. Although not typically associated with observations of Bragg scatter, weather radar operating at S-Band are capable of detecting returns from clear-air turbulence (Melnikov et al., 2013). We are not aware of any such reports at higher frequency bands such as C-Band, X-Band, K-Band, W-Band, and so forth.

*Combined Use:* In February and March of 2014, a projected hosted by NCAR was conducted in Colorado called LATTE (Lower Atmospheric and Thermodynamics and Turbulence Experiment). As part of the experiment, the NCAR S-Pol weather radar and the NCAR 449-MHz RWP were deployed in such a manner that RHI (range height intensity) scans with S-Pol were directed over the RWP. The RWP was operated in RIM mode. S-Pol was configured to operate in a mode that would increase sensitivity and allow observations of Bragg scatter. Results are shown in Figure 3. The layer in the S-Pol data at a height of about 4 km is the result of Bragg scatter generated by winds coming across the Rocky Mountains. An enhancement of the backscattered signal detected by the RWP at the same time and height is seen the right-hand plot. Ceilometer data and ground-based cameras indicated that there were no clouds over the RWP site at the time.

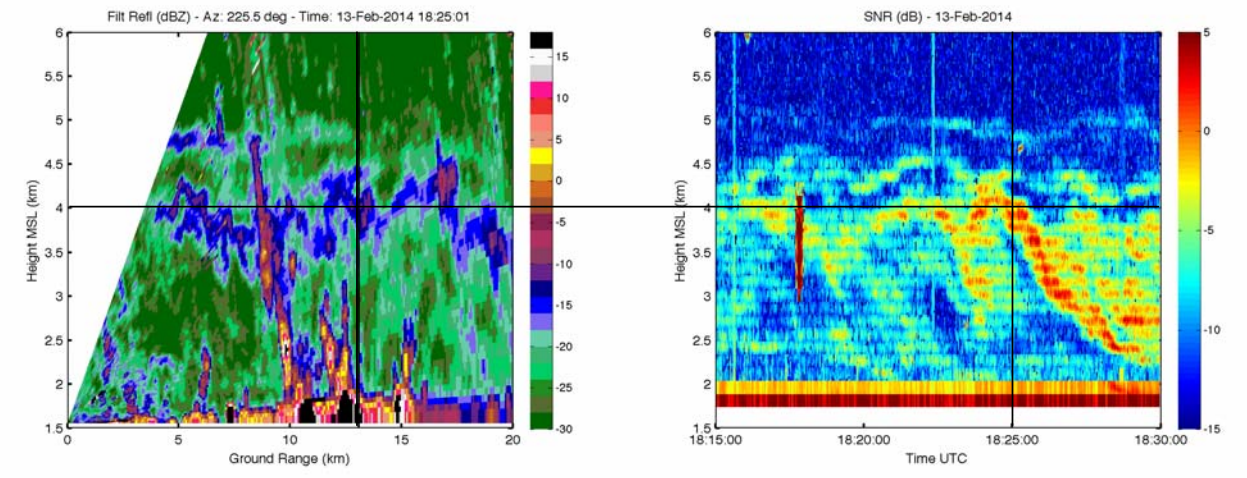


FIGURE 3. Plots of data from the NCAR S-Pol (left, showing radar reflectivity) and the NCAR 449-MHz RWP (right, showing SNR). The horizontal black lines simply show a height of 4-km AGL. For S-Pol, the vertical black line shows the location of the RWP and for the RWP the black line shows the time when the S-Pol data were collected.

## DOPPLER LIDAR

Coherent Doppler lidars bear many similarities to radar. They transmit pulses of collimated laser radiation into the atmosphere, which is backscattered by aerosols and cloud particles. The received backscattered radiation is used to infer the radial velocity of the scatterers density and the density of the scatterers. Scanning strategies utilized by Doppler lidar are similar to those of RWPs or weather radar, depending on the lidar. As the price of Doppler lidars has dropped, these instruments are increasingly being deployed in atmospheric research. Figure 5 shows an example of data collected during a low-level jet event. Doppler lidar are expected to have a significant impact on future boundary layer studies.

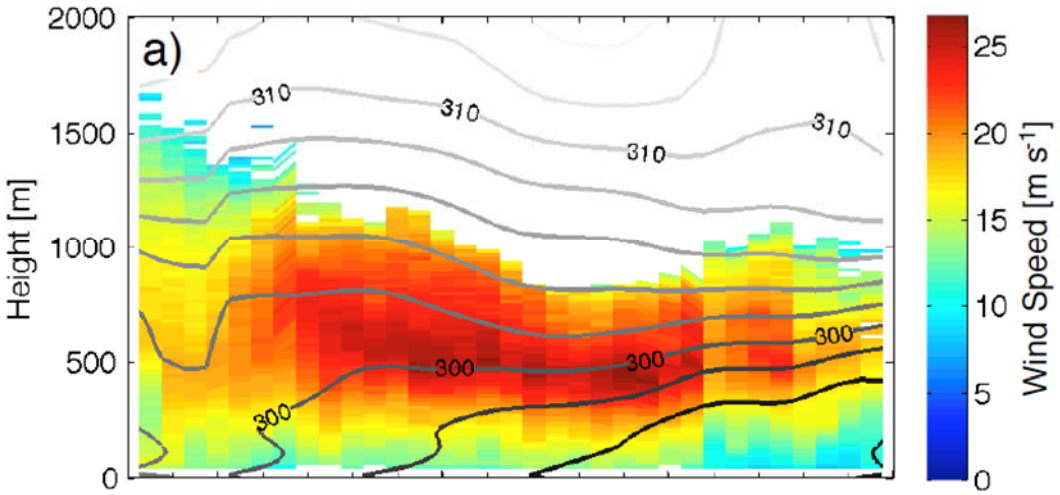


FIGURE 5. Wind speed recorded using a scanting Doppler lidar corresponding to a low-level jet. The contours show values of potential temperature. Data were collected in northern Oklahoma. Image taken from Bonin, (2015).

## SUMMARY & OUTLOOK

Ground-based active electromagnetic remote sensing methods have a long history of application in boundary layer research. We continue to see new developments in these methods, which are impacting their ability to dive deeper into understanding the processes that drive boundary layer development and evolution. Most radar-based boundary layer research is conducted using RWPs. One limitation of BLRs is their spatial resolution. The horizontal resolution can be addressed through spaced antenna techniques, especially when coupled with radar imaging. RIM is being used to improve vertical resolution. Unlike conventional phase coding techniques, RIM processing can be applied adaptively. It is recommended that both angular and range imaging could be further developed and explored. In the case of weather radars, it has been shown that S-Band weather radar can be used to monitor the atmospheric boundary layer, especially the depth of the boundary layer. S-Band weather radar can also be used to visualize and investigate scattering layers in the free atmosphere. It is recommended that the potential of using weather radar for boundary layer research be further developed. Finally, there has been a dramatic increase in the number of Doppler lidars being used in the atmospheric sciences. They offer robust estimation of the wind and have good range resolution. Moreover,

techniques are being developed to investigate atmospheric turbulence using Doppler lidar. All of these remote sensing techniques are expected to continue providing valuable observations to the boundary layer research community.

## References

Bonin, T., 2015: Nocturnal Boundary Layer and Low-Level Jet Characteristics Under Different Turbulence Regimes, *PhD Dissertaion, University of Oklahoma,* 183p.

Eaton, F. D., S. A. McLaughlin, and J. R. Hines, 1995: A new frequency-modulated continuous wave radar for studying planetary boundary layer morphology, *Radio Sci*, **30**, 75–88.

Froidevaux, M., C. W. Higgins, V. Simeonov, P. Ristori, E. Parkyjak, I. Serikov, R. Calhoun, H. van den Bergh, and M. Parlange, 2013: A raman lidar to measure water vapor in the atmospheric boundary layer, *Adv. Water Resources*, **51**, 345-356.

Hocking, W. K., J. Röttger, R. D. Palmer, T. Sato, and P. B. Chilson, 2016: Atmospheric Radar: Application and Science of MST Radars in the Earth's Mesosphere, Stratosphere, Troposphere, and Weakly Ionized Regions, *Cambridge University Press*, 854p.

Jacobsen, E, 2014: Prospects of Clear Air Monitoring with the Multi Mission Phased Array Radar, *MS Thesis, University of Oklahoma*, 157p.

Lundquist, J. K., et al., 2017: Assessing the state-of-the-art capabilities for probing the atmospheric boundary layer, The XPIA Field Campaign, Bull. Amer. Meteorol. Soc., 289-314.

Melnikov, V. M., R. J. Doviak, D. S. Zrnic, and D. J. Stensrud, 2013: Structure of Bragg scatter observed with the polarimetric WSR-88D, *J. Atmos. Oceanic Tech.*, **30**, 1253-1258.

Palmer, R. D., T.-Y. Yu, and P. B. Chilson, 1999: Range imaging using frequency diversity, *Radio Sci.*, **34**, 1485-1496.

Schween, J. H., A. Hirsikkoo, U. Löhnert, and S. Crewell, 2014: Mixing-layer height retrieval with ceilometer and Doppler lidar: from case studies to long-term assessment, *Atmos. Meas. Tech.*, **7**, 3685-3704.

Sullivan, P. P., C.-H. Moeng, B. Stevens, D. H. Lenschow, and S. D. Mayor, 1998: Structure of the entrainment zone capping the convective atmospheric boundary layer. *J. Atmos. Sci.*, **55**, 3042–3064.

Weckwerth, T. M., K. J. Weber, D. D. Turner, and S. M. Spuler, 2016: Validation of a water vapor micropulse differential absorption lidar (DIAL), *J. Atmos. Oceanic Tech.*, **33**, 2353-2372.

# Wind, Current, Wave, and Stress Coupling in the Boundary Layer

Mark Bourassa and Qi Shi
EOAS and COAPS, Florida State University

The transfer of energy, momentum, and gas across the air-sea interface is a critical component of the Earth system on weather and climate timescales. Variability within the marine atmospheric boundary layer is often fast enough that a constellation of three or four satellites would be required to measure the atmospheric variables associated with air-sea coupling on the short timescales needed for both weather and climate. Consequently, the observing system for both the ocean and atmospheric boundary layers has been more focused on understanding and modeling processes with goals related to data assimilation, state estimation and forecasting. The future observing system must be designed to measure key variables in processes we know are important, and to push the existing boundaries so that additional processes that we suspect are important can be studied and better included in models. This talk emphasizes modeling applications, because consistent and accurate model physics in the atmospheric and oceanographic boundary layers is needed for climate, medium-range weather, and many other scientific and societal applications. Furthermore, improved model physics can be used to fill observational gaps in spatial and temporal sampling.

Surface stress, the vertical flux of horizontal momentum, is one of the key links between the atmospheric boundary layer and the ocean's mixed layer. Stress is sensitive to winds, waves, currents, and buoyancy. Insufficient stress causes models to have higher wind speeds, weaker mean currents, and shorter-lived ocean eddies. Stresses are highly dependent on the characteristics of surface waves, which are in turn substantially altered by strong currents. The eddy kinetic energy input into the ocean is equal to the dot product of the stress and current products; hence, winds, waves, currents, and stress all appear to be critical to coupling the ocean and atmosphere. A modeling study will be used to demonstrate the importance of currents and waves on stress and ocean mixing, as well as on heat fluxes. Comparisons to satellite observations will be used to show that currents and waves are indeed critical, and to recommend the related needs for our future observing psystem. Only some of these variables need to be observed because waves can be well modeled given stress (or winds) and currents. Observing equivalent neutral winds (which are equivalent to stress) and currents addresses many issues related to atmospheric and oceanic boundary layers, and provides a way forward to push the frontiers of our understanding of air-sea interaction.

# Advances, challenges, and opportunities for remote sensing of the atmospheric surface layer and air-sea fluxes

Carol Anne Clayson
Physical Oceanography Department
Woods Hole Oceanographic Institution

Exchanges of energy, moisture, and mass at the atmosphere-ocean interface represent a critical coupling within the climate system. The radiative and turbulent heat fluxes are the main contributor to heating and cooling of the oceans, which also influences the surface mixing. They also supply energy and moisture to the atmospheric boundary layer affecting changes in static stability, moist static energy, and convection. Therefore, it is of great importance that these fluxes are properly quantified through careful observation and correctly parameterized in coupled modeling, including general circulation models.

Estimating turbulent fluxes from satellites require estimates of sea surface temperature (SST), near-surface wind speed (Wspd), specific humidity (Qair), and temperature (Tair). Recent intercomparison efforts by Brunke et al. (2011), the Ocean Heat Flux project (Bentamy et al. 2017) and the WCRP Working Group on Air-Sea Fluxes [WGASF] (Fairall et al. 2010) indicate that Tair and Qair are primary sources of uncertainty in producing accurate turbulent flux estimates using satellites, and this talk will focus mainly on these parameters.

Several relatively independent efforts are currently being undertaken to produce latent and sensible heat fluxes over the global oceans. While sharing the use of the bulk flux approach, specific choices must be made however, including parameterization of exchange coefficients, spatial and temporal resolution of bulk variables, sources of nearsurface observations, and interpolation methodology. The details of implementation often differ resulting in divergent estimates. Both latent heat and sensible heat fluxes show inter-product differences of 5-10 Wm-2 globally. Several of the products show a moderate trend from the early 1990's, in contrast to some reanalysis products. At the global scale, both Qair-Qsurf, SST - Tair differences and Wspd differences appear to be important, and offsetting in some cases.

In this talk I will highlight some of the challenges still remaining for the development of accurate, precise, and consistent climate data records of Qair, Tair, and the turbulent latent and sensible heat fluxes. In particular, I will demonstrate that large conditional/regional biases affect current remote sensing based estimates of near-surface air temperature and humidity, particularly under different cloud regimes. However, these challenges also point the way to possible advances still to be made given current (and past) satellite datasets. Three main areas open for advances and opportunities will be discussed:

*Improved data fusion*. New methods for combining satellite data from multiple satellite sensors and systems will be discussed, as well as possibilities for improvements from integrating atmospheric models within the analyses.

*New approaches to handling cloud impacts*. Microwave brightness temperature will be shown to be sensitive to cloud types and microphysical characteristics. Possible approaches for

new algorithms for ameliorating these biases will be outlined, as well as thoughts for making use of this understanding for blending datasets.

*New sensor development*. Virtually all of the sensors that are currently used for analysis of the near-surface atmospheric properties were not developed for this purpose. Several possibilities for new sensors will be discussed.

# Emerging Technologies for Remote Sensing of Boundary Layer Clouds, Precipitation, and Thermodynamics

Matthew Lebsock
NASA-JPL, California Institute of Technology

Both weather and climate models have longstanding biases in their representation of clouds within the planetary boundary layer. There are typically compensating errors in cloud amount and cloud brightness. These biases have persisted for decades despite improvements in physical parameterizations and observing systems. Boundary layer clouds over the ocean have a disproportionate influence on global temperatures owing to their strong short wave and minimal long wave radiative effects on the top of atmosphere energy balance. The response of these clouds in the subtropical ocean are the largest source of uncertainty in projections of global mean temperature change. Despite recent optimism that the low cloud feedback is well-understood and of positive sign it is difficult to reconcile the shared inability of models to represent the mean state of these clouds with fidelity with a well understood cloud feedback.

This talk focuses on the observing system relevant to improved understanding of boundary layer clouds. Cloud is the result of interactions between the surface fluxes, boundary layer mixing, microphysical, and radiative processes. The balance of these processes give rise to clouds as a product of their thermodynamic environment. Specifically, they represent the saturated tail of the joint distribution of total water and temperature. Meaningful advances in the representation of clouds must therefore be coupled to improved representation of thermodynamics and an observing system should reflect this fact by coupling these observations.

The current state of the art remote sensing platform for clouds is NASA's A-Train constellation. Cloud properties are derived from passive optical and microwave imagers, the CloudSat radar and CALIPSO lidar. The profiling capabilities of the active sensor have had a profound impact in characterizing boundary layer cloudiness. In addition, the first spaceborne identification and quantification of light precipitation comes from CloudSat. These observations, as they stand, are good enough to expose the significant cloud and precipitation biases that exist in models. However, only limited boundary layer thermodynamic profiling is available from the AIRS sensor in the A-Train. We do know that the boundary layer profiles from AIRS, and models, have significant biases in their characterization of the boundary layer when compared with coincident radiosonde measurements. Thermodynamics then is the weak link in the observing system and it is arguable that improvements to the representation of clouds may best be facilitated through improved thermodynamic observations coupled to cloud observations.

In this talk several points will be made including:

- It is critical that the cloud and precipitation data record established with the A-Train be continued. Specifically, this applies to the combined radar/lidar data record.
- Minor technological advances will facilitate more accurate characterization of clouds. Specifically adding radiometric channels to a follow-on radar will improve cloud liquid water path retrievals and shortening radar pulse lengths to probe closer to the earth surface will improve precipitation retrievals.
- Cloud observations must be coupled in space and time to observations of thermodynamics following the successful constellation approach of the A-Train.
- Major improvements in the observing system are necessary to characterize the atmospheric thermodynamic environment.
- Improvements to radio occultation receivers and retrieval methodologies will soon allow occultation retrievals of water vapor profiles to within several hundred meters above the earth surface whereas they have been limited to above 1-2 km in the past.
- Technology development is improving the achievable spatial resolution of infrared observations which will have the capability to (1) see between clouds and (2) quantify small scale variance in thermodynamics.
- Revolutionary advances in active profiling techniques for water vapor will likely be possible from space within the next decade. These include both lidar for clear sky and radar for cloudy sky profiling. Each technique still requires continued funding to advance the technology for spaceborne deployment.
- In-cloud radar sounding of water vapor requires specific allocation of the radio-frequency spectrum in and around the protected 183 GHz band, which will require advocacy from the scientific community.

# Biogenic emissions and interactions with the atmospheric boundary layer

Allison L. Steiner
University of Michigan

The terrestrial biosphere emits a broad suite of gases and particles into the atmospheric boundary layer, and many of these compounds undergo transformations contributing to ozone and fine particulate matter. From the chemical perspective, understanding the fate of these emissions and their impact on weather and climate strongly depend on boundary layer dynamics. The vertical mixing out of the surface layer can strongly influence the distribution of primary emissions and the formation of secondary compounds in the atmosphere. Many gas-phase compounds are short-lived climate forcers, and particles can act as cloud condensation nuclei influencing the formation of boundary layer clouds. Because many of these emissions are sensitive to environmental changes such as temperature, changes in climate and vegetation species distribution would alter the emissions and their feedback to boundary layer processes.

Gas phase biogenic volatile organic compounds (VOC), such as isoprene ($C_5H_8$), monoterpenes ($C_{10}H_{16}$) and a suite of oxygenated VOC, are emitted naturally from most photosynthesizing vegetation, and are dependent on environmental conditions such as temperature and light. Once emitted, these compounds are mixed up and out of the forest canopy, and the efficacy of this mixing is a function of the canopy structure and vertical heterogeneity. Primary emissions (e.g., isoprene and terpenes) react with atmospheric oxidants on similar time scales as turbulent boundary layer mixing. Modeling studies of these timescales vary, but large-eddy simulation models indicate that isoprene chemical lifetimes can be shorter than turbulent mixing timescales and the chemistry of isoprene oxidation can be influenced by convective conditions, cloud formation and other boundary layer processes (Figure 1). As a result, boundary layer conditions can influence the reactivity of isoprene and other VOC within the PBL (Li et al., 2016). In addition to the reactions that form ozone, many biogenic VOC contribute to heterogeneous chemistry in the atmosphere, undergoing aqueous chemistry within clouds and influencing gas and aqueous chemistry in the cloud layer (Li et al., 2017).

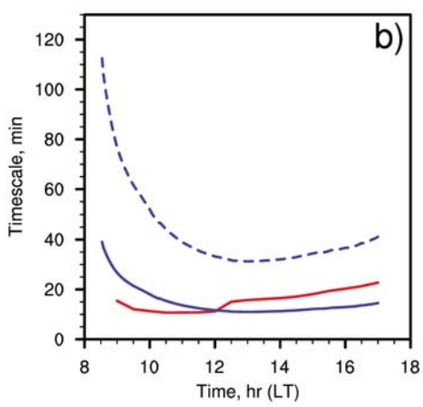


FIGURE 1. Diurnal timescales of the turnover time (red), isoprene lifetime (blue) and methacrolein (blue-dashed, isoprene oxidation product) lifetime, based on LES simulations of convective conditions during the DISCOVER-AQ 2011 field campaign (Li et al., 2016).

Bioaerosols such as anemophilous (or wind-driven) pollen are emitted by terrestrial vegetation in large quantities to transmit genetic material between plants. These compounds also can mix throughout the boundary layer and be transported large distances despite their relatively large size (20-50 microns on average). Additionally, pollen grains can easily rupture when wet, releasing smaller organic particles that are known to be cloud-active (Steiner et al., 2015). Ground-based lidar studies with depolarization at the University of Michigan Biological Station has shown distinct signatures from pollen throughout the boundary layer after flowering (Figure 2). These observations provide a way to quantify when and where pollen emissions may be contributing to the atmospheric particle burden. Further, modeling studies suggest that these particles can suppress precipitation through the second aerosol indirect effect to the order of 1040% during spring when emissions are high (Wozniak et al., in preparation).

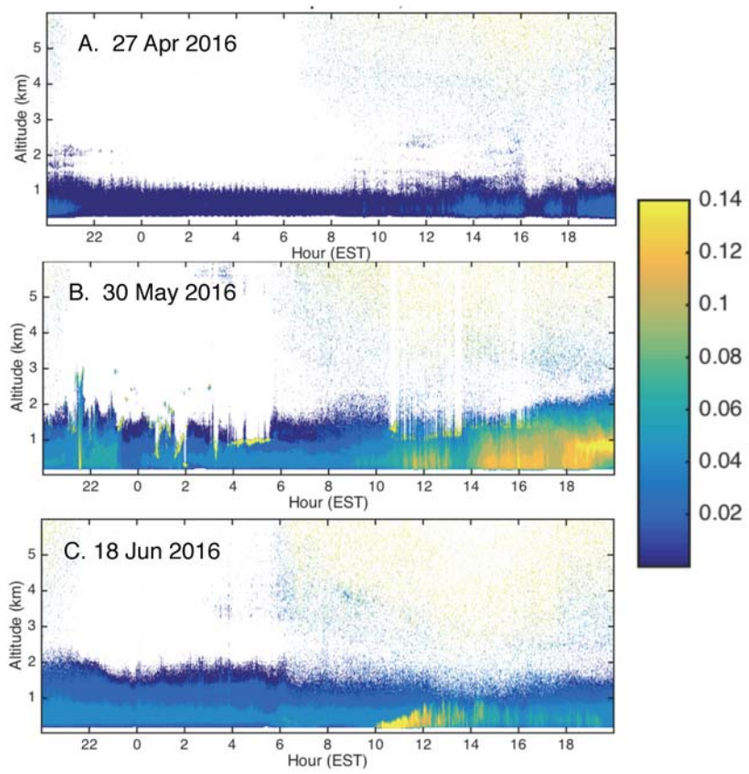


FIGURE 2. Diurnal depolarization ratios (color bar) over the lower atmosphere as detected by the Mini Micro-Pulse Lidar (MPL) at the University of Michigan Biological Station (UMBS) for three selected days during 2016 observations: (A) prior to leaf out and flowering periods (27 April), (B) five days following the emergence of red oak flowers (30 May), and (C) four days after the first detection of white pine cone emergence (18 June). Note the higher depolarization ratios during pollination time periods starting at approximately 10AM EST.

To understand these fluxes from the biosphere to the atmosphere, we rely on a suite of ground-based or flight-based observing systems (and to some extent remote sensing, although this has some unique limitations due to chemical lifetimes). Forest flux sites with comprehensive measurements are relatively sparse (e.g., about six sites in the US that are well-instrumented for atmospheric chemistry over the past decade, and many with relatively short and single-year field seasons). Flight-based observations are also typically limited to single field campaigns that may span one month. Additionally

tools to provide more observations over more ecosystem types, and particularly those that are maintained over several years, are greatly needed to understand the changing role of chemistry.

To fill these gaps, we rely on modeling systems that focus on emissions modeling and understanding the fate of these compounds in the atmosphere. These tools range from one-dimensional canopy-meteorology models, to Large-Eddy Simulation (LES) systems, up to regional and global scale models that rely on boundary layer parameterizations. For comparison with site observations, single-column models have been especially useful as they resolve multiple layers within the forest canopy and can account for atmospheric chemistry within the canopy and identify specific physical and chemical processes that may be important. However, these models tend to be weak on boundary layer dynamics, and moving up in scale to LES can work to alleviate some of the common problems identified within the boundary layer. However, far more common than these two methods are chemistry transport models (CTMs), which rely on weather models or reanalysis products to drive the mixing within the boundary layer. Also, coupled models with chemistry and meteorology (e.g., WRF-Chem) provide an interactive tool that allows for interactive emissions schemes. However, there is frequently a mis-match between these scales, and the boundary layer height as simulated by LES and WRF-Chem can differ greatly.

To better understand the role of biogenic emissions on boundary layer processes, observing systems are needed over longer time scales and broader spatial scales to (1) understand chemical and physical processing within the cloud layer, e.g., how compounds are entrained and mixed between the boundary layer and free troposphere, or reacting within clouds layers, and (2) develop an understanding of interannual variability of these processes and how the boundary layer could be influencing emissions from year to year.

## REFERENCES

Li, Y., M.C. Barth, G. Chen, E.G. Patton, S.-W. Kim, A. Wisthaler, T. Mikoviny, A. Fried, R. Clark and A.L. Steiner (2016) Large-eddy simulation of biogenic VOC chemistry during the DISCOVER-AQ 2011 campaign, *JGR-Atmospheres*, 121, 8083-3105, doi:10.1002/2016JD024942.

Li, Y., M.C. Barth, E.G. Patton and A.L. Steiner (2017) Impact of in-cloud aqueous processes on the chemistry and transport of biogenic volatile organic compounds, *JGR-Atmospheres*, doi:10.1002/2017JD026688.

Steiner, A.L., S.D. Brooks, C. Deng, D.C.O. Thornton, M. Pendleton and V. Bryant (2015) Pollen as atmospheric cloud condensation nuclei, *Geophysical Research Letters*, DOI: 10.1002/2015GL064060.

Wozniak, M.C., F. Solmon, and A.L. Steiner, The impact of pollen rupture on precipitation, in preparation.

# Characterizing Constraints to Land-Atmosphere Carbon, Water and Energy Exchange with Spaceborne Remote Sensing

Kyle C. McDonald
Department of Earth and Atmospheric Sciences
City College of the City University of New York

Surface temperature and water status are key state variables controlling carbon, water and energy exchange at the land-atmosphere boundary in terrestrial biomes. Wetlands exert major impacts on global biogeochemistry, hydrology, and biological diversity. In northern high latitudes, the landscape transition between seasonally frozen and non-frozen conditions occurs each year over more than 50 million km2 of the biosphere, affecting hydrological and ecological processes and associated trace gas dynamics profoundly. Combined, surface moisture and water status define a surface hydrospheric state that is key to linking terrestrial water and energy cycles, and is a principal determinant of the terrestrial carbon cycle.

Providing reliable, consistent multi-temporal observations, remote sensing measurements from Earth-orbiting satellites are well-suited for characterizing the vegetation structure and distribution, and temporal dynamics of surface temperature and moisture fields. Passive and active and microwave sensors such as radiometers scatterometers and Synthetic Aperture Radars (SARs) can provide observations of structure and water status without the fundamental limitation cloud cover, atmospheric contaminants or available light that are common constraints to optical and infrared sensors. Optical/IR sensors provide critical measurements of surface structure, temperature and photochemistry. LIDAR technologies offer unique capabilities for detailed characterization of vegetation canopy structure.

Current and planned Earth science remote sensing missions offer a developing array of datasets supporting mapping and monitoring of land surface state variables as associated with boundary layer characterization. This presentation reviews science issues associated with the surface state variables and the associated capabilities addressed by such mission data sets. Selected current and planned missions and their capabilities are discussed. Products related to characterization of processes governing carbon, water and energy cycles in terrestrial ecosystems are considered. Development of integrated approaches employing multiple data products to support assessment regional and global scale processes are discussed.